



## ARBS Annual Review of Biomedical Sciences

pdf freely available at <http://arbs.biblioteca.unesp.br>

2008;10:105-159

---

### Histochemistry, General and Special\*

Tetsuji Nagata<sup>†</sup>

Department of Anatomy and Cell Biology, Shinshu University School of Medicine, Matsumoto, and  
Department of Anatomy, Shinshu Institute of Alternative Medicine and Welfare, Nagano, JAPAN

Received: 25 April 2007; accepted 13 July 2008

Online on 13 December 2008

---

#### Abstract

Nagata T. *Histochemistry, General and Special. ARBS Annu Rev Biomed Sci* 2008;10:105-159. Histochemistry has been developed between the morphology and functionology, employing both anatomy and biochemistry to fill up the gap between both. Histochemistry localizes chemical components of cells and tissues on histological sections by using various techniques. This field was first established by developing techniques for demonstrating phosphatase activity in 1930's. I had aimed at studying histochemistry by developing new techniques using various principles since 1950's. I had formerly proposed to classify these methods into 3 categories, *i.e.*, chemical, physical and biological techniques. The histochemical techniques have been well developed and systematized by the end of the 20<sup>th</sup> century to demonstrate various components such as enzymes, proteins, nucleic acids, glucides, lipids, etc. As a result, many text books are now available dealing with the methodology, which has been well developed in the late 20<sup>th</sup> century to form a new scientific field which should be designated as "General Histochemistry". These techniques should be applied to all the organ systems of men and animals as applications of histochemistry to special histology. The results of these applications to all the organs should be collected to form a new field, *i.e.*, "Histochemistry of the Organs" like the histology of the organs or special histology. These results should form a new field in medical sciences, which can be designated as "Special Histochemistry" developing to a part of the microscopic anatomy together with the special histology. These data include not only 3-dimensional structure of the organs but also the 4-dimensional structure in connection with the individual aging.

© by São Paulo State University – ISSN 1806-8774

**Keywords:** methodology, chemical methods, physical methods, biological methods, application to the organs

---

\*This study was sponsored by Grants-in-Aids for Scientific Research from the Ministry of Education, Science and Culture of Japan (No. 001054, 801066, 501010, 501533, 56870001, 58015046, 02454564) and Grants-in-Aids for Scientific Research from the Japan Society for Promotion of Sciences (No.18924034, 19924024, 20929003).

#### <sup>†</sup>Correspondence

Tetsuji Nagata. Department of Anatomy and Cell Biology, Shinshu University School of Medicine, Matsumoto 390-8621, and Department of Anatomy, Shinshu Institute of Alternative Medicine and Welfare, Nagano 380-0861, Japan. E-mail: [nagatas@po.cnet.ne.jp](mailto:nagatas@po.cnet.ne.jp)

---

## Table of Contents

1. Introduction
    - 1.1. Historical review on histochemistry and cytochemistry
    - 1.2. Classification of histochemical methods
      - 1.2.1. Chemical methods
      - 1.2.2. Physical methods
      - 1.2.3. Biological methods
      - 1.2.4. Histochemistry: general and special
  2. Histological and Histochemical Techniques
    - 2.1. Animal treatment and tissue processing
    - 2.2. Fixation of tissues and cells
      - 2.2.1. Chemical fixation for insoluble compounds
      - 2.2.2. Chemical fixation for soluble compounds
      - 2.2.3. Cryo-fixation for soluble compounds
    - 2.3. Embedding and sectioning
      - 2.3.1. Cryo-sectioning without embedding
      - 2.3.2. Freeze-drying and embedding
      - 2.3.3. Freeze-substitution and embedding
      - 2.3.4. Dry sectioning of freeze-dried or freeze-substituted materials
    - 2.4. Observation of histochemical specimens by microscopy
      - 2.4.1. Light microscopy
      - 2.4.2. Electron microscopy
      - 2.4.3. Image analysis of histochemical reactions
  3. Histochemical Methodology - General Histochemistry
    - 3.1. Chemical methods in histochemistry
      - 3.1.1. Color reactions for light microscopy
      - 3.1.2. Electron dense deposits for electron microscopy
    - 3.2. Physical methods in histochemistry
      - 3.2.1. Methods using high or low temperatures
      - 3.2.2. Methods using lights with different wave lengths
      - 3.2.3. Methods using radiations
    - 3.3. Biological methods in histochemistry
      - 3.3.1. Immunohistochemistry
      - 3.3.2. Lectin histochemistry
  4. Special Histochemistry - Histochemistry of the Organs
    - 4.1. The skeletal system
    - 4.2. The muscular system
    - 4.3. The circulatory system
    - 4.4. The digestive system
    - 4.5. The respiratory system
    - 4.6. The urinary system
    - 4.7. The reproductive system
    - 4.8. The endocrine system
    - 4.9. The nervous system
    - 4.10. The sensory system
  5. Concluding Remarks
  6. Acknowledgments
  7. References
-

# 1. Introduction

The researches in medical and biological sciences or bio-medical sciences aim at clarifying the morphology and functions of human and animal bodies by means of various research methods. The medical and biological sciences dealing with morphology are anatomy and pathology, while those dealing with functions are biochemistry and physiology, which can be designated as functionology (Nagata, 2004a). The two basic medical sciences, morphology and functionology, cover not only all fields of basic medical sciences but also all fields of clinical sciences such as internal medicine and surgery. Anatomy and pathology describe the form and structure of the human and non-human animal bodies, while functionology analyzes functions on these being by applying chemistry and physics. Recent advances in research methodology in medical and biological sciences have been made at the frontiers between the morphology and functionology, between anatomy-pathology and biochemistry-physiology. This new frontier is designated as histochemistry and cytochemistry, which is a field to localize chemical components of cells and tissues on histological sections by using various techniques and analyze the functions based on morphology. When I started the career as anatomist and histologist in 1955, after graduating from a medical school in Japan, I first aimed at studying cytochemistry by developing new special techniques using various principles such as enzyme cytochemistry, microincineration, microspectrophotometry, radioautography, cryo-techniques, X-ray microanalysis and immunocytochemistry. We have first concentrated to develop methodologies from 1960's to 1970's. However, since these technologies were well developed in 1970-80's, we then concentrated to apply these special techniques to various kinds of cells and tissues in men and other animals. Formerly, I had proposed to classify these cytochemical methods into 3 categories, *i.e.*, chemical, physical and biological techniques (Nagata, 1995b, 1999b). Recently, the methodology has been well developed to form a new field, which should be designated as general histo- and cytochemistry similarly to the general histology. On the other hand, these techniques should be applied to all the organ systems of men and other animals, such as the skeletal, muscular, digestive, respiratory, urinary, reproductive, endocrine, circulatory, nervous and sensory systems. The results of these applications to all the organ systems should be collected to accumulate a new field, *i.e.* histochemistry of organs like histology of organs. We made efforts to apply these techniques to various organ systems of men and other animals since 1970's to the present time (Nagata, 1999b, 2001a,b, 2002, 2004c, 2005a,b, 2006a,b, 2007a,b) and collected data from all the organs including the aging process from prenatal, postnatal development to adult and senescent stages. The data include not only 3-dimensional structure of the organs but also the 4-dimensional structure taking the time dimension into account, by labeling cells and tissues in connection with the individual aging (Nagata, 1995c, 1997b, 1999a, 2000a,c).

## 1.1. Historical review on histochemistry and cytochemistry

The histochemistry and cytochemistry is as old as histology itself (Lison, 1936, 1960; Pearse, 1953, 1968, 1980). In early 19<sup>th</sup> century, histochemical researches to study chemical components of biological structure in combination with chemistry and biology started first in botany in France (Raspail, 1825). He stained starch in plant tissues blue with potassium iodide solution under the light microscope and demonstrated its localization microscopically (Raspail, 1825). Then, he published an essay on microscopic chemistry for the first time (Raspail, 1830). Later, from the 1840's to 1870's, histochemistry in zoology and medicine was developed mainly as biological chemistry, together with histology introducing methods involving tissue destruction to analyze chemical components in Germany (Lehmann, 1842). Among these zoologists, anatomists and pathologists who were at that time interested in analyzing chemical constituents in animal tissues including men, Miescher (1874) was the first to introduce cell fractionation to analyze nucleic acids in nuclei of leukocytes. During these times in the 19<sup>th</sup> century, this new field was called as "microchemie" in French or "Mikrochemie" in German, which meant microchemistry in English. Microchemistry was, in other words, microscopic chemistry or chemical microscopy and meant to observe chemical reactions *in situ* under microscopy.

In early 20<sup>th</sup> century, aniline dyes were frequently used to stain tissues in anatomy and pathology. Normal histology was studied not only in anatomy but also in physiology. Histologists and pathologists were much interested in new dyes and less interested in histochemistry at that time. When Lison (1936)

published his famous book entitled “Histochemie Animale”, many histologists were again interested in histochemistry. Lison classified histochemical techniques into two categories, “*méthodes extra situm*” or “*méthodes extractives*” and “*méthodes histochimiques in situ*” or “*méthodes topochimique*” in French. The former included cell fractionation and microchemistry, while the latter included *in situ* histochemistry, which he proclaimed to be the new “science” studying the chemical components of tissues without tissue destruction. Then, many histologists, anatomists, pathologists, physiologists started to study this new field and published many original papers and books dealing with histochemistry and cytochemistry. Innumerable literature, as well as textbooks and handbooks, are available from the 1950’s to 1990’s. Representative books in the mid 20<sup>th</sup> century are Glick (1949), Gomori (1952), Danielli (1953), Lillie (1954), Eränko (1955) and Pearse (1953, 1961, 1968, 1980, 1985, 1991). These books only referred to the histochemical techniques, classifying these methods into several categories such as tissue processing, staining procedures for nucleic acids, proteins, carbohydrates, lipids, enzymes, fluorescence microscopy, radioautography, immunostaining, and so on. On the other hand, series of handbook in 27 volumes, edited by Graumann (partly with Neumann), appeared from 1958 to 1998 treating various topics including not only methods but also results, as well as another series of handbook on the progresses in histochemistry edited by Graumann (succeeded by Disse). In the 1960’s to 1990’s, many histochemists studied to develop new methodologies employing various principles and published innumerable original papers in various journals.

Since I started the career as anatomist and histologist in 1955, after graduating from a medical school in Japan, I first aimed at studying histochemistry and cytochemistry by developing new special techniques using various principles such as enzyme histochemistry (Nagata, 1956, 1974), microincineration (Nagata *et al.*, 1957), microspectrophotometry (Nagata, 1961a,b,c, 1966, 1972a), radioautography (Nagata, 1985, 1992), cryo-techniques (Nagata, 1994a) and X-ray microanalysis (Nagata, 1991, 2000d, 2003, 2004b). I had first concentrated to develop methodologies in the 1960’s to 1970’s. However, since these technologies were well developed in the 1970’s, then I had concentrated to apply these special histochemical and cytochemical techniques to various tissues and cells in men and other animals. The special histo- and cytochemical techniques are now well developed and systematized. At the present time many text books of histo- and cytochemistry are available, which deal with only the methodology, consisting of techniques for tissue processing and demonstrating chemical components in tissue sections. Such books should be regarded as the textbooks of general histochemistry and cytochemistry. Formerly, I had proposed to classify these methods into 3 categories, *i.e.*, chemical, physical and biological techniques (Nagata, 1995b, 1999b). Recently, the methodology has been well developed to form a new field, which should be designated as “general histo- and cytochemistry” similarly to general histology (Nagata, 1995b, 2001a). The term histochemistry and cytochemistry was sometimes used under different definitions, such as Lison (1936) who defined that histochemistry meant the methods *in situ* while cytochemistry meant the methods *extra situ*. However, we recently have usually used the term such as that histochemistry treats the tissue while cytochemistry treats the cell.

## 1.2. Classification of histochemical methods

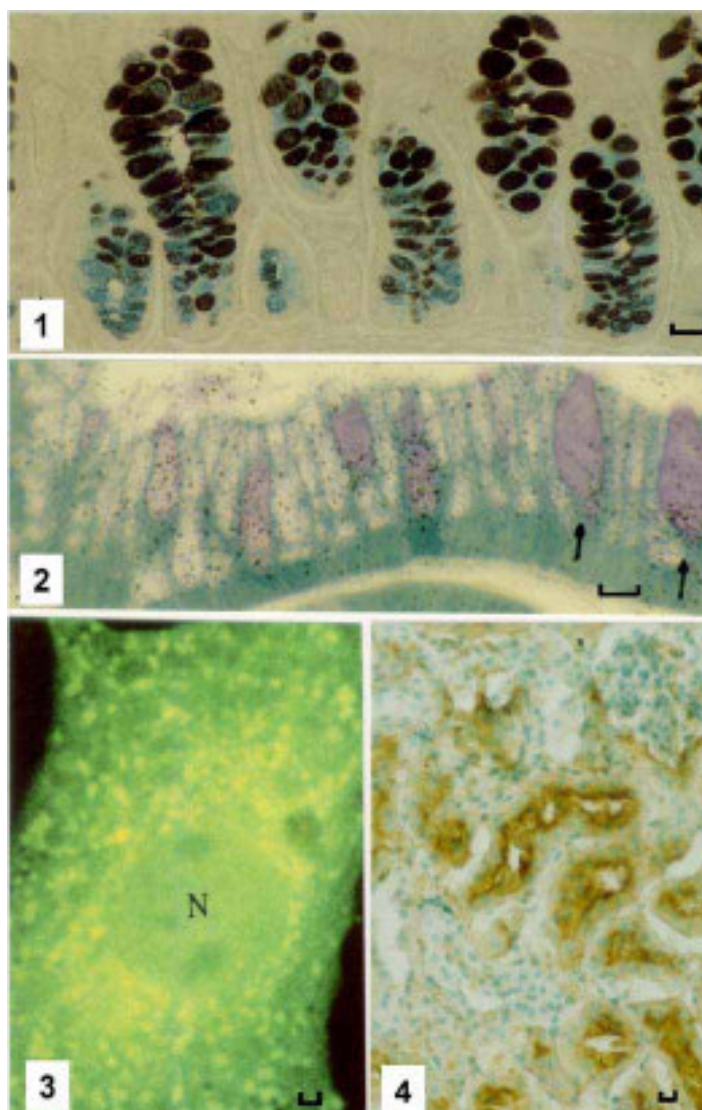
As mentioned above, I had formerly proposed to classify the histochemical techniques into 3 categories; chemical methods such as chemical reactions by staining (Fig. 1), physical methods such as radiations (Fig. 2) and biological methods such as immunity (Fig. 3) or affinity (Fig. 4), according to the principles used in the procedures (Nagata, 1995b, 1999b, 2001ab).

### 1.2.1. Chemical methods

The chemical methods in histochemistry consist of various chemical reactions, *e.g.* the historical color staining of DNA with Feulgen reaction. The principles and methods can be divided into two categories: color reactions for light microscopy and dense deposits for electron microscopy. The color reactions were first developed in histochemistry such as DNA Feulgen reaction, staining of proteins with Millon reactions, glucides with PAS reaction or HID-AB (Fig. 1), lipids with Sudan, and some enzymes such as alkaline and acid phosphatases. The bases of these chemical reactions are well understood. On the other hand, the electron dense deposits for electron microscopy such as PA-TCH-SP



method for glucides, PEI for glycoproteins or metal precipitation methods for enzymes were later developed.



Figures 1—4. Color reactions for light microscopy in general histochemistry. From Nagata (2001a). Permission from Academic Press. **Fig 1.** Chemical reaction. Light microscopic photograph of the colon of an adult mouse stained with HID-AB sequence. The goblet cells in the top region (upper half of the picture) of the crypts stained black with HID (high iron diamine), while the goblet cells in the deeper region (bottom) stained blue with AB (Alcian blue). x480. **Fig 2.** Physical reaction. Light microscopic radioautogram of the colon of a mouse injected with  $^{35}\text{SO}_4$ , fixed at 180 min., sectioned, radioautographed and stained with toluidine blue. Many black silver grains demonstrating radiosulfate incorporation can be seen over the apical portions of the mucous droplets in the 2 goblet cells (arrows) in the lower region of the colonic crypt (right) indicating rapid transfer, while the silver grains over the other 4 goblet cells (no arrow) show the localization over the whole mucous droplets indicating that they transferred slowly in the upper region of the colonic crypt (left). x1,200. Bar=5 $\mu\text{m}$ . **Fig 3.** Biological reaction. Fluorescence micrograph of a primary culture hepatocyte from a Wistar rat on a cover-slip was fixed and stained with FITC-labeled anti-catalase antibody for immunostaining, demonstrating the localization of catalase. The fluorescent particles disseminating in the cytoplasm, surrounding the nucleus (N), are peroxisomes including catalase. x3,500. Bar=1 $\mu\text{m}$ . **Fig 4.** Biological reaction. Light micrograph of an adult mouse kidney cortex, cryosectioned, stained with biotinylated Lotus lectin and ABC complex. The reaction products appear as dark brown deposits of DAB. The reaction products for Lotus were localized in the cytoplasm and the brush borders of proximal tubules of adult cortex. x 200. Bar=10 $\mu\text{m}$ .

### 1.2.2. Physical methods

The principles and methods using physical reactions consist of various physical reactions such as changes of temperature of specimens as microincineration or cryo-techniques, and effects of wavelength on absorption such as microspectrophotometry, fluorescence microscopy, confocal laser scanning microscopy, or utilization of radiation such as radioautography (Fig. 2) and X-ray microanalysis.

### 1.2.3. Biological methods

The biological methods in cytochemistry consist of mainly two biological reactions, which can be observed in living organism both plants and animals. The biological reaction was first introduced into cytochemistry by Coons *et al.* (1941), when they demonstrated the localization of proteins by the fluorescent antibody method using the immunity (Fig. 3). Later, the lectins obtained from plants were also introduced into cytochemistry as another biological reaction to demonstrate sugar residues of glycoproteins (Fig. 4).

### 1.2.4. Histochemistry: general and special

The details in respective three methods, *i.e.*, chemical, physical and biological methods will be described in details in sections 2.1., 2.2., 2.3., 2.4., 3.1., 3.2., 3.3., which should be designated as general histochemistry. On the other hand, the applications of these methods should be designated as special histochemistry and will be described at the end of this article in sub-sections of section 4.

## 2. Histological and Histochemical Techniques

Conventional histological and histochemical techniques, which we usually employ in this study, should be described briefly according to the procedures.

### 2.1. Animal treatment and tissue processing

Fundamental techniques dealing with the tissues and cell in histochemistry and cytochemistry are almost the same as in classical histology. All the small experimental animals, such as mice and rats, were anesthetized by intraperitoneal injections with such anesthetics as pentobarbital sodium (Nembutal, Abbott Laboratories, Chicago, Ill., USA) after any experiments and are sacrificed at given time either by decapitation or by perfusing via the left ventricles of the hearts with 2.5% glutaraldehyde in 0.1 M cacodylate buffer at pH 7.2, depending on whether insoluble or soluble compounds should be fixed. For conventional histochemistry, to demonstrate insoluble compounds the perfusion fixation can be used and the tissues from various organs were taken out, cut into small pieces (1 x 1 x 1 mm), soaked in the same glutaraldehyde fixative at 4°C for 1 h and postfixed in 1% osmium tetroxide in the same buffer for 1 h, dehydrated with graded ethanol and embedded in epoxy resin (Epon 812 or Epok 812, Oken Co., Tokyo, Japan). On the other hand, *in vitro* labeling of cultured cells and tissue blocks obtained from either animals or human biopsy materials were incubated in media containing any experimental drugs, using CO<sub>2</sub> incubator under normal conditions at 37°C for given time, usually 1 h or up to a few hours. They were then rinsed in Hanks' solution, fixed in the same buffered glutaraldehyde and osmium tetroxide solutions, dehydrated and embedded in epoxy resin as above.

For the soluble compounds, however, perfusion fixation cannot be used. The whole bodies of the small animals or organs and tissues taken out after decapitation without using any solution should be immediately cryo-fixed by either metal contact method or immersion method cooled with liquid nitrogen. Then, the frozen organs and tissues can be processed by cry-sectioning followed by freeze-drying. Otherwise, the frozen organs and tissues can be freeze-dried or freeze-substituted and embedded into epoxy resin.

Embedded tissues in epoxy resin can be used for either LMRAG or EMRAG. For LMRAG, thick sections at 2 µm are cut on an ultramicrotome and picked up onto clean glass slides and warmed for extension and drying. For electron microscopy, ultrathin sections of 100 nm thickness are cut in general using a conventional transmission electron microscope with the accelerating voltage at 100 kV. It is generally accepted that the thinner the section is the better the resolution, but the less the radioactivity

it contains and the longer the exposure time in case of radioautography. If any intermediate high voltage electron microscope is available at such accelerating voltages as 200, 300 or 400 kV, thicker sections at 200 or 300 nm thick can be used for observing such thicker sections. We prefer to use semithin sections at 200 nm thickness at 400 kV to shorten the exposure time in case of radioautography (Nagata, 2002). Semithin sections are cut on a Porter-Blum MT-2B ultramicrotome (Dupont-Sorvall, Newtown, CONN, USA). Ultramicrotomes of mechanical feeding type are preferable than thermal feeding type because of the accuracy of the section thickness, which effect on the number of silver grains by radioautography. Ultrathin or semithin sections are picked up onto either platinum or gold meshes to prevent the copper meshes from rusting through the histologic and radioautographic treatment especially by the development. Alternatively, collodion coated copper grid meshes can be used. For collodion coating, copper grid meshes (100-200 meshes) are soaked into 2% collodion solution for a few min, spread on a filter paper in a Petri dish and dried at 37°C for a few hours in an incubator.

## **2.2. Fixation of tissues and cells**

We have developed simple routine standard techniques to demonstrate insoluble compounds in various cells and tissues of experimental animals and to quantify the contents of synthesized macromolecules in each cell and cell organelle by both light and electron microscopy. The localization of silver grains developed by means of ordinary radioautography, however, demonstrates only the insoluble compounds such as radioactive substances such as DNA, RNA or proteins bound to the macromolecules fixed in the cell with the chemical fixatives used (Nagata, 2002). On the other hand, any soluble chemical compounds such as radioisotopes bound to the small molecules, which are not fixed with ordinary chemical fixatives, are washed away through conventional routine procedures such as fixation, dehydration, embedding, sectioning, and radioautographic procedures, so that these compounds cannot be demonstrated. Ordinary radioautographic procedures can be designated as wet-mounting radioautography, since the tissues are processed through both conventional wet treatments and applying wet radioautographic emulsions to the specimens. In order to demonstrate any soluble radioactive compounds, special techniques are required in accordance with the characteristics of the radioisotopes used for radioautography. The techniques for microscopic radioautography developed in our laboratory can be divided into 2 categories, *i.e.*, wet-mounting radioautography for insoluble compounds, such as macromolecular synthesis, and dry-mounting radioautography for soluble compounds, such as small molecular compounds.

### **2.2.1. Chemical fixation for insoluble compounds**

Small animals such as mice and rats are anesthetized and sacrificed either by decapitation or by perfusing via the left ventricles of the hearts with 2.5% glutaraldehyde in 0.1M cacodylate buffer at pH 7.2 and the tissues from various organs are taken out, cut into small pieces, soaked in the same glutaraldehyde fixative at 4°C for 1 h and postfixed in 1% osmium tetroxide in the same buffer for 1 h, dehydrated with graded ethanol and embedded in epoxy resin. On the other hand, cultured cell and tissue blocks, incubated in media containing any experimental compounds *in vitro*, using CO<sub>2</sub> incubator under normal conditions at 37°C for given times, are rinsed in Hanks' solution, fixed in the same buffered glutaraldehyde and osmium tetroxide solutions, dehydrated and embedded in epoxy resin as above. The tissue blocks are cut on an ultratome for either LM (2 µm thick) or EM (0.1-2 µm) and picked up onto either glass slides or grid meshes using water. In some cases, the whole mount cells on either glass coverslips or coated meshes *in vitro* are fixed, dried and used for conventional histochemistry to observe the whole cells without sectioning (Nagata, 2001b). In order to observe isolated cells obtained from the tissues *in vivo*, small tissue blocks are oscillated in Ranvier's alcohol and isolated, smeared on glass slides, fixed in Carnoy's fluid, and stained for histochemistry.

### **2.2.2. Chemical fixation for soluble compounds**

The techniques of histochemistry for soluble compounds can be theoretically classified into two categories from the viewpoint of fixation used. In the precipitation method, the soluble compound

is fixed in a mixture containing a substance which reacts with the soluble compounds forming a precipitation, so that the fixed tissues can be processed through routine histological procedures followed by a routine wet techniques. This principle was first used in detecting soluble  $^{45}\text{Ca}$  (Nagata & Shimamura, 1958, 1959a,b) in light microscopic radioautography of several tissues fixed in a formaldehyde solution containing ammonium oxalate to form calcium oxalate precipitation. This procedure, however, is limited to the soluble compounds which can be precipitated with any other specific compounds. Moreover, there are many possibilities of diffusion of the soluble compounds when they are precipitated with the fixatives.

### 2.2.3. Cryo-fixation for soluble compounds

By the freezing method, on the other hand, the tissues are quickly frozen in a cooled liquid such as isopentane or propane cooled to its melting point with liquid nitrogen. Then the tissues can be cut by cryo-microtomy. At the light microscopic level, the frozen tissues can be cut in a cryostat and the frozen sections are placed in contact with radioautographic emulsions by various methods in case of radioautography. At the light microscopic level, the frozen tissues can be cut in a cryostat at a thickness around 20-30  $\mu\text{m}$  and the frozen sections are placed in contact with radioautographic emulsions by various techniques. To demonstrate soluble small molecular compounds, cryo-fixation and dry-mounting radioautography should be routinely employed for both LM and EM radioautography.

After the tissues are taken out without using any solution from the experimental animals which had received injection of any experimental compounds, such as radioisotopes, they are trimmed as small as 1 x 0.5 x 0.5 mm with two pieces of razor blades on a cold plate cooled to 0°C with ice and water. The tissue blocks are attached to small pieces of aluminum foils, 5 x 5 mm in size (13) or directly onto the surface of a metal block. Cultured cells are centrifuged at 500 rpm for 10 min after incubation in the media containing radioactive compounds, and the pellet is placed on a piece of aluminum foils or metal blocks.

For fixing the tissues quickly by cryo-fixation, we soak the tissues into a quenching fluid which is cooled with a cooling agent. The quenching fluids we usually use are propane (melting point -169°C), isopentane (-161°C), or hexane (-94°C). These reagents are liquids at low temperatures and conduct heat very well. They also bubble when they contact tissues. Among them, propane is explosive, while hexane has a rather higher melting point. Therefore, isopentane is very often used. Instead of quenching fluids, a pure copper block is sometimes used in direct contact with the tissues. As cooling agents, the following substances or mixtures of two substances are generally used: liquid helium (boiling point -269°C), liquid nitrogen (196°C), liquid air (-190°C), dry ice and ether (-60°C), dry ice and nonane (53°C). Among these, liquid nitrogen is most frequently used. We usually use the combination of isopentane or propane as the quenching fluid and liquid nitrogen as the cooling agent, or a copper block as metal contact and liquid nitrogen as the cooling agent. Ready-made cryo-instruments such as RF-2 (Eiko, Tokyo, Japan), JFD-RFA (JEOL, Tokyo, Japan), cryoblock or cryovacublock (Reichert-Jung, Germany) are commercially available. Liquid nitrogen (200-300 ml) is carefully poured into a Dewar flask. A 50 ml beaker is placed in the liquid nitrogen, and 20-30 ml of isopentane or propane is poured into the beaker. We prefer isopentane to propane. Within a few minutes the liquid isopentane begins to solidify at its melting point of -160°C as it is cooled by the liquid nitrogen at -196°C. The tissue blocks or free cells adhering to a small piece of aluminum foil are plunged quickly into the isopentane with a pair of forceps. The frozen tissues are then removed from the isopentane, using a small cup, which is made with a piece of aluminum foil 3 cm x 3 cm in size, molded with a No. 00 gelatin capsule to prevent ice crystal formation, and transferred into liquid nitrogen in a Dewar flask, and stored under the liquid nitrogen until processing. In this process, if the tissues are exposed to the air, ice crystals will grow larger, and the fine structure will be damaged. The frozen tissues are then processed through freeze-drying or freeze-substitution (Nagata, 1972b). The frozen tissues are then removed from the isopentane, using a small cup, which is made with a piece of aluminum foil 3 cm x 3 cm in size, molded with a No. 00 gelatin capsule to prevent ice crystal formation, and transferred into liquid nitrogen in a Dewar flask, and stored under the liquid nitrogen until processing. In this process, if the tissues are exposed to the air, ice crystals will grow larger, and the fine structure will be damaged. The frozen tissues are then processed through freeze-drying or freeze-substitution procedures. In case of metal contact method, using cryo-



instruments, frozen tissues are removed from the copper blocks and stored in the liquid nitrogen as well.

## **2.3. Embedding and sectioning**

### **2.3.1. Cryo-sectioning without embedding**

The frozen tissues can directly be cut by cryo-sectioning without any embedding. The procedures for cryo-sectioning can be divided into two, light microscopic and electron microscopic cryo-sectioning.

For light microscopic cryo-sectioning, the frozen tissues can be cut in a cryostat at  $-80^{\circ}\text{C}$ , then the frozen sections are placed on glass slides. Various techniques were employed. We use the cryostat in a conventional bright room cutting cryo-sections and then they are coated with the emulsion in a darkroom with a large wire-loop method for radioautography. We use a conventional rotary type cryostat. The frozen tissues are transferred into a cryostat kept at around  $-30^{\circ}\text{C}$  and dry sections at  $20\text{--}30\text{ }\mu\text{m}$  are cut. They are transferred onto glass slides and either air-dried at room temperature or freeze-dried at  $-30^{\circ}\text{C}$  for a few hours.

For electron microscopic cryo-sectioning, the technique of ultrathin cryo-sectioning, or simply cryo-ultramicrotomy, was first reported by Bernhard and Leduc (1967) for radioautography. Then, it was improved by Tokuyasu (1973), employing preincubation in sucrose solution and picking up sections with sucrose droplets. For radioautography, however, his technique is not applicable because of the diffusion of radiolabeled compounds. We use LKB ultratomes 4800 equipped with an LKB cryokit 14800 or LKB-NOVA (LKB, Bromma, Sweden). Other types of any ultramicrotomes, such as DuPont-Sorvall or Reichert-Jung with cryokits, can also be used. The temperature of the specimens is usually set at  $-100^{\circ}\text{C}$  to  $-120^{\circ}\text{C}$  and that of the glass knives at  $-80^{\circ}\text{C}$  to  $-100^{\circ}\text{C}$ . The optimal temperature depends on the kind of tissues used. Dry sections are picked up with dry eyelash probes onto grids and covered with another grid as a sandwich and pressed with copper rods. Grids used for this purpose are coated with collodion applied by soaking copper grids in 1% collodion solution and dried at  $37^{\circ}\text{C}$  for 1 h. As controls, wet sections are picked up with sucrose droplets. Grids carrying dry sections are dried through freeze-drying at  $-50^{\circ}\text{C}$  for 24 h, like the freeze-drying procedure of tissue blocks as described above. Among the drying procedures tested, *i.e.* freeze-drying, freeze-substitution, and air-drying, the freeze-drying procedure was the best from the viewpoint of preservation of both cell structure and soluble compounds such as radioisotopes. In order to freeze-dry cryosections, we use a rotary cryotransfer apparatus. The rotary disc, which carries 5 grids with cryosections, is changed every 5 grid and transferred into a carrier, which consists of a tube and a cylinder which can contain 5 discs in its shelves, thus containing 25 grids. The carrier is transferred into the desiccator of the freeze-drying apparatus, which is operated for 3 h at  $-80^{\circ}\text{C}$ . After the cryosections are dried, they are coated with carbon and are processed through the dry-mounting radioautographic procedure. Recently, cryotransfer apparatuses are commercially available affiliated to respective cryo-kit equipped ultramicrotomes such as LKB, Sorvall or Reichert.

### **2.3.2. Freeze-drying and embedding**

The freeze-drying technique was first used by Altmann (1889, 1894), then was applied for light and electron microscopy by Gersh (1932, 1956). The freeze-drying apparatus we are using was designed and constructed in our laboratory (Nagata, *et al.*, 1969). It consists of a cold trap, a desiccator, which is set in the cold trap, three Geisler, discharge and ionization vacuum gauges, and two rotary and oil diffusion vacuum pumps. The cold trap consists of a stainless steel cylinder containing liquid nitrogen. The desiccator, which is set in the cold trap, has 96 sets of thermoelements which can be controlled with electric current at temperatures between  $-80^{\circ}\text{C}$  to  $+60^{\circ}\text{C}$ . The whole apparatus is capable of maintaining a pressure of less than  $10^{-6}$  Torr. A similar apparatus is now commercially available from several makers. The frozen tissues are transferred into the freeze-drying apparatus ladled with a small aluminum cup. The freeze-drying should be carried out at first with the operation of the rotary pump for about 1 h until the pressure reaches  $10^{-3}$  Torr. The two pumps (RP and DP) are then operated for about 24 h to complete drying, while the desiccator is kept at  $-80^{\circ}\text{C}$ . After the completion of freeze-drying, the temperature over several hours by changing the electric current of thermoelement, so that the whole drying procedure

takes about 30 h in case of tissue blocks. In case of cryo-sections on grids, however, freeze-drying for only 12 h is enough. Before completion of the procedure, the epoxy embedding mixture is placed in the dripping unit which should be evacuated for 10 min by means of another rotary pump at a pressure of 10-3 Torr. After completion of drying, the embedding medium, epoxy resin mixture, is dripped down into the specimen chamber, the tissues are infiltrated and the two pumps are stopped. When the drying procedure is completed, the tissues adhering to aluminum foil will sink in the embedding medium. Fixation is not required before the embedding, although Pearse (1953) maintains that the unfixed freeze-dried tissues are easily damaged. In case when fixation is preferable before embedding, in order to enhance contrast, freeze-dried tissues can be exposed to osmium vapor for 30 min in a tight jar containing a small piece of osmium tetroxide crystal. Freeze-dried tissues are taken out and infiltrated with fresh embedding medium overnight at room temperature, and polymerized at 35°C, 45°C and 60°C for 12 h each. When cultured cells or cryo-sections on grids are freeze-dried, no embedding is necessary. The cultured cells freeze-dried on grids are processed directly through radioautography and can be observed by high voltage electron microscopy (Nagata, 2002).

### **2.3.3. Freeze-substitution and embedding**

The technique of freeze-substitution or freeze-thawing was first applied to light microscopy and developed by Lison (1936). At the electron microscopic level, several papers describing the morphology of freeze-substituted cells have been later published. The principle of freeze-substitution is to dehydrate the frozen tissues in a solvent at a very low temperature without thawing the tissues, and substitute the ice with the solvent. The usual solvents are acetone, ethanol or ether. The coolants used are dry ice-acetone mixture (-78°C) or dry ice-ethanol (-78°C). We applied this principle to radioautography for the first time (Nagata, *et al.*, 1969). The routine procedure is as follows: 1) Dry ice and acetone are mixed in a Dewar flask; 2) A small test tube or sample tube containing 20-30 ml of absolute acetone is put in the Dewar flask and cooled to -78°C; 3) Tissues are frozen according to the procedure described above in liquid nitrogen, and transferred with aluminum foil cups into the test tube containing absolute acetone; 4) The transferred tissues are kept in the substituting fluid for 72 h to substitute the ice with the solvent. The present authors use a deep freezer (Tabai, Tokyo, Japan) in which the Dewar flask is stored and the temperature is kept at -80°C; 5) After the substitution is completed, the temperature is gradually raised to 20°C over several hours. The tissues are transferred into Epon/ acetone mixture, then processed through Epon mixture and polymerized. In general, it is useful to use cryoprotective agents such as glycerin, DMSO, or sucrose in order to reduce the ice crystal formation artifacts. However, for the purpose of demonstrating soluble radioactive compounds by means of radioautography, it is preferable not to employ such techniques. Recently, freeze-substitution instruments such as CS-auto (Reichert-Jung, Germany) are commercially available which can be controlled automatically.

### **2.3.4. Dry sectioning of freeze-dried or freeze-substituted materials**

The embedded tissues after freeze-drying or freeze-substitution should be cut dry without using any water. We usually cut dry sections from epoxy resin embedded tissues for both light and electron microscopy without water. By sectioning the Epon or Epok blocks of freeze-dried or freeze-substituted tissues, it is necessary to cut sections without using water in the knife trough in order to prevent diffusion artifact of labeled soluble compounds. Complete dry sectioning without any liquid is very difficult in expanding dry sections. It is also difficult to pick them up onto glass slides or grid meshes. Among many knife trough liquids which we tested, ethylene glycol was the best for flotation and expansion of the dry sections (Nagata *et al.*, 1969, 1984b, 2000b). It wets the glass knife to the very edge but does not wet the plastic sections. It does not resolve soluble labeled compounds. Sections are not so easily expanded on ethylene glycol as on water, but can be expanded when they are warmed with a tungsten lamp for a few minutes. They are picked up onto collodion coated glass slides or 150 mesh grids. We use glass slides or grids which are previously coated with collodion by dipping them into 1% collodion solution and drying them at 37°C for 1 h.

## **2.4. Observation of histochemical specimens by microscopy**

After the specimens are processed through various procedures as described the specimens stained and observed by light or electron microscopy.

### **2.4.1. Light microscopy**

Light microscopic specimens are observed by either conventional transmission light microscopy or dark field incident light microscopy or ultraviolet light microscopy depending upon the histochemical reactions. By the conventional microscopy, histochemical color reactions appear with the background sections, so that the localization of the histochemical reaction is clear but sometimes confusing with densely stained structures such as secretory granules. By ultraviolet light microscopy, fluorescent staining such as immuno-staining can be recognized. On the other hand, by the dark field incident light microscopy, silver grains by radioautography or inorganic substances by microincineration appear as bright specks over the dark sections like stars in the dark sky, so that we can recognize the silver grains but can not observe the sections well. In this case, stainings are not necessary. Either method has its advantages and disadvantages. It depends on the preference of each scientist.

### **2.4.2. Electron microscopy**

Electron microscopy can usually be carried out with conventional transmission electron microscopes with standard voltage around 100 kV. However, we prefer to use such intermediate high voltage electron microscopes as accelerating voltages at 200, 300 or 400 kV when available for obtaining better contrast between the histochemical reactions such as silver grains or immuno-gold staining and the cell structures as well as better transmittance through thicker specimens especially by radioautography when we use thicker sections containing much more RI-labeled compounds. We use either a Hitachi H-700 electron microscope at 200 kV or a JEOL JEM-4000EX electron microscope at 300 or 400 kV in our laboratory (Nagata, 2002).

### **2.4.3. Image analysis of histochemical reactions**

To analyze these histochemical reactions quantitatively, we can make use of various kinds of image analyzers now commercially available (Nagata, 1993). For example, the number of labeled nuclei per total cell populations labeled with  $^3\text{H}$ -thymidine by radioautography for calculating the labeling index, or the number of silver grains per cell body or per unit area labeled with other macromolecular precursors for calculating the relative incorporation rates are measured and calculated. On the other hand, direct quantification of silver grains on EMRAG is possible by using energy dispersive X-ray microanalyzers equipped with intermediate high voltage electron microscopes with either STEM or TEM modes (Nagata, 2004a,b,c).

## **3. Histochemical Methodology - General Histochemistry**

### **3.1. Chemical methods in histochemistry**

The chemical methods in histochemistry consist of various chemical reactions such as the historical staining of DNA with Feulgen reaction, staining of proteins with Millon reactions, glucides with PAS reaction or HID-AB (Fig. 1), lipids with Sudan and some enzymes. The bases of these chemical reactions are well understood. The principles and methods can be divided into two categories, color reactions for light microscopy and dense deposits for electron microscopy.

#### **3.1.1. Color reactions for light microscopy**

Various kinds of color reactions for demonstrating various substances have been developed. Among of them, we mainly used such color reactions whose intensities and absorbances are parallel with the concentrations of the substances for applying them to microspectrophotometry when we prefer to quantitate such color reactions (Nagata, 1972a). The methods which we used in histochemistry will be briefly described (Figs. 1-4).

- **Nucleic acids.** The most specific chemical reaction for nucleic acids well-known in histochemistry should be the reaction of Feulgen (1924). This reaction depends on the hydrolysis by hydrochloric acid of the purine-desoxypentose linkage of the DNA in nuclear chromatin resulting in aldehyde, which is colored purple by Schiff's reagent. Since the color density and the absorption of this reaction were first shown by Widström (1928) to be parallel with the DNA contents of respective cells, it was used for microspectrophotometry. We used a modified Feulgen reaction for quantification of DNA in various cell nuclei (Nagata, 1966a, 1972a).
- **Proteins.** Proteins consist of polypeptides. Total proteins consisting of various amino acids can be stained with such color reactions as mercuric bromphenol blue or naphthol yellow S. On the other hands, some basic proteins are stained with Fast green and gallocyanine chrome alum, or only some amino acids in proteins can be stained with specific dyes such as tryptophane and tyrosin with Millon reactions, tyrosin with diazotization-coupling, tryptophane with p-dimethylaminobenzaldehyde-nitrite, arginin with Sakaguchi reaction. These color reactions for proteins can also be utilized for quantitative studies by microspectrophotometry (Nagata, 1966a, 1972a).
- **Glucides.** Glucides are classified into several categories, monosaccharides, disaccharides, oligosaccharides and polysaccharides. Several procedures for demonstrating glucides with color reactions based on the periodic acid-Schiff (PAS) reaction are available. The theory of the reaction is based on the fact that aqueous periodic acid oxidizes 1,2 glycol groups in cells which consist of carbohydrates, to produce aldehydes which are colored by Schiff's reagent, basic fuchsin. Among of the modified procedures, we formerly used PAS reaction for microspectrophotometry. We also used PAS-AB or HID-AB (high iron diamine-alcian blue) sequence to differentiate mucosubstances in the goblet cells in the intestines (Nagata & Kawahara, 1999). The HID-AB sequence is considered to differentiate black stained sulfated complex carbohydrate from blue stained carboxylated mucosubstance lacking sulfate esters (Fig. 1).
- **Lipids.** Lipids are insoluble in water and extracted from cells by only fat solvents. They consist of fatty acids and alcohols and can be classified into simple lipid esters and compounds lipids. The old and common procedures for demonstrating simple lipid droplets in cells are fat-soluble Sudan dyes, which were discovered by Daddi (1896). Later Lillie (1944) developed this method in pathology. We used either Sudan III or Sudan black in 70% alcohol for staining.
- **Enzymes.** It is well known that the recent development of histo- and cytochemistry began from enzyme histochemistry when Takamatsu (1938, 1939) and Gomori (1939) found the principle for demonstrating alkaline phosphatase activity independently by hydrolyzing the substrate with the enzyme activity and producing lead precipitation colored black with sulfide. Then, varieties of techniques for demonstrating various enzymes have been developed in 1950-1960's so extensively that Pearse (1953) described in his famous textbook, "Although a few years ago only 2 or 3 enzymes could be demonstrated in the tissues by histochemical means, there are now techniques for at least 18," but after 5 years he (Pearse, 1953) amended the description to "for at least 45." Now in early 21<sup>st</sup> C, this sentence must be amended to read "for at least 200," employing several principles resulting in color reactions such as, metal precipitation, azo-dyes, tetrazolium salts, and DAB osmium. Since around 2,100 enzymes were registered by the Enzyme Committee of the International Union of Biochemistry (1979), the number of enzymes demonstrable cytochemically is too small. Among them, we developed and studied several enzymes such as cytochrome oxidase (Nagata, 1956), urate oxidase (Yokota & Nagata, 1973, 1977), catalase (Yokota & Nagata, 1974), acid and alkaline phosphatase, non-specific esterase (Nagata & Murata, 1980), arylsulfatase (Murata *et al.*, 1975), lipase (Fig. 5) (Nagata, 1974) and phospholipase (Nagata & Iwadare, 1984).
- **Pigments.** Several pigments can be found in various cells and tissues, such as melanin, lipofuscin, ceroids, hemoglobin, hemosiderin, bilirubin etc. Among them, we studied the localization of melanin and its precursors in the skin by argentaffine reaction (Nagata *et al.*, 1957a).



- **Inorganic Substances.** Varieties of methods for demonstrating inorganic elements, especially metals, by color reactions have been developed since many years. The color reaction produced by union of a dye with a metal or metal salt is called as lake-formation. Numerous techniques exist for the demonstration of metals such as iron, copper, gold, silver, mercury, lead, nickel, aluminum, zinc etc. Among them, color reactions for inorganic iron were frequently used such as Prussian blue or Turnbull blue. However, the specificities of these techniques were mostly unsatisfactory. We have not tried these color reactions so much. On the contrary, we employed only physical techniques, micro-incineration (Nagata *et al.*, 1957b) (Figs. 6, 7) and radioautography (Nagata *et al.*, 1977b) for demonstration of inorganic substances.

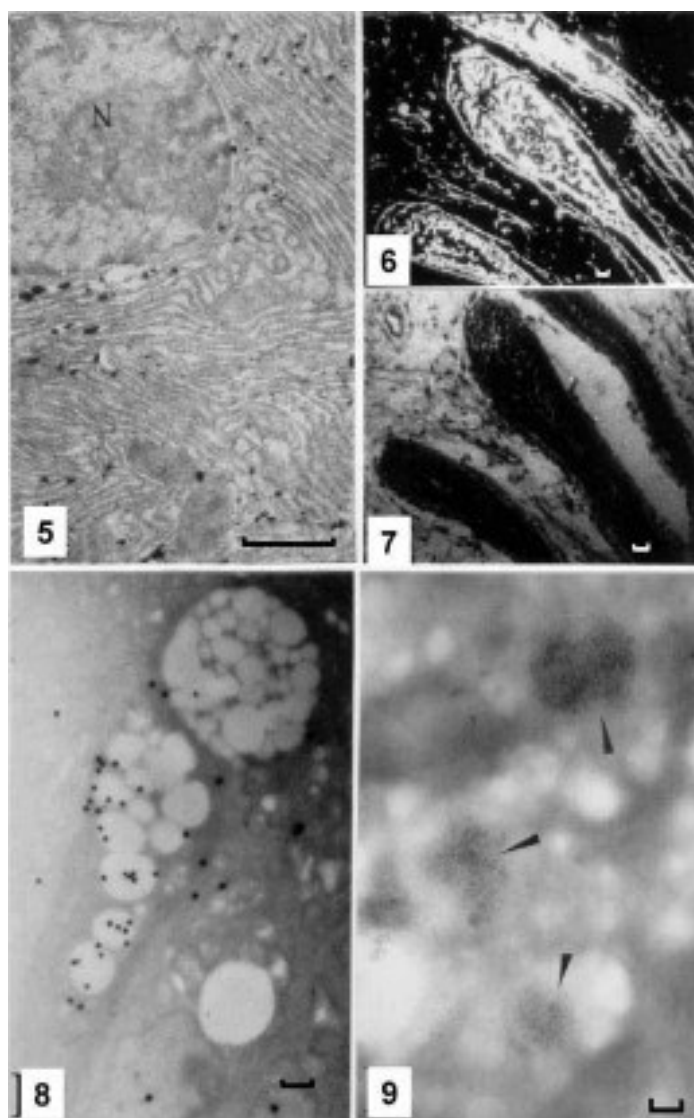
### 3.1.2. Electron dense deposits for electron microscopy

When electron microscopes were developed and applied to biology in 1950's, the histologists and pathologists observed thin sections obtained from tissues and cells after electron staining with uranium and lead to increase contrast in specimens. Later, histochemists who studied localization of chemical components in tissues and cells started to use electron microscopy for localizing *in situ* chemical reactions in 1960's by producing electron dense deposits at cell organelle levels. Such field of study on subcellular localization of chemical components of cells was designated as electron microscopic cytochemistry or ultracytochemistry. Various kinds of enzyme activities were first demonstrated by means of the similar techniques used for light microscopy resulting in metal precipitation such as lead deposits for acid phosphatase. Other metal deposits, such as copper, gold, barium, cerium, cadmium, strontium were also used for demonstration of various enzyme activities. Then, electron dense macromolecules produced by azo dyes and tetrazolium salts were used for enzyme cytochemistry. Likewise, varieties of macromolecules, *i.e.* DNA, RNA, proteins, glucides, lipids and amines were lately demonstrated by labeling with electron dense deposits, for example using enzyme-gold complex localizing DNA and RNA. Among of these techniques we developed and applied several methods for both macromolecules, PEI for glycoproteins (Duan & Nagata, 1993) and PA-TCH-SP for glucides (Nagata, 2000c), as well as enzymes, such as lipase (Nagata, 1974) (Fig. 1), phospholipase (Nagata & Iwadare, 1984), catalase (Yokota & Nagata, 1974) and urate oxidase (Yokota & Nagata, 1973, 1977).

- **PA-TCH-SP for glucides.** Typical glucides such as glycogen particles contained in various cells can be demonstrated by PAS color reaction at light microscopic level as well as several techniques resulting electron dense deposits at electron microscopic level, specific for vicinal hydroxyl groups in glycogen with periodic acid-thiocarbohydroazide-silver proteinate method (Thiéry, 1967). We improved this method (PA-TCH-SP) and found it to be the most suitable from the viewpoints of reaction specificity, reproducibility, sufficiency of electron density (Murata *et al.*, 1977a,b). After the staining, fine electron dense reaction products were observed in the cytoplasm of the megakaryocytes and blood platelets of rabbits as well as in the mucous granules in the goblet cells in mouse colonic epithelium (Nagata, 2000c).

- **PEI for glycoproteins.** Polyethyleneimine (PEI) stains anionic sites of proteoglycans in various tissues (Sauren *et al.*, 1991). We improved the staining methods and the PEI binding sites in the glomerular extracellular matrices of mouse kidney (Duan & Nagata, 1993) and the hyaline cartilage of mouse trachea (Li *et al.*, 1994) were demonstrated.

- **Enzyme cytochemistry.** The techniques for demonstrating enzyme activity at the light microscopic level were extensively developed in 1950's to 1970's. Then, the techniques for demonstrating enzyme activity at the electron microscopic level, producing electron dense deposits, followed. The principle for demonstrating enzyme activity employs several procedures to produce electron dense deposits such as, metal precipitation, azo-dyes, tetrazolium salts, and DAB osmium. Among them, we developed and studied several enzymes such as cytochrome oxidase (Nagata, 1956), urate oxidase (Yokota & Nagata, 1973, 1977), catalase (Yokota & Nagata, 1974), non-specific esterase (Nagata & Murata, 1980), arylsulfatase (Murata *et al.*, 1975), lipase (Nagata, 1974) (Fig. 5) and phospholipase (Nagata & Iwadare, 1984). Other enzyme activities such as DAB reaction for peroxisomes, glucose-6-phosphatase (G-6-Pase) activity for endoplasmic reticulum, thiamine pyrophosphatase (TPPase)



Figures 5-9. Black and white reactions either electron dense deposits for electron microscopy and spodogram for light microscopy in general histochemistry. From Nagata (2001a), Permission from Academic Press. **Fig 5.** Electron micrograph showing lipase activity in pancreatic acinar cells of an adult mouse. The pancreatic tissue was prefixed in buffered glutaraldehyde, incubated in a medium for lipase, postfixed in buffered osmium tetroxide, embedded, sectioned and observed by electron microscopy. Electron dense deposits which demonstrate lipase activity are localized in endoplasmic reticulum. x15,000. Bar=1 $\mu$ m. **Fig 6.** Dark field light micrograph of a dog skin tissue, fixed in ethanol formalin, dehydrated, embedded in paraffin, sectioned, heated at 600°C in an oven and observed by dark field microscopy. The white figures demonstrate spodogram of inorganic substances, mainly calcium, in the hair follicles. x 200. Bar=10 $\mu$ m. **Fig 7.** A control serial section of the same tissue as in Fig. 6, but stained with H-E. Compare with Fig. 6. The white structure in Fig. 6 corresponds to the hair follicles in Fig. 7. x200. Bar=10 $\mu$ m. **Fig 8.** Electron radioautogram of a goblet cell in the deeper crypt of the colonic epithelium of an adult mouse after injection with  $^{35}\text{SO}_4$ , fixed at 30 min., sectioned and radioautographed and observed by electron microscopy. Many electron dense silver grains are localized over the Golgi zone and mucous droplets in the goblet, demonstrating incorporation of radiosulfate into sulfomucins. x 4,800. Bar=1 $\mu$ m. **Fig 9.** Electron micrograph of a mouse liver, prefixed in glutaraldehyde, rapidly frozen, cryosectioned with a cryo-ultramicrotome, immunostained with ferritin-anti-urate oxidase conjugate and stained negatively with phosphotungstic acid. Electron dense ferritin particles are seen in peroxisomes in the hepatocyte. x 52,000. Bar=0.1 $\mu$ m.

activity, acid phosphatase activity (AcPase) for lysosomes, cytochrome oxidase activity for mitochondria and ZIO reaction for Golgi apparatus were also employed to demonstrate these marker enzymes in respective cell organelles for 3-dimensional observation of cell organelles in thick specimens by high voltage electron microscopy (Nagata, 1995c, 1997b, 1999a, 2000a).

### 3.2. Physical methods in histochemistry

The principles and methods using physical reactions consist of various physical reactions such changes of temperature of specimens as microincineration at high temperatures or cryo-techniques at low temperatures, and effects of light wave-length on absorption such as microspectrophotometry, fluorescence microscopy, confocal laser scanning microscopy, or utilization of radiation such as radioautography and X-ray microanalysis (Nagata, 1994a).

#### 3.2.1. Methods using high or low temperatures

For preparing histochemical specimens, both very high temperatures at several hundreds degree C and very low temperatures at below minus 100°C are employed.

- **microincineration.** Since most cells and tissues, except the bones and the teeth, consist mostly of organic compounds the technique of microincineration was first developed to study the inorganic components, mainly the metals, in various cells many years ago (Raspail, 1830). Lately, the routine technique was established by Scott and Horning (1953). We studied the inorganic elements in the skin using microincineration modifying Scott technique, by fixing tissues in a mixture of absolute ethanol and neutral formalin, dehydrating, embedding in paraffin, sectioning, and the slides carrying sections were heated to 600°C in an oven, and observed by dark field microscopy (Nagata *et al.*, 1957b). By the dark field light microscopy, the spodograms consisting of the inorganic substances such as calcium or magnesium appear as bright specks over the dark sections like stars in the dark sky (Fig. 6), so that we can recognize the inorganic substances but cannot observe the sections well. In such cases stainings for the control serial sections are necessary and can separately be observed by conventional microscopy. (Fig. 7).
- **cryo-techniques.** The cryo-techniques applied to cytochemistry consist of 3 techniques, cryo-fixation followed by cryo-sectioning, freeze-drying and freeze-substitution. Varieties of combination of these procedures were successfully utilized for cytochemistry to prevent loss of soluble compounds in cells, displacement of cell constituents by diffusion and denaturation of chemical components especially of enzymes. Historically the cryo-technique to fix and freeze-dry tissues was first introduced by Altmann (1889, 1894). The procedure was later improved by Gersh (1932) for light microscopy and then for electron microscopy (Gersh, 1956). We used these techniques by designing freeze-drying apparatuses (Nawa *et al.*, 1965, 1969) and applied for both radioautography demonstrating soluble radio-labeled compounds (Nagata *et al.*, 1969; Nagata, 1972b, 1994a,b; Nagata & Murata, 1977) and enzyme cytochemistry (Yokota & Nagata, 1973, 1974, 1977) by electron microscopy.

#### 3.2.2. Methods using lights with different wave lengths

In cytochemistry both visible and invisible lights with various wave lengths from ultraviolet rays to ultrared rays were employed by light microscopy. Ultraviolet rays were used to observe the absorption bands of both DNA and RNA, while visible rays at definite wavelengths were used for microspectrophotometry of different color reactions. We used microspectrophotometry using both invisible ultraviolet rays and visible spectrum (Nagata, 1966, 1972a).

- **ultraviolet rays.** Using ultraviolet rays, we could measure the nucleic acid contents in respective cells (Nagata, 1966a, 1972a). The DNA and RNA which contain purin and pyrimidine have the absorption band in the wave length of 260 mμ. Since the absorption is proportional to the concentration of the nucleic acids when measured by using this wave length, the content of each cell before fixation can be determined. However, only the total sum of both DNA and RNA was obtained. By using fixed cells, DNA and RNA could be measured separately by

removing either DNA or RNA with DNase or RNase. However, this method is not used at present because errors could be caused during the extraction of DNA or RNA.

- **microspectrophotometry.** Microspectrophotometry was originally developed by Caspersson (1936) and widely used to measure the contents of nucleic acids of various cells. We used an Olympus single-beam microspectrophotometer Model MSP-A-IV (Nagata, 1966). The procedure for measuring the contents of various cytochemical compounds in the cells is based on the same principle as ordinary spectrophotometry using different wave-lengths, both visible and invisible ultraviolet rays, depending upon the chemical components we measured. As visible rays we used 560 nm for DNA stained with Feulgen reaction, 650 nm for RNA stained with Azur B, 585 nm for RNA stained with cresyl violet, 435 nm for total proteins stained with Naphthol yellow S, 610 nm for total proteins stained with mercuric bromphenol blue, 635 nm for basic proteins stained with fast green, 500 nm for basic proteins stained with gallocyanine chromalum, 500 nm for tyrosin and tryptophane stained with Millon reaction, 520 nm for tyrosin stained with diazotization-coupling, 625 nm for tryptophane stained with p-dimethyl-aminobenzaldehyde-nitrite reaction, 520 nm for arginine stained with Sakaguchi reaction and 560 nm for glucides stained with PAS reaction. Some of the enzyme reactions could also be measured using absorptions at different wave-lengths (Nagata, 1961a,b,c, 1972a).

### 3.2.3. Methods using radiations

The radiations due to electromagnetic waves can physically be divided into 4, alfa-rays, beta-rays, gamma-rays and X-rays according to the wave-length from short to long length. Three methods were employed using radiations in cytochemistry, *i.e.*, microradiography, microradioautography and X-ray microanalysis.

- **microradiography.** Microradiography is a technique to observe the picture of small tissue specimens penetrated by radiation from soft X-rays resulting in negative images such as chest X-ray films. The small X-ray films are observed by light microscopy. In cytochemistry, microradiography is used to observe hard tissues such as the bone and the teeth, penetrated by soft X-rays resulting in negative images. We used microradioautography to observe the sliced bone tissues (Nagata, 1995b). By this procedure differences of mineralization in tissue sections can be observed by light microscopy.

- **radioautography.** Radioautography is a technique to demonstrate the patterns of localization of radioactive substances in various specimens incorporating radioactive compounds. The radioautograms can be observed by both light and electron microscopy (Figs. 2, 8). The specimen which consists of tissues and cells in contact with the photographic emulsion containing developed silver grains is called radioautograph, while the pattern of silver grains on the radioautograph is called radioautogram and the procedure to produce radioautographs is designated as radioautography. Radioautograph is the autograph produced by radiation. Autograph is a positive picture made by itself. Therefore, the term radioautogram means etymologically the positive picture produced by radiation which is emitted from the object itself resulting in autogram. To the contrary, autoradiograph consists of auto and radiograph. The suffix auto means automatic, while the term radiograph means the picture of the object which is penetrated by rays resulting in negative images such as microradiogram or chest X-ray films. Thus, autoradiograph etymologically means a negative picture of the specimen produced automatically with radiation emitted from another radiation source away from the specimens (Nagata, 1992, 1994c,d, 2002). However, it is now accepted that the both terms, radioautography and autoradiography, are considered to be the synonyms. I had advocated a new concept, named "radioautographology." This new term is the coinage synthesized from radioautography and ology, expressing a new science derived from radioautography. The concept of radioautographology is a science to localize the radioactive substances in the structure of the objects and to analyze and to study the significance of these substances in the structure (Nagata, 1998a,b, 2002). The science, radioautographology, can be divided into 2 parts, general



radioautographology and special radioautographology. The former deals with the principle and techniques of radioautography, while the latter deals with the application of radiography to various materials (Nagata, 1998b, 2002). General radioautographology is the technology including all the natural sciences to produce the specimens, which contain radioactive compounds, procedures for tissue preparations and the methods to make tissues contact with the photographic emulsions and to give exposure for a certain period of time to produce the latent images of the radioactive substances in the specimens, then to develop the emulsion to produce the silver metal grains, thus enabling to compare both the specimens and radioautograms in order to learn the localization of radioactive substances in the specimens. We developed the technologies for light and electron microscopic radioautography (Nagata, 1998a) and applied them to cell biology and cytochemistry (Nagata, 1991, 1992, 1994c,d, 1996a,b, 1997a, 1998b, 2002). General radioautographology is the technology including all the natural sciences to prepare the specimens, which contain radioactive compounds, procedures for tissue preparations and the methods to make tissues contact with the photographic emulsions and to give exposure for a certain period of time to produce the latent images of the radioactive substances in the specimens, then to develop the emulsion to produce the silver metal grains, thus enabling to compare both the specimens and radioautograms in order to learn the localization of radioactive substances in the specimens. The radioactive compounds used in radioautography are mainly composed of inorganic or organic compounds which are artificially labeled with radio-isotopes (RI) and can be incorporated into human or animal bodies by experiments. The radioactivity emitted from the radioactive isotopes are divided into 3 kinds of rays, *i.e.*, alpha, beta and gamma rays. Among these 3 rays, the beta ray is the best for radioautography because of its shorter range and the strongest ionization. For radioautography various kinds of RIs are used. Among them,  $^3\text{H}$ ,  $^{14}\text{C}$ ,  $^{35}\text{S}$  and  $^{125}\text{I}$  are very often utilized because they can be labeled to various inorganic compounds which are usually used in biological and medical researches. The RI-labeled compounds used for radioautography can be classified into 2 categories, *i.e.*, the precursors which are incorporated into macromolecules such as nucleic acids (DNA and RNA), proteins, glucides and lipids, and the other target tracers which are small molecular compounds such as hormones, neurotransmitters, vitamins, inorganic substances, drugs and others. The macromolecular syntheses are labeled with  $^3\text{H}$ -thymidine (for DNA),  $^3\text{H}$ -uridine (for RNA) amino acids such as  $^3\text{H}$ -glycine or  $^3\text{H}$ -leucine (for proteins),  $^3\text{H}$ -glucose or  $^{35}\text{SO}_4$  (for glucides) and  $^3\text{H}$ -glycerol or  $^3\text{H}$ -fatty acids (for lipids). Embedded tissues can be used for either light or electron microscopy. For light microscopy thick sections at 2  $\mu\text{m}$  are cut, while ultrathin sections at 100 nm thickness are cut for conventional transmission electron microscope with the accelerating voltage at 100 kV. It is generally accepted that the thinner the section is the better the resolution, but the less the radioactivity it contains and the longer the exposure time for radioautography. We prefer to use semithin sections at 200 nm thickness by observing with high voltage electron microscopy at 400 kV in order to shorten the exposure time (Nagata, 1998a). We have developed simple routine standard techniques to demonstrate both soluble and insoluble compounds in various cells and tissues of experimental animals and to quantify the contents of synthesized macromolecules in each cell and cell organelle by both light and electron microscopy. The techniques for microscopic radioautography developed in our laboratory can be divided into 2 categories, *i.e.*, wet-mounting radioautography for insoluble compounds such as macromolecular synthesis and dry-mounting radioautography for soluble compounds such as small molecular compounds using cryo-techniques such as cryo-fixation, cryo-sectioning, freeze-drying, freeze-substitution (Nagata, 1992, 1994b, 1996b, 1998b).

- **x-ray microanalysis.** X-ray microanalysis is carried out by means of analytical electron microscopes which consist of scanning or transmission electron microscopes equipped with X-ray analyzers. To analyze trace elements in small biological specimens, electron beams (with diameters 5-100 nm) are irradiated at a small spot (with diameters 5-100 nm) and the emitted X-rays are analyzed with either energy dispersive X-ray analyzer (EDX) or wave-dispersive X-ray analyzer (WDX). To analyze the elements in biological specimens, EDX is usually preferred to WDX because all the elements can be detected by EDX. We used transmission analytical

electron microscopes equipped with X-ray microanalyzers, *i.e.*, Hitachi H-700 with EMAX-1800E (Horiba, Kyoto, Japan), JEOL JEM 200CX with Kevex 7000-77 (Kevex, U.K.), and JEOL GEM-4000EX with TN-5400 (Tracor-Northern, Middleton, USA) at accelerating voltages from 100 kV to 400 kV. X-ray microanalysis is an excellent method to qualify and quantify basic elements in biological specimens. We quantified the end products of cytochemical reactions such as Ag in radioautograms or Ce in phosphatase activity or endogenous trace elements such as Zn, Ca, S and Al which originally exist in karyoplasm, cytoplasm or cell organelles of various cells and intracellular matrix after conventional chemical fixation or cryo-fixation. From our results, it was shown that X-ray microanalysis using intermediate high voltage transmission electron microscopy at 300 or 400 kV was very useful resulting in high P/B ratios for quantifying these trace elements in biological specimens (Kametani & Nagata, 2005, 2006, 2007; Nagata, 1991, 1993, 2000d, 2004b; , Kametani 2002).

### 3.3. Biological methods in histochemistry

The biological methods in cytochemistry employ the biological reactions which can be observed in living organism both plants and animals. They were later developed than the chemical and physical methods. The biological reaction was first introduced into cytochemistry by Coons *et al.* (1941), when they demonstrated the localization of proteins by the fluorescent antibody method. Later, the lectins obtained from plants were also introduced into cytochemistry as another biological reaction to demonstrate sugar residues of glycoproteins (Sharon & Lis, 1972). We used both techniques to demonstrate proteins and glycoproteins.

#### 3.3.1. Immunohistochemistry

Coons *et al.* (1941) first demonstrated the localization of proteins by the fluorescent antibody method making use of the very high specificity of immune reactions of animals producing antibody in the localization of antigenic proteins. Then, various techniques have been developed by many scientists to label and visualize the localization of antigenic proteins at both light and electron microscopic levels using such markers as fluorochrome (FITC, RITC) and enzymes (HRP) for light microscopy (Fig. 3) and metals (ferritin or colloidal gold particles) for electron microscopy (Fig. 9). Among these techniques, we made use of immunofluorescence and PAP techniques (Usuda & Nagata, 1991) for light microscopy and developed immunoferritin and immunogold techniques for localizing some enzymes for electron microscopy (Yokota & Nagata, 1973, 1974, 1977; Usuda & Nagata, 1991; Usuda *et al.*, 1991a,b,c, 1994, 1995, 1996).

- **fluorescence or color staining for light microscopy.** We first used to label the antibodies with fluorochromes such as FITC (fluorescein iso-thiocyanate) to localize the antigens in cultured cells. Some cell strains cultured on cover slips from experimental animals such as hepatocytes from Wister rats or primary cultures of human biopsies materials such as thyroid cancer tissues were fixed in absolute acetone and stained with FITC-labeled antibodies such as anti-catalase, a peroxisomal enzyme, or anti-keratin and vimentin with anti-rabbit IgG. The antibody localization was observed by fluorescence microscopy (Fig. 3). Then, we used a modified technique of PAP (peroxidase-anti-peroxidase) method by Sternberger (1979) to demonstrate the localization of several enzymes such as protein kinase C in the retina and the cerebellum (Usuda *et al.*, 1991a), and the thyroid (Shimizu *et al.*, 1991). We first purified protein kinase C from rabbit retina and studied immunohistochemical localization of protein kinase C isozymes (types I, II and III) in the retina and cerebellum using monoclonal antibodies. Frozen sections were cut on a cryostat microtome, stained with rabbit anti-mouse IgG and mouse peroxidase-antiperoxidase complex. Some other immunostaining such as PCNA/cycling (Hanai *et al.*, 1993), BrdU and Ki-67 (Xiao-Lin *et al.*, 1996) were also employed using ABC (avidin-biotin-peroxidase complex) followed by DAB reaction.

- **metal-conjugate staining for electron microscopy.** We used two kinds of metal-conjugates, ferritin first and then colloidal gold later. Ferritin, one of the metaloproteins, containing 23%

iron, can be observed as electron opaque particles by electron microscopy. The approach to label the antibody with ferritin was first introduced by Singer (1959). In order to demonstrate the localization of urate oxidase and catalase in peroxisomes by electron microscopy (Fig. 9), we first used immuno-ferritin staining in combination with cryo-sectioning, since the immuno-ferritin conjugate could not penetrate into the intact cells because of its large molecular weight (Yokota & Nagata, 1973, 1974, 1977). The tissues were prefixed with 2% glutaraldehyde or 4% formaldehyde in 0.1M phosphate buffer, pH 7.4, frozen in liquid nitrogen and cryo-sections were cut, stained with ferritin-antibody conjugate and refixed with 2% glutaraldehyde in 0.1M phosphate buffer (Yokota & Nagata, 1973, 1974, 1977). Recently, colloidal gold particles conjugated with protein A to antibodies, frequently used instead of ferritin particles because of the better contrast of gold particles than ferritin by electron microscopy. The protein A-colloidal gold method was first introduced by Roth *et al.* (1978). Since the homogeneous sizes of gold particles can be used, 2 or 3 antibodies can be stained and observed simultaneously. Moreover, the density of colloidal gold particles are in proportion to the concentration of the bound antibody, the quantification of immuno-staining can be carried out. We developed the protein A-gold immuno-staining by post-embedding technique in combination with the cryo-technique by rapid freezing and freeze-substitution without chemical fixatives for demonstrating peroxisomal enzymes such as urate oxidase, catalase, D-amino acid oxidase, L- $\alpha$ -hydroxiacid oxidase, glycolate oxidase, acyl-CoA oxidase, etc. in rat liver, kidney and intestine (Usuda *et al.*, 1990, 1996; Usuda & Nagata 1991). To observe 2 antibodies on the same section, for example, one side of the section was stained with the antibody for D-amino acid oxidase antibody and 15-nm protein A-colloidal gold particles, and the other side of each section was stained with the antibody for catalase and 5-nm protein A-colloidal gold particles (Usuda *et al.*, 1991c).

### 3.3.2. Lectin histochemistry

Lectins were found as carbohydrate-binding proteins obtained from various plants such as Ricinus communis agglutinin from castor beans, concanavalin A from Jack beans, peanut agglutinin from peanut Arachis hypogaea or animals such as Helix pomatin agglutinin from snails which specifically bind to sugar residues in glycoproteins such as lactose, mannose, N-acetyl-galactosamine or N-acetyl-glucosamine, respectively. These specificities were applied to demonstrate the localization of these sugar residues by labeling the lectins with such markers as FITC, HRP, avidin-biotin, ferritin or gold particles as lectin-conjugates for visualizing the lectin-binding sites by both light and electron microscopy (Roth & Binder, 1978). We used some lectin-conjugates to demonstrate several sugar-residues in various specific cells by light and electron microscopy (Hanai, 1993; Hanai *et al.*, 1993a,b).

- **avidin-biotin staining for light microscopy.** We studied the compositional changes in glycoconjugates in mouse kidney and retina using 16 kinds of biotinylated lectins, followed by ABC (avidin-biotin complex) and DAB method for light microscopy (Hanai *et al.*, 1994a,b,c,d). The frozen sections were picked up onto glass slides, and stained with biotinylated lectins followed by ABC (avidin-biotin-complex). As the results, lectin binding sites for specific sugar residues with brown positive reaction can be localized, while control reactions should be negative (Fig. 4).
- **protein A gold staining for electron microscopy.** For electron microscopy, we studied the compositional changes in glycoconjugates in mouse kidney and retina using 16 kinds of biotinylated lectins, followed by protein A-gold technique instead of ABC (avidin-biotin complex) and DAB method for light microscopy (Hanai *et al.*, 1994d), slightly modified from Roth (1983). Ultrathin sections were cut and stained by biotinylated lectin conjugates followed by streptavidin colloidal-gold complex. After routine electron staining with uranyl acetate and lead citrate, the positive sites can be demonstrated with gold particle localization (Hanai *et al.*, 1994d).

## 4. Special Histochemistry - Histochemistry of the Organs

When various methods to demonstrate various chemical components in cells and tissues have been well developed, the applications of these technologies gradually increased at the end of the 20<sup>th</sup>

Century. The applications of the general histochemistry to anatomy of men and animals are called as special histochemistry and cytochemistry or histochemistry of the organs similarly to special histology or histology of the organs (Nagata, 1999b). On the other hand, the applications of general cytochemistry to cell biology should be designated as special cytochemistry. In special histochemistry and cytochemistry, the stresses are placed on the cell organelles in respective cell types in various organ systems.

Special histochemistry and cytochemistry consists of the following sections dealing with the respective organ systems. Because of the page limit for this paper in this journal, only several examples will be here mentioned. For further information in detail, readers are recommended to refer to other recent review articles on cytochemistry (Nagata, 2001) and radioautographology (Nagata, 2002).

#### 4.1. The skeletal system

The skeletal system consists of the bones and the joints. With regards the bones, we studied the bones of aging salamanders from hatching to senescence (Nagata, 1998c, 2006c). The bones of juvenile salamanders at 4-8 weeks consisted of the hyaline cartilage or chondrocytes. Examination of radioautograms labeled with  $^3\text{H}$ -thymidine showed that some of the nuclei of cartilage cells at the epiphyses were labeled with silver grains at 4 weeks (Fig. 10), and the labeling indices were 15-18%, then decreased from 6 to 8 weeks around 7-8%, and finally to 1-2% at 10 weeks. In the adults at 8-12 months and to 5 years, the numbers of the cartilage cells decreased and the labeling indices reached almost zero. Thus, the DNA synthesis in the bones was shown to increase and decrease due to aging of animals.

The joints consist of a few bones which are connected with the ligaments and the synovial membranes. We studied the yellow ligaments of the human patients who were suffering from the ossification of the ligaments (Ono, 1991; Ono & Nagata, 1988, 1992; Ono *et al.*, 1994). We first investigated the biopsied specimens taken from the yellow ligaments of patients at various ages suffering from lumbar pains and fixed the specimens by both chemical fixation in buffered glutaraldehyde and osmium tetroxide followed by conventional dehydration, epoxy embedding and wet sectioning as well as the cryo-fixation at  $-192^\circ\text{C}$  followed by cryo-sectioning, freeze-drying without using any water and observed by electron microscopy (Fig. 11) using X-ray microanalysis (Fig. 12). The results showed that much more Ca and P were detected in the latter specimens than in the former specimens demonstrating the soluble compounds (Ono, 1991; Ono & Nagata, 1988, 1992; Ono *et al.*, 1994).

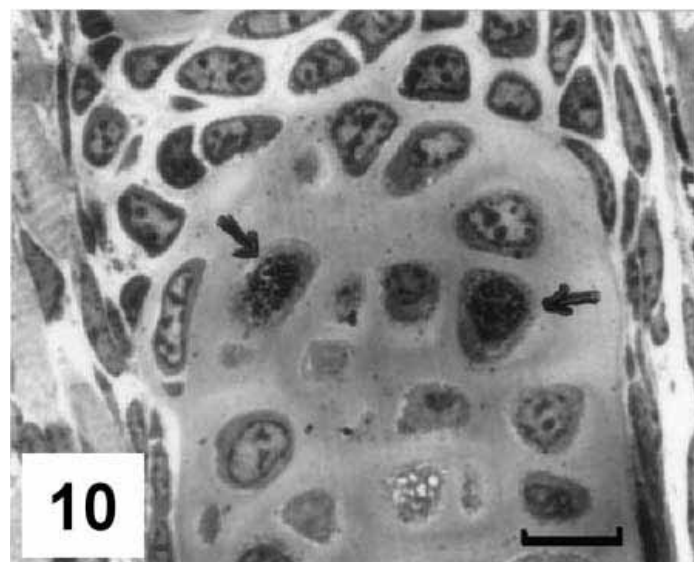


Figure 10. Light microscopic radioautogram (LMRAG) of the bone of a forelimb of a salamander at 4 weeks after hatching, labeled with  $^3\text{H}$ -thymidine. Many nuclei of cartilage cells are labeled with silver grains showing DNA synthesis.  $\times 1,600$ . Bar=10  $\mu\text{m}$ . From Nagata. (2001a), Permission from Academic Press.



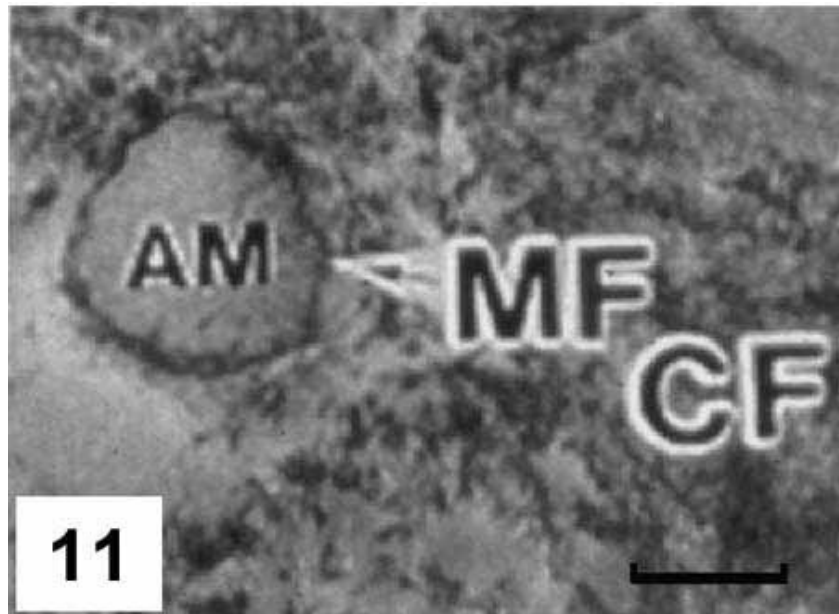


Figure 11. Electron micrograph of an Epon embedded section of the interlaminae portion of the human yellow ligament. Each elastic fiber contains a central amorphous material (AM) which is surrounded by myofilaments (MF) and many collagen fibers (CF).  $\times 10,000$ . Bar =  $1\ \mu\text{m}$ . From Nagata (2001a), Permission from Academic Press.

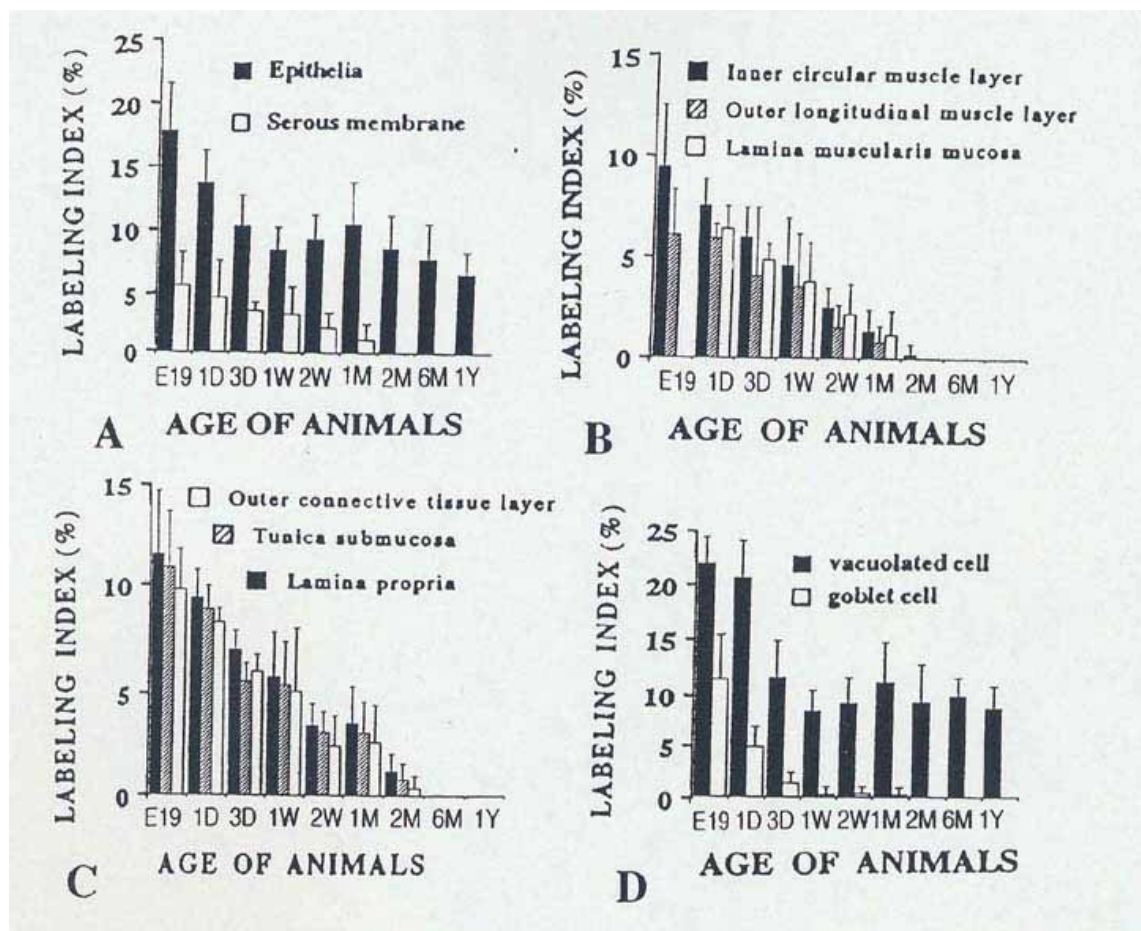


Figure 12. X-ray spectra obtained from chemically fixed Epon embedded sections (top) or cryo-fixed frozen-dried cryo-sections (bottom) of the yellow ligament of a patient suffering from lumbar canal stenosis. From Nagata (2001a), Permission from Academic Press.

## 4.2. The muscular system

The muscular system consists of many skeletal muscles in the whole body. The DNA synthesis of mouse intercostal muscles from prenatal day 13 through postnatal 24 months were studied by  $^3\text{H}$ -thymidine radioautography (Hayashi *et al.*, 1993). Many nuclei are labeled in myotubes at prenatal days 13-19. The labeling indices revealed chronological changes, reaching a peak at prenatal day 13, and decreasing gradually after birth to 0% at postnatal 3 months, showing an increase followed by a decrease. When thigh muscles of Wistar rats were mechanically injured and labeled with  $^3\text{H}$ -thymidine, satellite cells were labeled, showing that the regenerating muscle fibers originated from satellite cells (Sakai *et al.*, 1977). In the thigh muscle of dystrophy chickens,  $^3\text{H}$ -thymidine was incorporated into the satellite cells, demonstrating the regenerations in these cells which cannot be observed in normal muscles (Oguchi & Nagata, 1980, 1981). When  $^3\text{H}$ -taurine was injected administered to both normal and dystrophy mice and the skeletal muscle were fixed by either conventional chemical fixation followed by dehydration, Epok embedding, sectioning and wet-mounting radioautography or cryo-fixation, freeze-substitution, freeze-drying and dry-mounting radioautography (Fig. 13), much more silver grains were observed on the sarcoplasmic reticulum, myofilaments, mitochondria and sarcoplasmic membranes in the latter specimens than the former, demonstraing the soluble compounds in normal mice than dystrophy mice (Terauchi & Nagata, 1988, 1993).

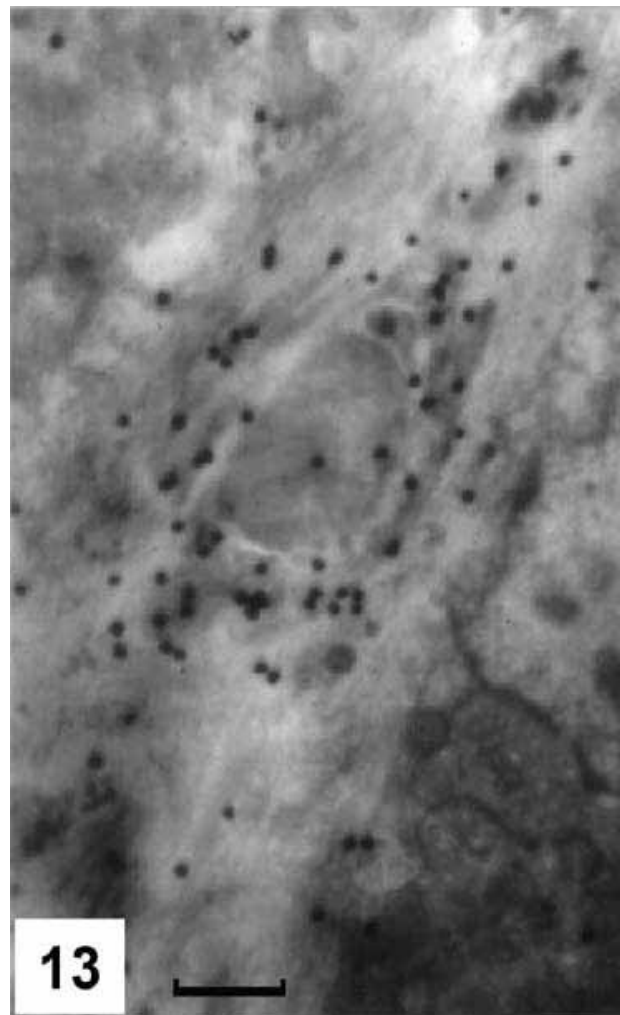


Fig. 13. Electron microscopic radioautogram (EMRAG) of the quadriceps femoris muscle of a normal adult mouse labeled with  $^3\text{H}$ -taurine, processed for freeze-substitution followed by dry-mounting radioautography. Many silver grains appeared on sarcoplasmic reticulum, myofilaments, mitochondria and sarcoplasmic membrane.  $\times 10,000$ . Bar=1  $\mu\text{m}$ . From Nagata.(2001a), Permission from Academic Press.

### 4.3. The circulatory system

The circulatory system consists of the heart, the blood vessels, the blood, the lymphatic vessels, the lymphnodes and the spleen.

We first studied histochemical changes of the cardiac muscle cells of rats during and after the global ischemia (Yanagiya, 1994; Yanagiya *et al.*, 1994). For demonstrating cytochrome oxidase activity in cardiac muscle mitochondria, DAB reaction was used and the intensity of the reaction products was quantified by densitometry. As the results, ultrastructural changes such as decreases of mitochondrial matrix granules and disruptions of cristae were observed from 60 min to 120 min ischemia. However, the cytochrome oxidase activity did not change until 240 min ischemia, showing a lag behind the ultrastructural changes (Yanagiya, 1994; Yanagiya *et al.*, 1994). We also studied nucleic acid synthesis in cultured heart muscle cells obtained from chicken embryo (Nagata & Nawa, 1966). The heart muscle fibroblasts *in vitro* showed incorporations of both  $^3\text{H}$ -thymidine and  $^3\text{H}$ -uridine in mononucleate and binucleate cells. The numbers of silver grains were much more in binucleate cells than mononucleate cells (Nagata & Nawa, 1966). The blood vessels, both arteries and veins, consist of 3 layers, the tunica intima, the media and the adventitia, from inside to outside. Those layers are formed with connective tissues and smooth muscles, covered inside with simple endothelial cells. We studied the localization of antihypertensive drugs in the supramesenteric arteries of spontaneous hypertensive rats by means of light microscopic radioautography (Suzuki *et al.*, 1994). Two kinds of antihypertensive drugs,  $^3\text{H}$ -benzidipine hydrochloride and  $^3\text{H}$ -nitrendipine were intravenously injected into rats and the arteries were taken out or the arteries were labeled *in vitro* by incubation in a medium containing  $^3\text{H}$ -antihypertensive drugs for 10 to 30 min, fixed by either chemical fixation or cryo-fixation, radioautographed by either wet-mounting or dry-mounting radioautography. The silver grains were observed over the plasma membranes and the cytoplasm of the fibroblasts in the intima and the smooth muscle cells in the media, suggesting the pharmacological active sites for the arteries (Suzuki *et al.*, 1994).

With regards the blood cells, we first studied enzyme cytochemistry, arylsulfatase B activity in the rabbit blood platelets (Murata *et al.*, 1975). The results showed that the reaction products were exclusively localized in the alpha granules of the platelets and the localization of the activity in each platelet showed different staining pattern, which suggested variable functional heterogeneity in the granules (Murata & Nagata, 1976). The ultrastructural localization of acid mucosubstances in the human basophilic leukocytes was studied with DI (dialyzed iron), which demonstrated that the DI-positive mucosubstances were localized on the cell membranes and specific granules of normal human basophilic leukocytes (Murata & Nagata, 1976). Mast cells are widely found to distribute in the loose connective tissues of most mammals. We studied the nucleic acid and mucosubstance syntheses in normal mast cells and mastocytoma cells in mice and rats (Murata *et al.*, 1977c, 1978a). The results showed that some of the normal mast cells as well as mastocytoma cells incorporated  $^3\text{H}$ -thymidine,  $^3\text{H}$ -uridine and  $^{35}\text{S}$ -sulfuric acid. The incorporation of  $^3\text{H}$ -thymidine was observed in the nuclei and mitochondria and the labeling index of  $^3\text{H}$ -thymidine incorporation in normal mast cells was very low (0.4%) while that of mastocytoma cells was high (Murata *et al.*, 1977b).  $^3\text{H}$ -uridine was incorporated into nuclei, nucleoli, mitochondria and ribosomes, while  $^{35}\text{SO}_4$  in the Golgi apparatus and the granules (Murata *et al.*, 1978b).

The spleen is one of the blood cell forming organs and is composed of the lymphatic tissues. We studied  $^3\text{H}$ -thymidine and  $^3\text{H}$ -uridine incorporations into splenic cells of aging mice in connection with the lysosomal enzyme (Olea, 1991; Olea & Nagata, 1991, 1992a,b). The acid phosphatase activity as demonstrated by means of the cerium substrate method was observed in the splenic tissues at various ages from newborn day 1 to postnatal month 10. Electron dense deposits were localized in the lysosomes of macrophages, reticular cells and littoral cells in all the aging groups. The intensity of reaction products as visually observed to increase from day 1 to week 1, reaching the peak at week 1, and then decrease from week 2 to month 10, was quantified by X-ray microanalysis in the TEM mode at accelerating voltage of 400 kV. The P/B ratio expressing cerium peak spectra increased from postnatal day 1 to week 1 and decreased from week 2 to month 10, which accorded well with the results of visual grain counting.

The blood cells are classified into 3 types, the erythrocytes, the leukocytes and the blood platelets. They are produced in the bone marrow. We studied macromolecular synthesis and cytochemical

localization in leukocytes, magkaryocytes and blood platelets in the rabbit bone marrow. We observed the normal rabbit granulocytes by EM radioautography, after labeling with  $^{35}\text{S}$ -sulfuric acid, that  $^{35}\text{S}$  was incorporated into the Golgi apparatus and then it migrated into the 3 kinds of granules, heterophil, acidophil and basophil (Murata *et al.*, 1979). By X-ray microanalysis, S was detected in the 3 kinds of granules which contained acid glucosamines (Murata *et al.*, 1979).

#### 4.4. The digestive system

The digestive system consists of the digestive tract (oral cavity, pharynx, esophagus, stomach, small and large intestines) and the digestive glands (salivary glands, liver, pancreas). The enzyme activities based on several chemical reactions were applied to these glands (Fig. 1). On the other hand, the DNA, RNA and protein syntheses of the digestive tract and the glands such as submandibular glands, esophagus, the small and large intestines (Figs. 16, 17), the liver, and the pancreas of aging mice labeled with  $^3\text{H}$ -thymidine,  $^3\text{H}$ -uridine,  $^3\text{H}$ -amino acids and  $^3\text{H}$ -glucosamine were studied (Duan & Nagata, 1993; Duan *et al.*, 1992, 1993; Jin, 1996; Jin & Nagata, 1995a,b; Morita, 1993; Morita *et al.*, 1994; Ma, 1988; Ma & Nagata, 1988a,b, 1990a,b, 2000; Ma *et al.*, 1991; Nagata, 1995a,b, 1999c, 2000e; Nagata *et al.*, 2000b; Watanabe & Nagata, 2002). The goblet cells in the intestines include sulfomucins which are HID positive with HID-AB staining (Nagata & Kawahara, 1999). The goblets also show incorporations of  $^{35}\text{S}$ -sulfuric acid by LM and EM radioautography, demonstrating sulfomucin synthesis (Fig. 2). The sulfomucin incorporations fixed at 180 min after the radiosulfate injections into mice revealed that many silver grains were observed over the mucous droplets of the goblet cells in the lower regions of the colonic crypts demonstrating accumulations of the radiosulfate at the apical portions of the droplets, while the silver grains in the goblet cells in the upper regions showed the silver localization over the whole mucous droplets. The results suggested that the silver grains showing incorporations of the radiosulfate transferred slowly in the upper region of the crypt than the lower regions (Nagata, 2001a). The DNA, RNA and protein syntheses in large digestive glands such as the salivary glands (Figs. 14,15) (Nagata *et al.*, 2000b), the liver (Nagata, 2006b; 2007a,b,c,d; Nagata & Ma, 2005a,b) and the pancreas (Nagata, 2000e) were also studied. Among of these studies, we recently concentrated on the macromolecular synthesis such as DNA, RNA and proteins in the mitochondria of hepatocytes of aging mice from fetal stages to postnatal day 1 to month 1 and year 1 and 2 and found the increases and decreases of these syntheses due to aging (Nagata & Ma, 2005a,b; Nagata, 2006a,b, 2007a,b,c,d). Light and electron microscopic radioautography of prenatal and postnatal normal mice at various ages labeled with  $^3\text{H}$ -thymidine revealed that many silver grains were localized over the nuclei of various cell types composing the liver, such as hepatocytes (Fig. 18), sinusoidal endothelial cells (Fig. 19), stellate cells of Kupffer, Ito's fat-storing cells, bile-ductal cells, fibroblasts and hematopoietic cells in perinatal animals. Likewise, light and electron microscopic radioautography of prenatal and postnatal normal mice at various ages labeled with  $^3\text{H}$ -thymidine revealed that many silver grains were localized over the nuclei of various cell types composing the pancreas, such as pancreatic acinar cells (Fig. 20), centro-acinar cells (Fig. 21), ductal epithelial cells, fibroblasts and endocrine cells of Langerhans. On the other hand, the hepatocytes contain various enzymes, which are demonstrated by either chemical reactions or immunostaining. Cell organelles in hepatocytes can be cytochemically stained with respective marker enzymes such as DAB reaction for catalase in peroxisomes, TPPase or ZIO for Golgi apparatus, G-6-Pase for endoplasmic reticulum, cytochrome oxidase for mitochondria and these organelles are 3-dimensionally observed in thick sections or whole mount cultured cells using high voltage electron microscopy (Nagata, 2000a,c). We also developed immunostaining of peroxisomal enzymes by protein A-colloidal gold complex technique using freeze-substitution embedding for electron microscopy (Usuda *et al.*, 1990, 1991b,c, 1994,1996; Usuda & Nagata, 1991) and found that the activity of catalase was clearly demonstrated in the peroxisomes of rat hepatocytes (Fig. 3).



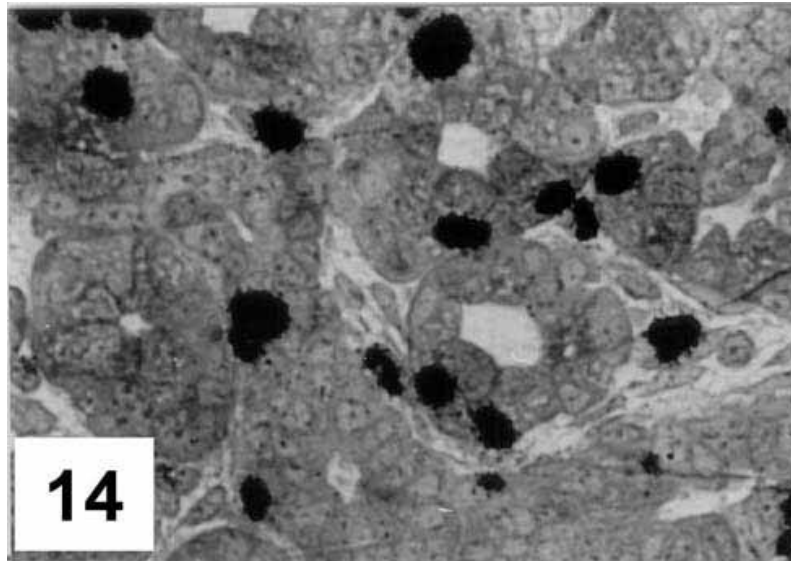


Figure 14. LMRAG of the submandibular gland obtained from a mouse embryo at fetal day 19, labeled with 3H-thymidine *in vitro* and radioautographed. Many nuclei of acinar cells and ductal cells are labeled with silver grains demonstrating DNA synthesis. x500. From Nagata . (2002), Permission from Urban & Fischer Verlag.

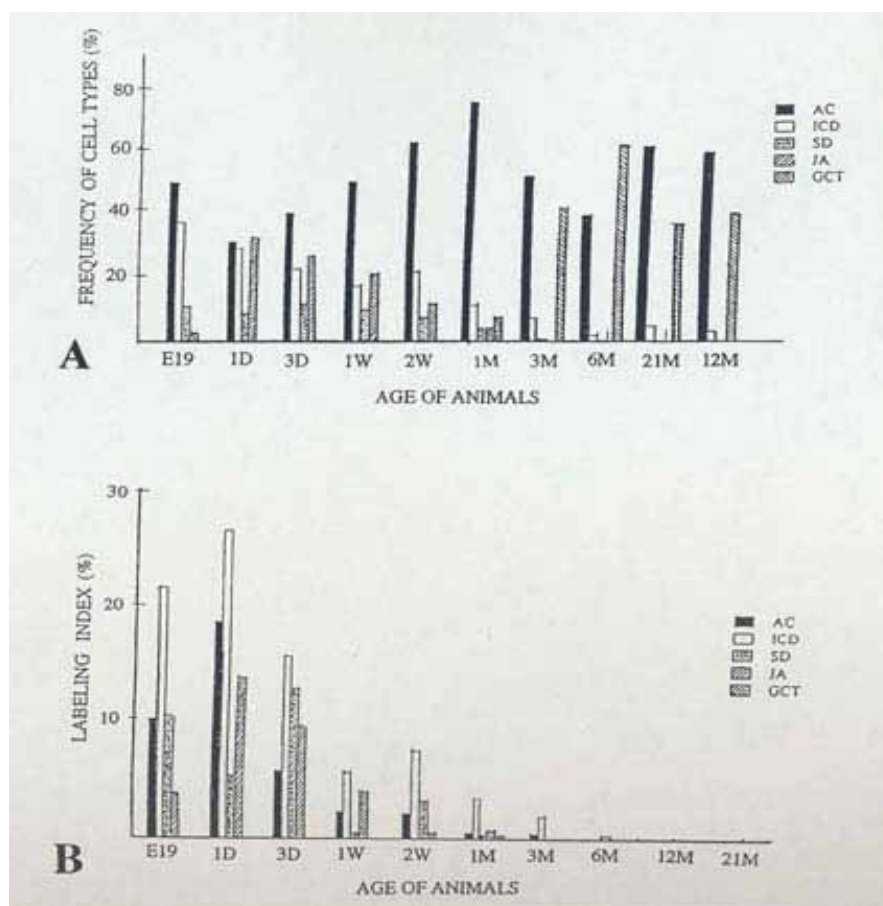


Figure 15. Histogram showing the frequencies and labeling indices of the five individual cell types in the submandibular glands of male ddY mice at respective ages. 15A. Frequencies of appearance of the five cell types. 15B. Labeling indices of the five cell types after 3H-thymidine injections. Abbreviations to the figures. AC; acinar cell, ICD; intercalated duct cell, SD; striated duct cell, JA; juxta-acinar cell, GCT; granular convoluted tubule cell. From Nagata, . (2002), Permission from Urban & Fischer Verlag.

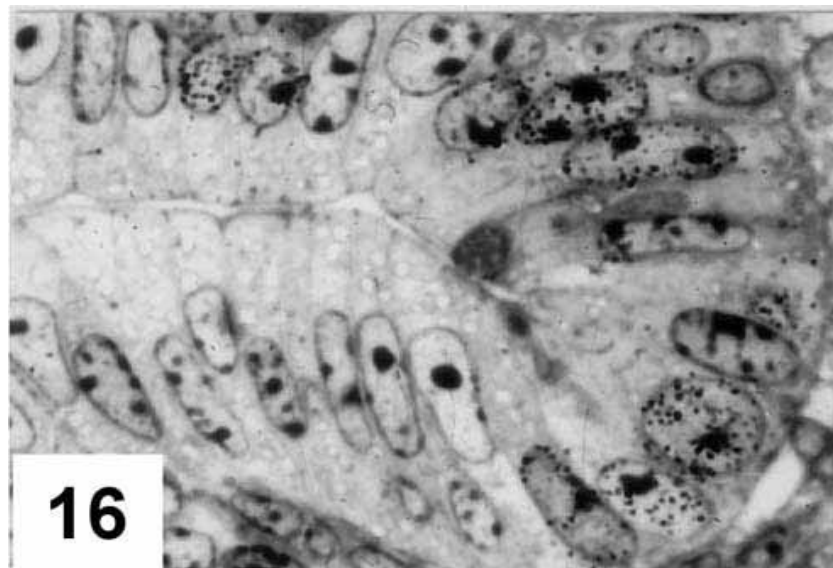


Figure 16. LM image of the colonic epithelial cells of a mouse embryo at fetal day 19, labeled with  $^3\text{H}$ -thymidine *in vivo* and radioautographed. Many silver grains are localized over the nuclei of several epithelial cells in the bottom of the crypt (right). x800. From Nagata . (2002), Permission from Urban & Fischer Verlag.

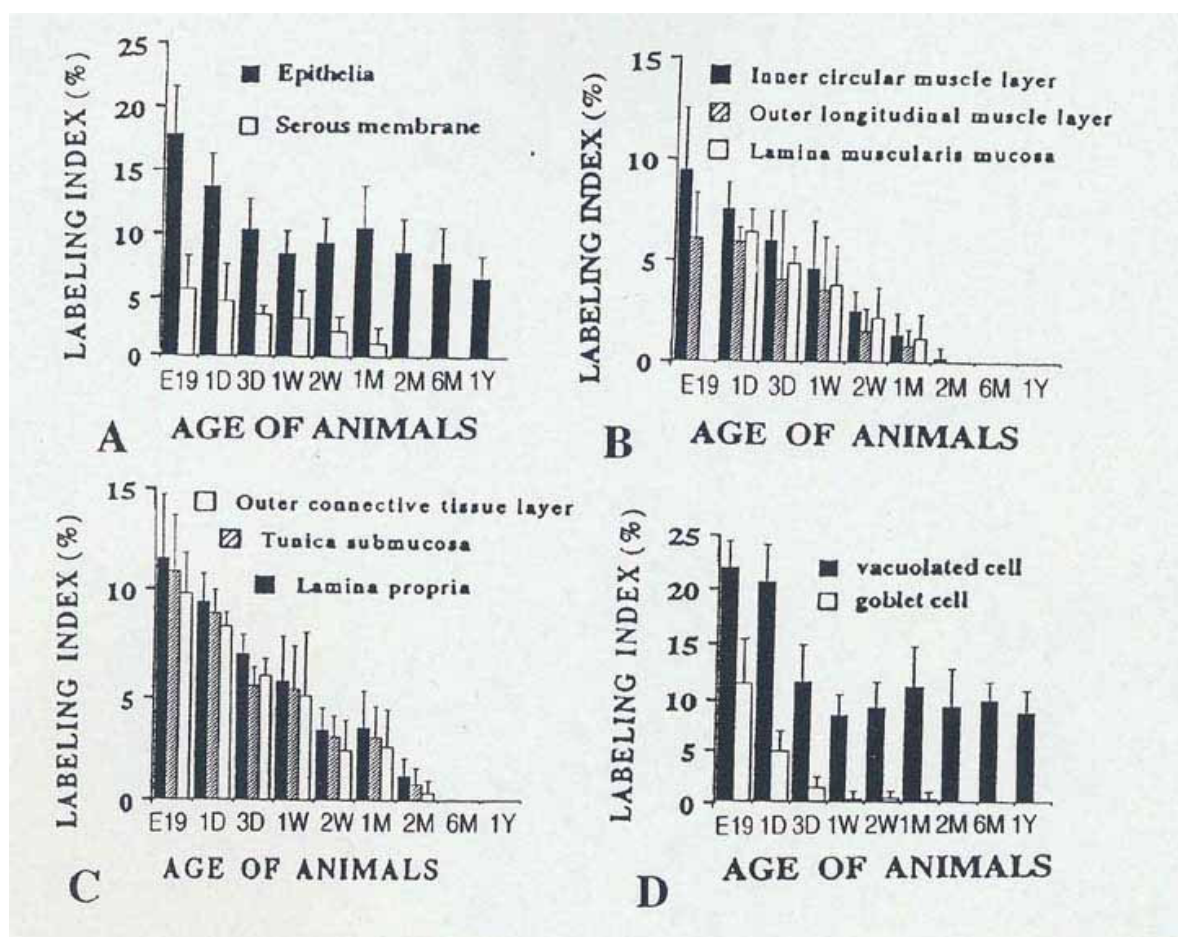


Figure 17. Histograms showing aging changes of average labeling indices in respective tissue layers and cells of mouse colon at various ages from embryo to postnatal 1 year labeled with  $^3\text{H}$ -thymidine. 17A. Labeling indices of the epithelia and the serous membranes. 17B. Labeling indices of the inner circular muscle layer, the outer longitudinal muscle layer and the lamina muscularis mucosae. 17C. Labeling indices of the lamina propria, the tunica submucosa and the outer connective tissue layer. 17D. Labeling indices of the vacuolated cells and the goblet cell. From Nagata . (2002), Permission from Urban & Fischer Verlag.

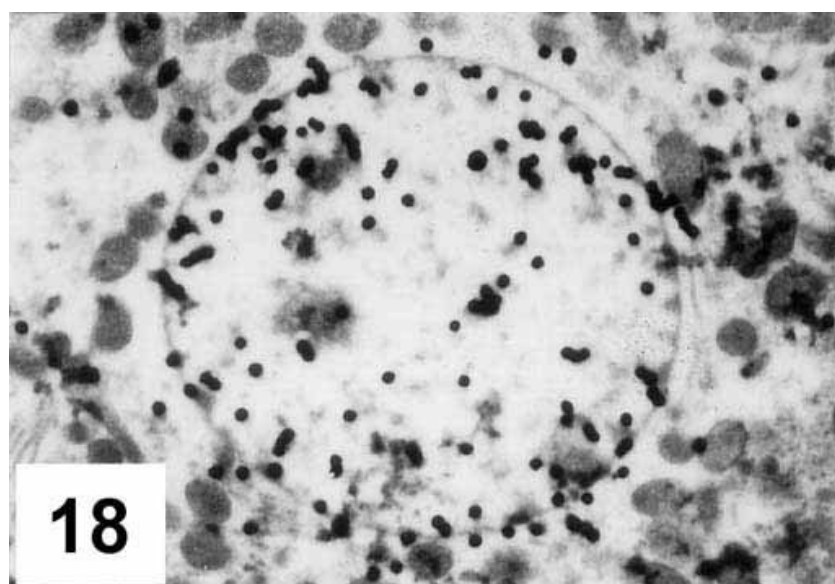


Figure 18. EMRAG of a hepatocyte of a 14 day old mouse, injected with <sup>3</sup>H-thymidine and radioautographed. Many silver grains are localized over the chromatin in the nucleus, showing DNA synthesis. x12,000. From Nagata (2002), Permission from Urban & Fischer Verlag.

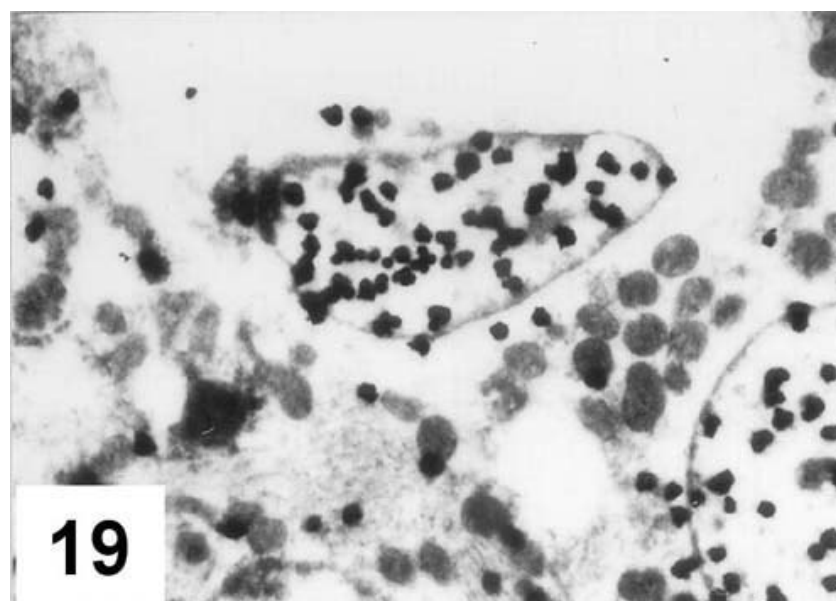


Figure 19. EMRAG of a sinusoidal endothelial cell in the liver of a 14 day old mouse, injected with <sup>3</sup>H-thymidine and radioautographed. Many silver grains are localized over the chromatin in the nucleus, showing DNA synthesis. x12,000. From Nagata (2002), Permission from Urban & Fischer Verlag.



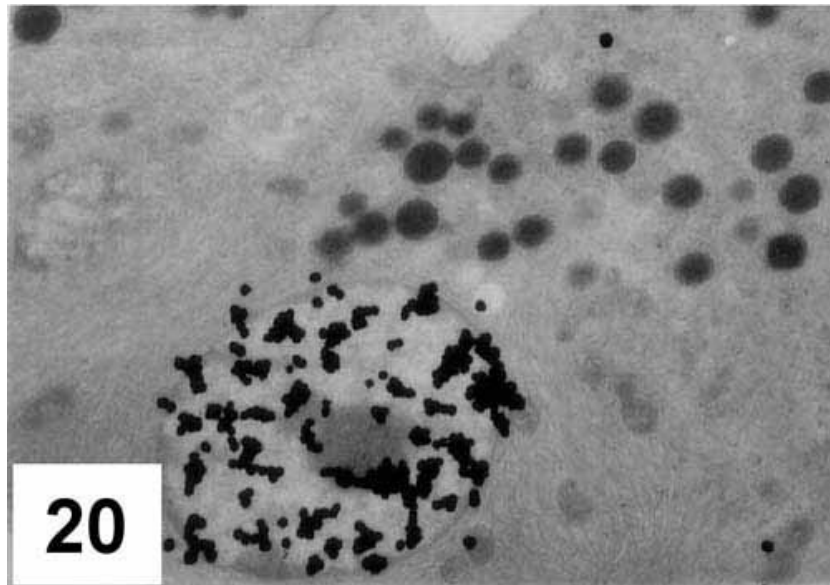


Figure 20. EMRAG of 2 pancreatic acinar cells of a young mouse at postnatal day 14, injected with  $^3\text{H}$ -thymidine and radioautographed. Many silver grains are localized over the chromatin in the nucleus of a cell at center, showing DNA synthesis.  $\times 10,000$ . From Nagata (2002), Permission from Urban & Fischer Verlag.

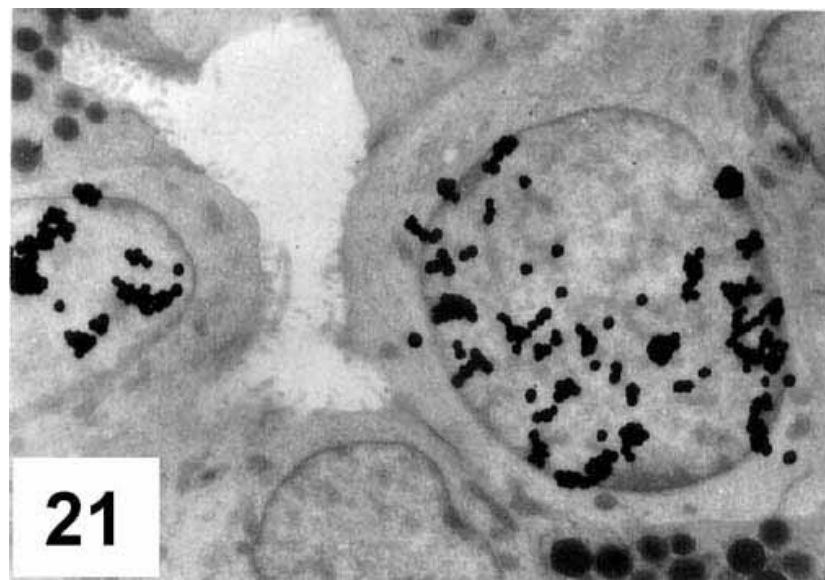


Figure 21. EMRAG of 2 pancreatic centro-acinar cells of a young mouse at postnatal day 14, injected with  $^3\text{H}$ -thymidine and radioautographed. Many silver grains are localized over the chromatin in the nuclei of 2 cells at left and right, showing DNA synthesis.  $\times 10,000$ . From Nagata (2002), Permission from Urban & Fischer Verlag.



## 4.5. The respiratory system

The respiratory system consists of the air way (nose, larynx, trachea) and the lungs. The DNA, RNA and protein synthesis of the trachea and the lungs of aging mice at various ages were studied (Nagata & Sun, 2007; Sun, 1995; Sun *et al.*, 1994, 1995a,b, 1997a,b).

The DNA synthesis in the nuclei of ciliated cells in the tracheal epithelia was observed only in the fetal animals (Fig. 22), while that of non-ciliated cells and basal cells found in both prenatal and postnatal animals (Fig. 23). The labeling indices of the epithelial cells showed the maxima on fetal day 18, then fell down from postnatal day 2 to year 2 (Fig. 24). The DNA syntheses of chondrocytes, fibroblasts, smooth muscle cells and glandular cells, were the highest on fetal day 18, then rapidly declined on postnatal day 3 and decreased due to aging. The glycoprotein synthesis with incorporations of  $^{35}\text{S}$ -sulfuric acid was also demonstrated in the tracheal cartilage matrices of fetal and newborn mice (Nagata, 2000f). The grain density was the maximum at fetal day 19 (Fig. 25), then decreased to postnatal day 1, 3 (Fig. 26), 9, 14 and 30, and reached zero from month 1 to 12. The DNA synthesis of aging mouse lung was studied by LMRAG and EMRAG (Sun *et al.*, 1994, 1995a,b). The labeling indices of DNA synthesis labeled with  $^3\text{H}$ -thymidine in the pulmonary cells also changed with aging. The index of type 1 epithelial cells (Fig. 27) was very low, which reached the peak on the postnatal day 3, then decreased gradually with aging reaching zero at postnatal month 6. The labeling indices of type 2 epithelial cells (Fig. 28), interstitial cells and endothelial cells, on the contrary, showed the peaks on fetal day 16, then fell down to postnatal day 1 and increased on postnatal day 3 again, and decreased (Fig. 29).

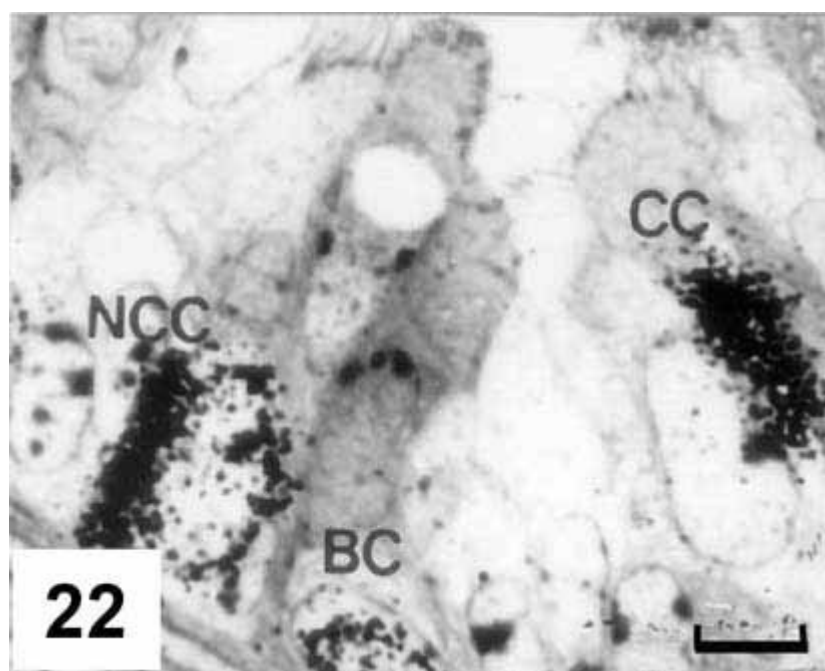


Figure 22. LMRAG of the trachea of a mouse embryo at fetal day 18, injected with  $^3\text{H}$ -thymidine and radioautographed. Many silver grains demonstrating DNA synthesis are localized over the 5 nuclei of epithelial cells, *i.e.* 3 nonciliated cells (NCC) at left, a basal cell (BC) at center and a ciliated cell (CC) at right. x1,500. From Nagata (2001a), Permission from Academic Press.

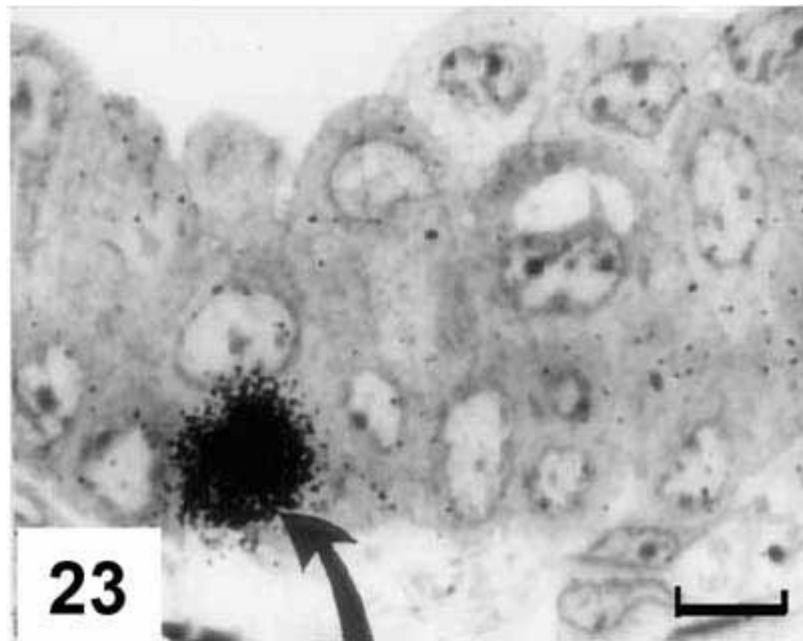


Figure 23. LMRAG of the trachea of an adult mouse at postnatal month 6, injected with  $^3\text{H}$ -thymidine and radioautographed. Many silver grains demonstrating DNA synthesis are localized over the nucleus of a basal cell (BC) at left (arrow). x1,500. From Nagata (2002), Permission from Academic Press.

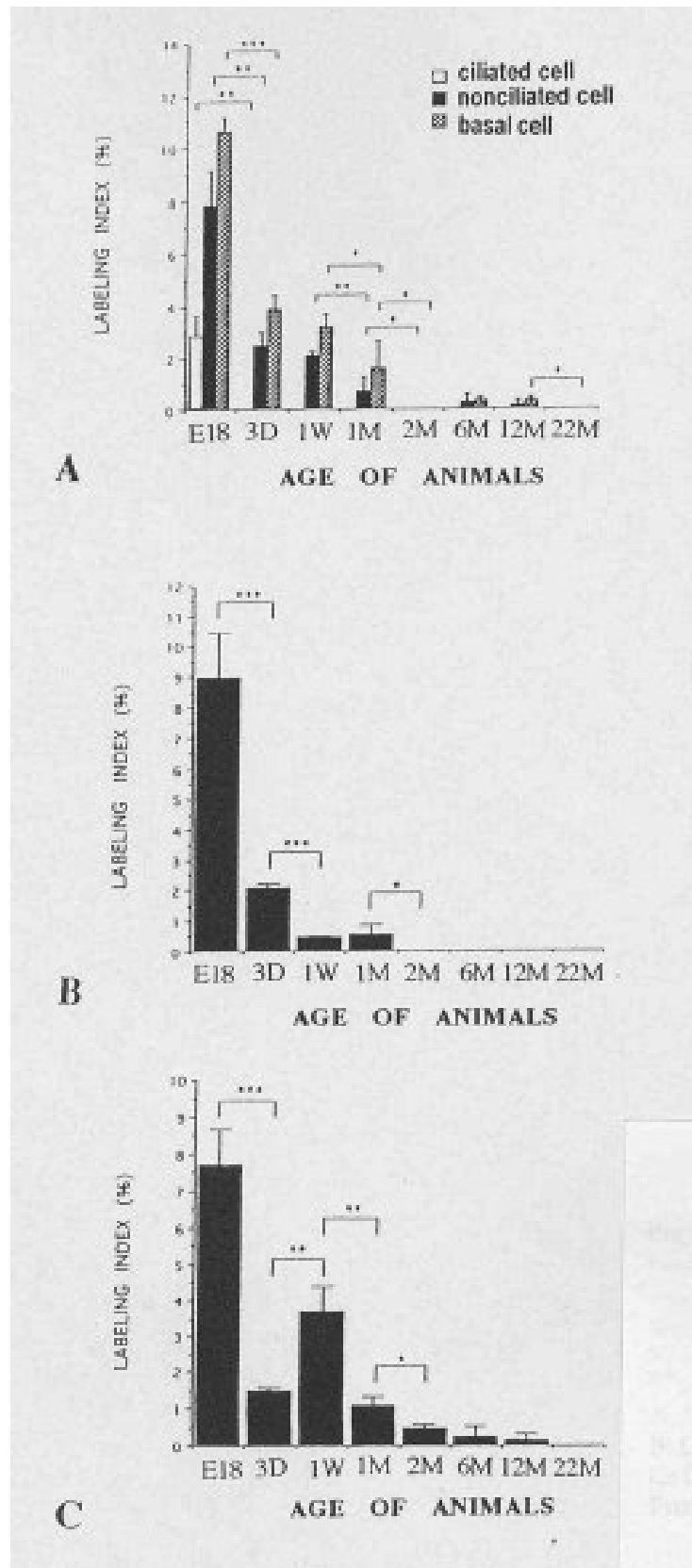


Figure 24. Histograms showing the aging changes in labeling indices of respective cell types in the tracheae of mice at various ages, labeled with  $^3\text{H}$ -thymidine. Mean  $\pm$  Standard deviation. \*significant at  $P<0.05$ . \*\*significant at  $P<0.01$ . A. Epithelial cells. B. Chondrocytes. C. Other cells. From Nagata (2002), Permission from Urban & Fischer Verlag.

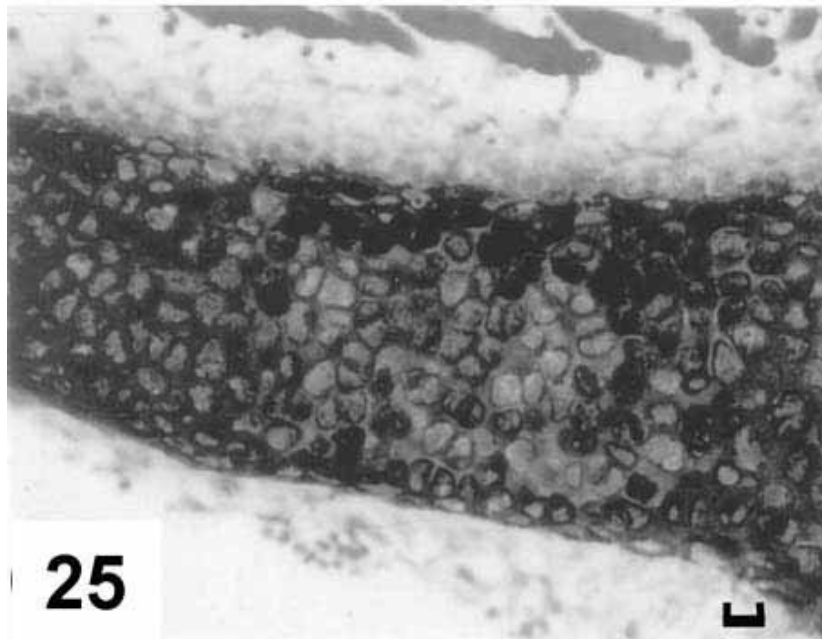


Figure 25. LMRAG of the trachea of a mouse embryo at fetal day 19, injected with radiolabeled sulfuric acid ( $^{35}\text{SO}_4$ ) and radioautographed. Many silver grains demonstrating sulfate demonstrating mucosubstance synthesis are localized over interterritorial and territorial matrices but not over the chondrocytes. x500. From Nagata (2001a), Permission from Academic Press.

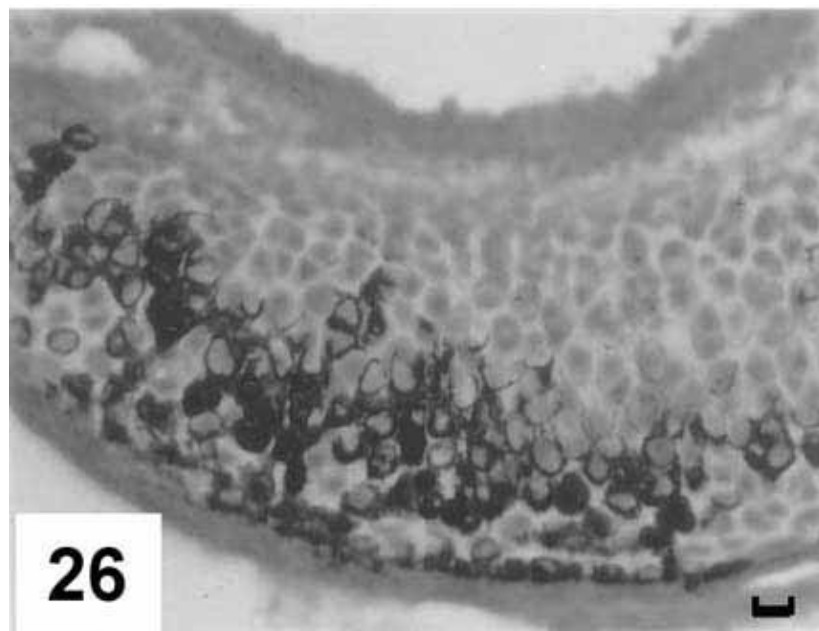


Figure 26. LMRAG of the trachea of a newborn mouse at postnatal day 3, injected with radiolabeled sulfuric acid ( $^{35}\text{SO}_4$ ) and radioautographed. Many silver grains demonstrating sulfate demonstrating mucosubstance synthesis are localized over interterritorial and territorial matrices. x500. From Nagata (2001a), Permission from Academic Press.



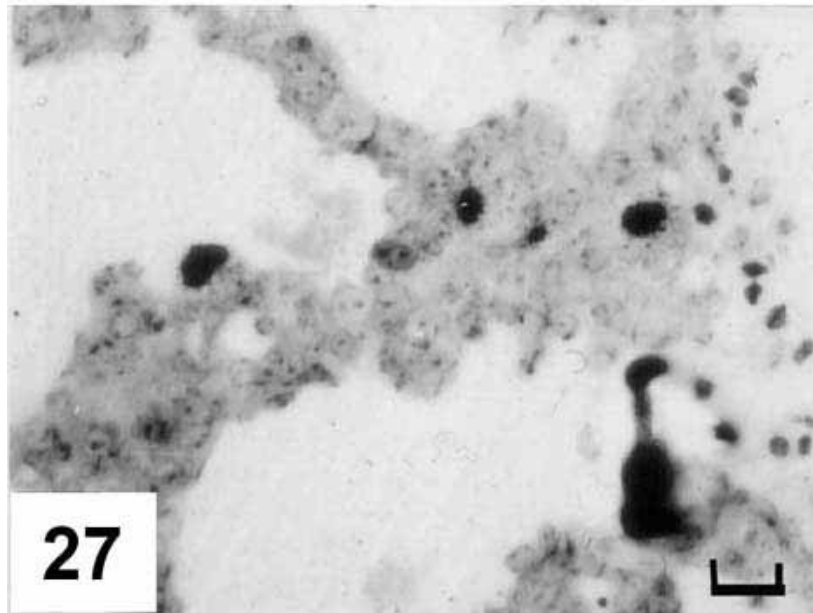


Figure 27. LMRAG of the lung of a newborn mouse at postnatal day 1, injected with  $^3\text{H}$ -thymidine and radioautographed. Many silver grains are localized the nuclei of type 1 epithelial cells and interstitial cells, showing DNA synthesis. x1,000. Bar=50 $\mu\text{m}$ . From Nagata (2001a), Permission from Academic Press.

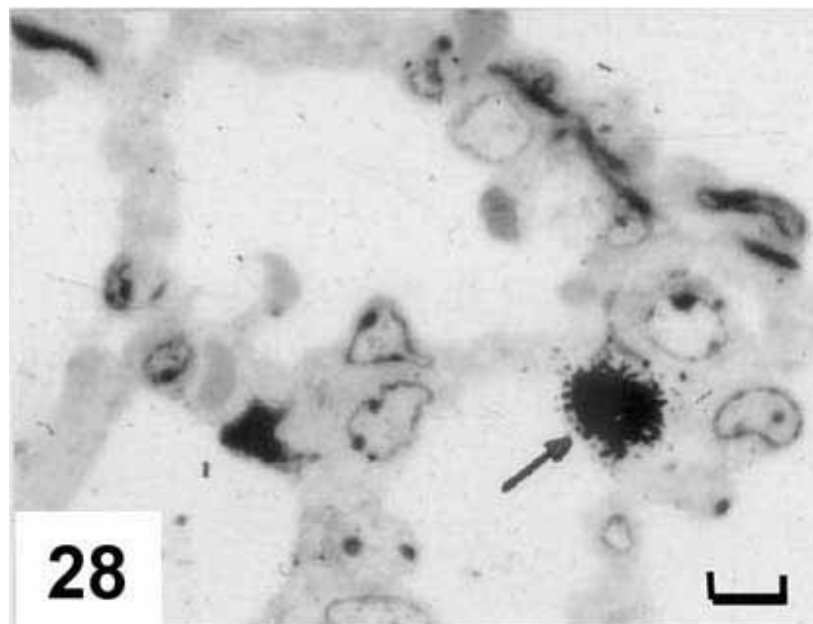


Figure 28. LMRAG of the lung of an adult mouse at postnatal 1 month, injected with  $^3\text{H}$ -thymidine and radioautographed. Many silver grains are localized over the nucleus of a type 2 epithelial cell (arrow), showing DNA synthesis. x1,000. Bar=50 $\mu\text{m}$ . From Nagata (2001a), Permission from Academic Press.

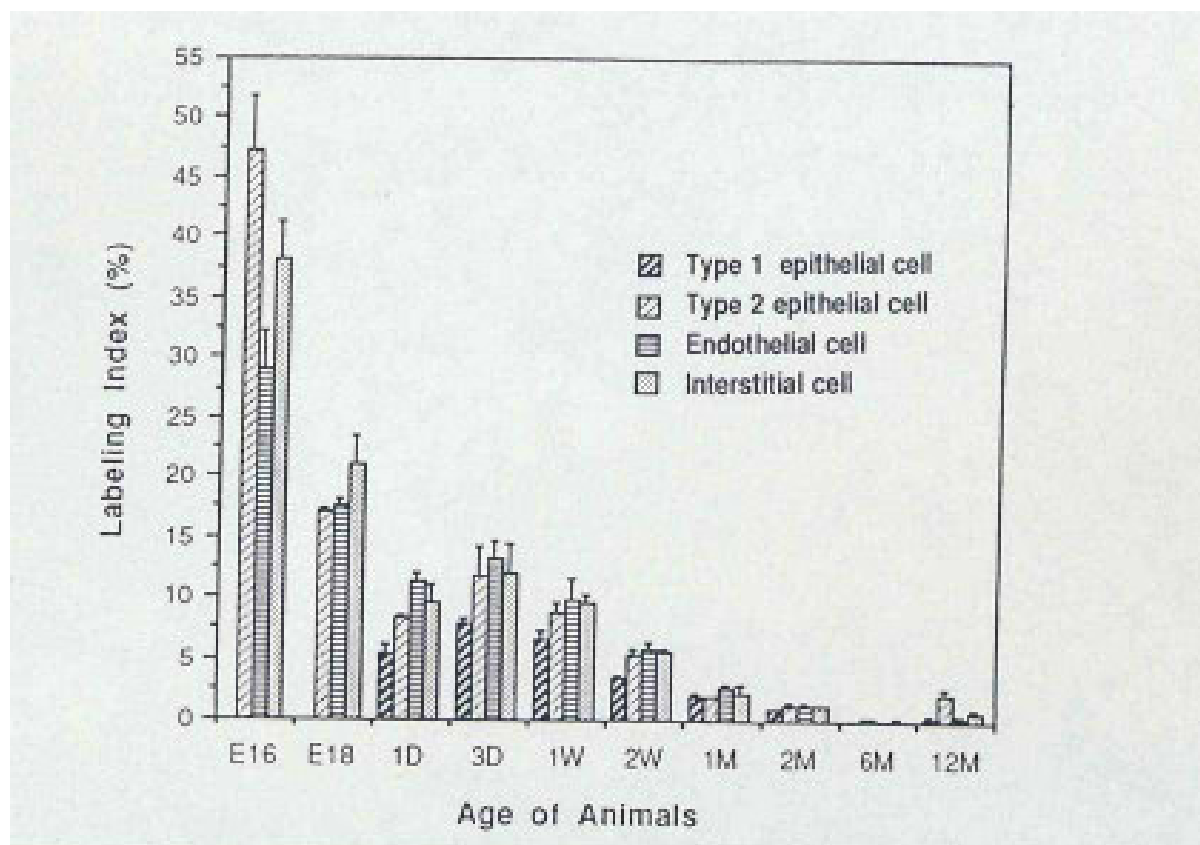


Figure 29. Histograms showing the aging changes in labeling indices of respective cell types in the lungs of mice at various ages, labeled with  $^3\text{H}$ -thymidine. Mean  $\pm$  Standard deviation. From Nagata (2002), Permission from Urban & Fischer Verlag.

#### 4.6. The urinary system

The urinary system consists of the kidneys and the urinary tracts (ureters, bladder, urethra). We studied the DNA, RNA and glycoprotein syntheses in the kidney of aging mice (Hanai, 1993; Hanai & Nagata, 1994a,b; Joukura & Nagata, 1995; Joukura *et al.*, 1996; Nagata, 2004c). The labeling indices of DNA synthesis in glomeruli and uriniferous tubules higher in the superficial layer than those in the deeper layer of the kidneys of the fetal (Fig. 30) and newborn mice (Fig. 31), which decreased with aging (Fig. 32) from juvenile animals to senescence (Hanai & Nagata, 1994a,b). The proliferative activity in the kidneys of aging mice was also evaluated by PCNA/cycling immunohistochemistry (Hanai *et al.*, 1993). The numbers of silver grains labeled with  $^3\text{H}$ -uridine, demonstrating RNA synthesis, in the glomeruli and uriniferous tubules were high at perinatal stages and decreased with aging (Hanai & Nagata, 1994b). The compositional changes in glycoconjugates of lectin binding pattern during fetal and postnatal development of renal corpuscles and uriniferous tubules of rat kidney was revealed by light and electron microscopy (Hanai *et al.*, 1994a,b). The  $^3\text{H}$ -glucosamine incorporations into the glomeruli and uriniferous tubules were high at the perinatal stages, reached the peak at postnatal day 1 and 3, then decreased to senescence at year 1 (Joukura & Nagata, 1995; Joukura *et al.*, 1996). These results showed that glucide synthesis in the kidney changed due to aging.

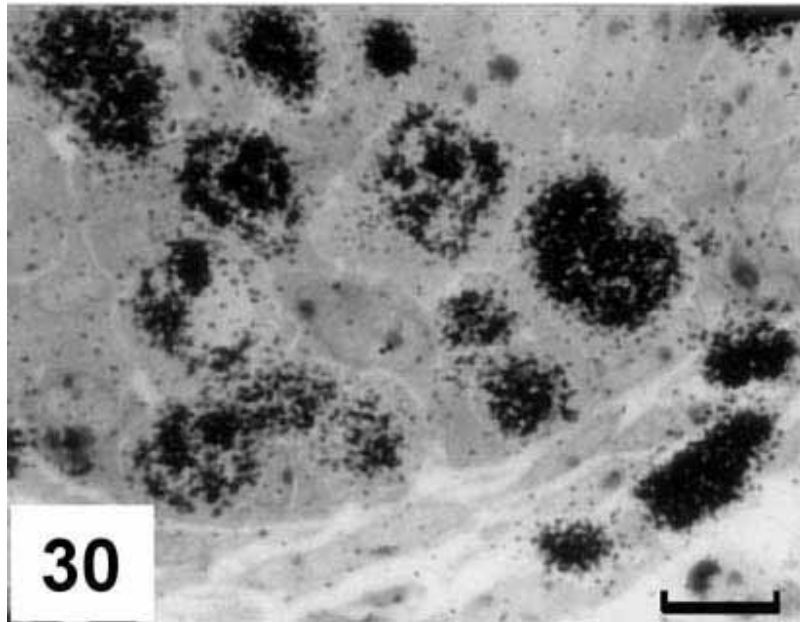


Figure 30. LMRAG of the metanephros of a mouse embryo at day 13.5 of the gestational stage, labeled with  $^3\text{H}$ -thymidine *in vitro*. Many labeled nuclei can be seen.  $\times 1,600$ . Bar= $50\mu\text{m}$ . From Nagata (2001), Permission from Academic Press.

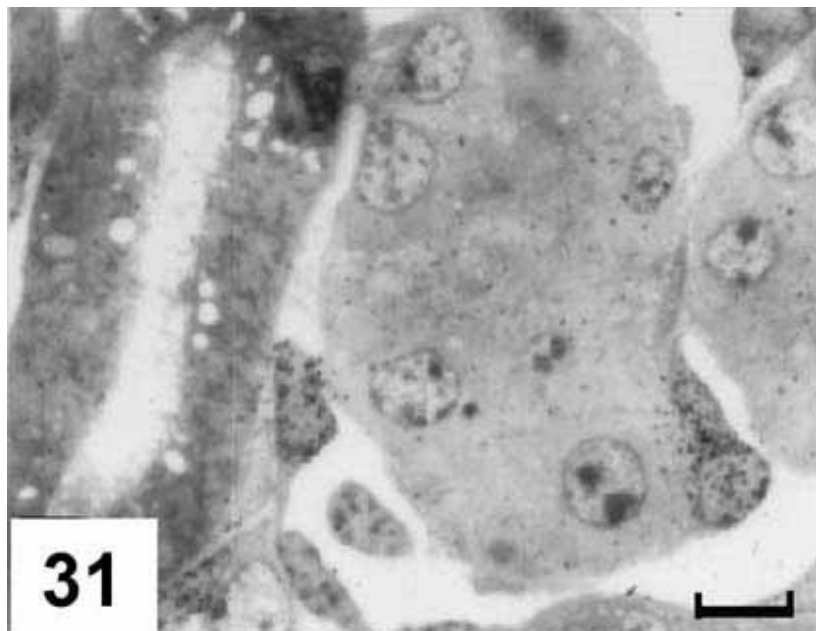


Figure 31. LMRAG of the metanephric cortex of a mouse embryo at day 15.5 of the gestational stage, labeled with  $^3\text{H}$ -thymidine *in vitro*. Less nuclei are labeled.  $\times 1,300$ . Bar= $50\mu\text{m}$ . From Nagata (2001a), Permission from Academic Press.

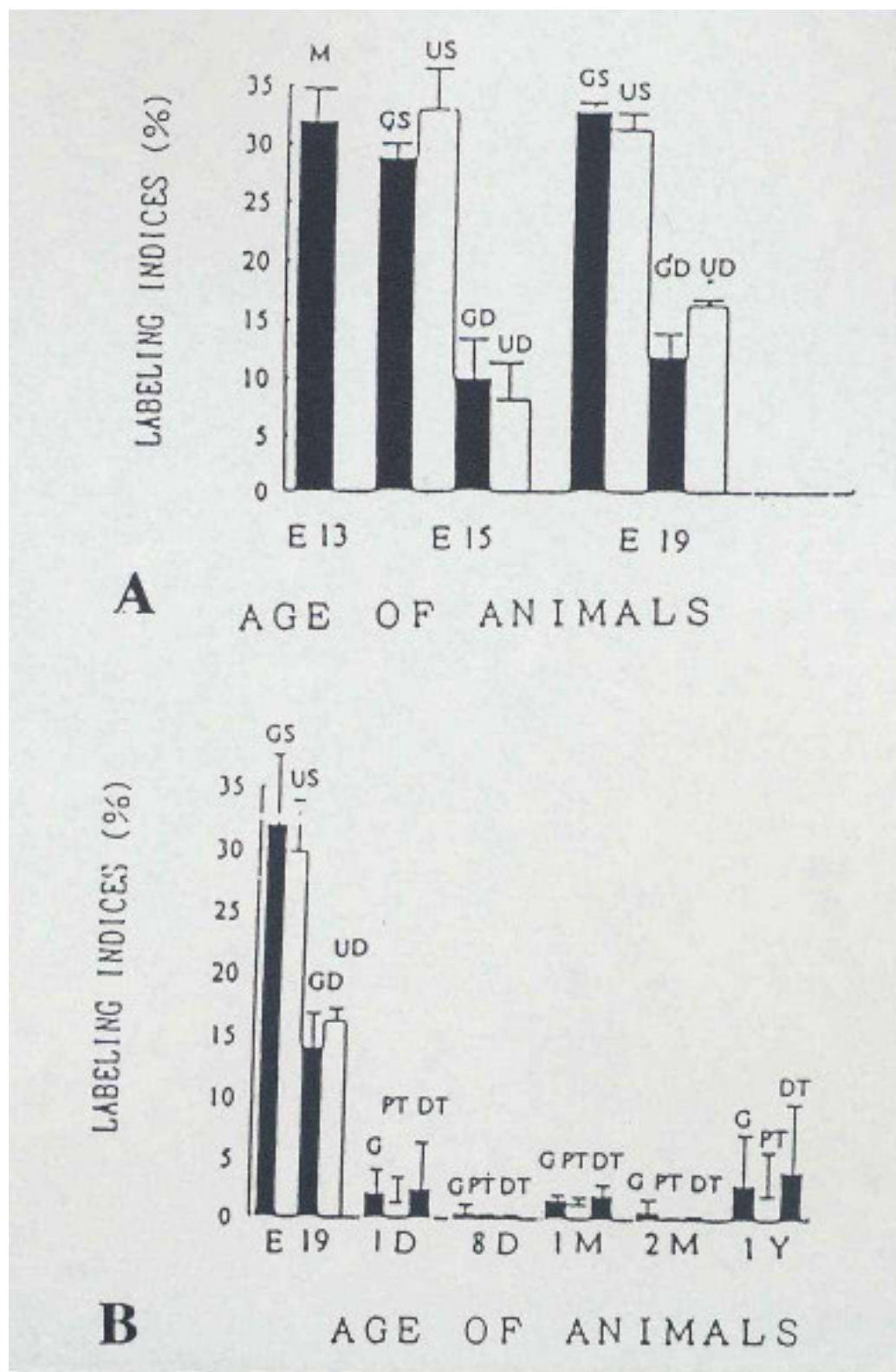


Figure 32. Histograms showing the labeling indices of mouse kidney cells, labeled with  $^3\text{H}$ -thymidine at various ages. 32A. Labeling indices of glomeruli and uriniferous tubules of the kidneys of mouse embryos from fetal day 13 to 19, labeled with  $^3\text{H}$ -thymidine *in vitro*. 32B. Labeling indices of glomeruli, proximal tubules and distal tubules in the kidneys of mouse embryos from prenatal day 19 to postnatal day 365, labeled with  $^3\text{H}$ -thymidine *in vivo*. Abbreviations to the figures. GS; glomeruli of the superficial layer, US; uriniferous tubules of the superficial layer, GD; glomeruli of the deeper layer, UD; uriniferous tubules of the deeper layer, G; glomeruli, PT; proximal tubules, DT; distal tubules. From Nagata (2002), Permission from Urban & Fischer Verlag.



#### 4.7. The reproductive system

The genital system consists of male (testis, ducts, glands, penis) and female genital organs (ovary, tube, uterus, vagina). We studied the DNA, RNA and protein syntheses of both male testis (Gao, 1993; Gao *et al.*, 1994) and female ovary, tube and uterus (Li, 1994; Li & Nagata, 1995) of normal female mice in aging and pregnant mice during activation of implantation window (Yamada, 1993; Yamada & Nagata, 1992a,b, 1993; Oliveira *et al.*, 1991, 1995).

At fetal and neonatal stages of male mice, the DNA synthetic activity of spermatogonia in the testis was weak and only a few labeled spermatogonia were found in the seminiferous tubules of the perinatal animals. Several labeled spermatocytes were recognized at postnatal day 4 to 7 (Fig. 33) and the number of labeled cells increased week 2 to month 1, keeping the high level to year 1 to 2 (Gao, 1993; Gao *et al.*, 1994). The labeling indices of spermatogonia and spermatocytes peaked at week 3 and kept the high level until senescence to year 2. The labeling indices of Sertoli cells and myoid cells, to the contrary, were high at fetal day to postnatal day 4, then decreased to senescence. The numbers of silver grains due to RNA and protein synthesis were low at the fetal and neonatal stages but increased at adult stage and maintained high levels until senescence (Gao *et al.*, 1994).

In the female reproductive organs, DNA and RNA syntheses were observed over all cell types, the surface epithelial cells, the stromal cells and the follicular cells of the ovaries of juvenile and adult female mice (Li, 1994; Li & Nagata, 1995). The labeling indices of DNA synthesis was high in newborn postnatal day 1 to 7, then decreased from day 14 (Fig. 34), month 1 to 2. The numbers of silver grains demonstrating RNA synthesis were high at neonatal stages from postnatal day 1 to 3, then decreased from day 7, 14 to month 1 and 2. On the other hand, the labeling indices of DNA synthesis in all the cell types, the epithelial, stromal and smooth muscle cells in the oviducts (tuba uterina) were high in newborn postnatal day 1 to 3, and decreased from day 7 to month 1 and 2 (Li *et al.*, 1992). The number of silver grains demonstrating RNA synthesis in all the cells of the oviducts were high at neonatal stages from postnatal day 1 to 3, and increased from day 7 to day 14, then decreased from month 1 and 2 (Li *et al.*, 1992). The labeling indices of DNA synthesis in all the cell types, the epithelial, stromal and smooth muscle cells in the uteri were high in newborn postnatal day 1 and decreased from day 3 to month 1 and 2 (Li, 1994; Li & Nagata, 1995). The number of silver grains demonstrating RNA synthesis in the epithelial cells of the uteri were high at neonatal stages from postnatal day 1 to 7, then decreased from day 14 to month 1 and 2, while the numbers of stromal and muscle cells increased from day 1 to 3 and decreased from day 7 to month 2 (Li & Nagata, 1995). We also studied PCNA/cyclin immunostaining in the ovary, oviduct and uterus of developing mice. The PCNA/cyclin positive cells were observed in the ovarian follicular epithelium, ovarian interstitial cells, tubal epithelial cells, tubal interstitial cells, uterine epithelial cells and uterine interstitial cells. The numbers of positive cells in these organs increased from postnatal day 1 to 3 and 7, then decreased from day 14 to senescence (Li & Nagata, 1995).

On the other hand, we also studied the changes of DNA, RNA and protein synthesis in the mouse endometrium during activation of the implantation, ovulation of female mice. The female BALB/C mice were controlled by pregnant mare serum gonadotropin and human chorionic gonadotropin, then they were ovariectomized on day 4 of pregnancy. The delay implantation state was maintained for 48 h after 0 to 16 h of estrogen supply, then RI-labeled precursors were injected and the intertransplantation sites, antimesometrial and mesometrial sites of the endometrium were taken out and radioautographed (Yamada, 1993; Yamada & Nagata, 1992a,b, 1993). The results showed that the labeling indices of DNA synthesis increased from 0 to 18 h, reaching the peak at 18 h after estrogen induction (Yamada & Nagata, 1992a,b), while the numbers of silver grains labeled with RNA and protein synthesis increased from 0 to 3 and 6 h, reaching peaks at 6 h, then decreased from 12 to 18 h (Yamada, 1993; Yamada & Nagata, 1993). The protein synthesis in the decidual cells of pregnant mice uteri was compared to the endometrium of virgin mice by  $^3\text{H}$ -prolin and  $^3\text{H}$ -tryptophane incorporations. The radioautograms demonstrated that silver grains were localized over the endoplasmic reticulum and the Golgi apparatus of fibroblasts and accumulated over collagen fibrils in the extracellular matrix, suggesting that the decidual cells produced collagen in the matrix (Oliveira *et al.*, 1991, 1995).

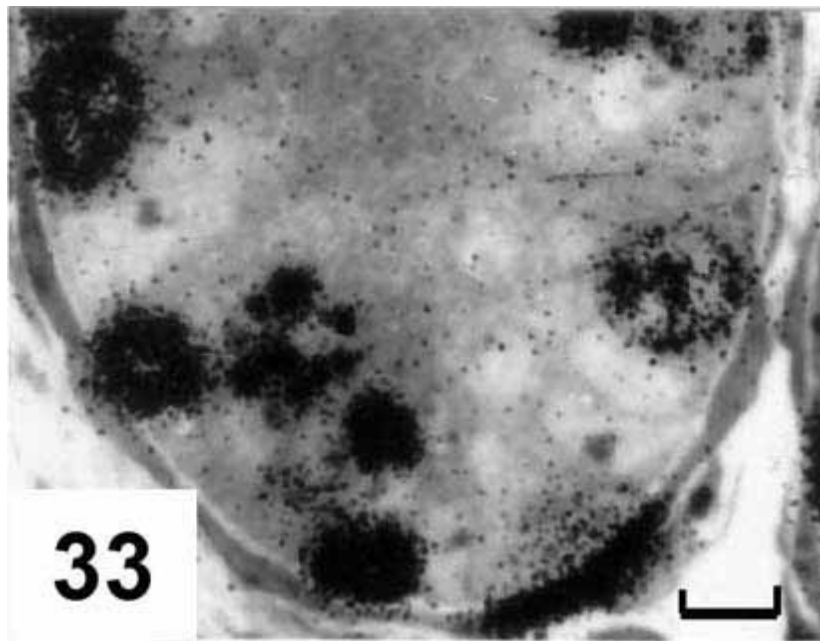


Figure 33. LMRAG of the testis of a male mouse at postnatal day 7, labeled with  $^3\text{H}$ -thymidine *in vitro*. x1,300. Bar=50 $\mu\text{m}$ . From Nagata (2001a), Permission from Academic Press.

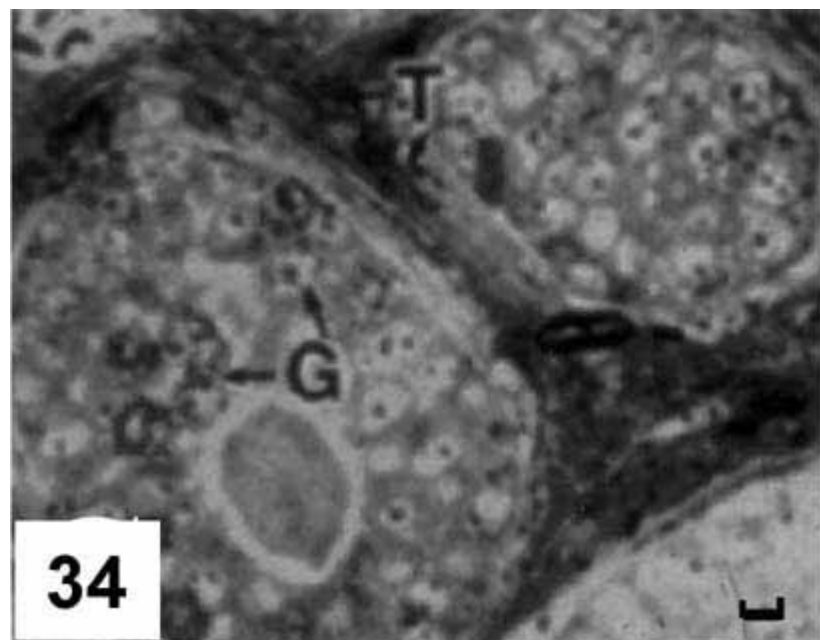


Figure 34. LMRAG of the ovary of a female mouse at postnatal day 14, labeled with  $^3\text{H}$ -thymidine *in vitro*. The nuclei of the granulosa (G) and theca (T) cells are labeled with silver grains. x500. Bar=50 $\mu\text{m}$ . From Nagata (2001a), Permission from Academic Press.

#### 4.8. The endocrine system

The endocrine system secretes various hormones and consists of the hypophysis, thyroid, parathyroid, thymus, pancreatic island of Langerhans, adrenal, and reproductive glands. We studied the DNA, RNA and protein syntheses in the adrenal glands of aging mice at various ages from prenatal day 19 to postnatal 2 years (Ito, 1996; Ito & Nagata, 1996; Liang, 1998; Liang *et al.*, 1999; Nagata, 2000b, 2008; Nagata *et al.*, 2000a). The DNA synthesis was found in all the 3 zones, zona glomerulosa (Fig. 35), fasciculata and reticularis, of the adrenal cortex as well as in the medulla (Ito, 1996; Ito & Nagata, 1996). The labeling indices were high at perinatal stages, then gradually decreased to senescence due to aging. The RNA synthesis was observed over all the cell types in both the cortex and medulla (Lian, 1998; Liang *et al.*, 1999). The numbers of silver grains were high at perinatal stages and decreased to senescence. The numbers of silver grains at the same aging stages were more in the zona glomerulosa (Fig. 36) than other 2 zones of the cortex, fasciculata and reticularis, and the medulla. The adrenal cortical cells contain many mitochondria which showed both DNA and RNA synthesis (Lian *et al.*, 1999; Nagata, 2008). The numbers of mitochondria, the numbers of labeled mitochondria and the labeling index of mitochondria per adrenal cortical cells labeled with RNA synthesis increased from perinatal stage to adult and senescence (Liang *et al.*, 1999). However, the labeled mitochondria and the labeling index labeled with DNA synthesis decreased from perinatal stage to senescence due to aging (Nagata, 2008). On the other hand, the DNA (Fig. 37), RNA (Fig. 38) and protein syntheses in other steroid secreting cells such as Leydig cells as well as ovarian follicular cells of mice were also studied, which also showed aging changes (Nagata, 2000b).

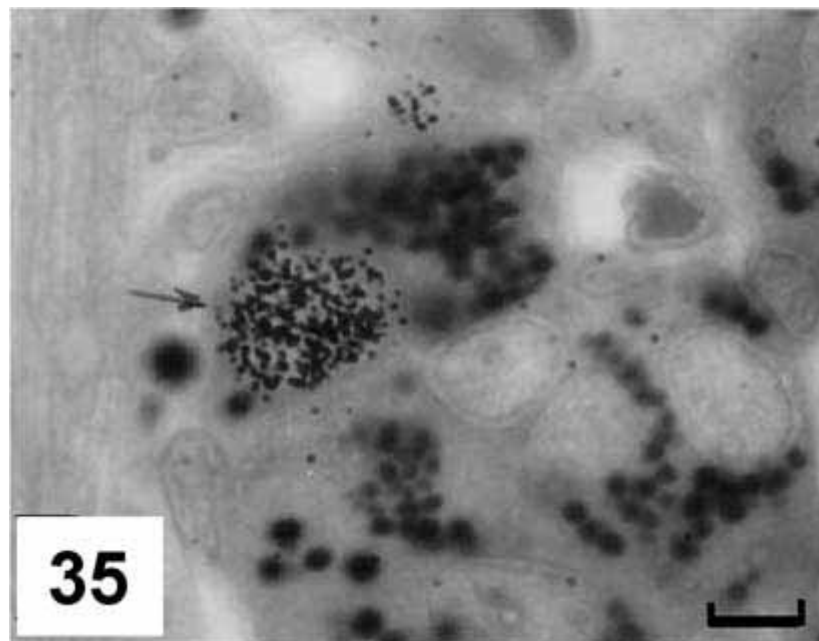


Figure 35. LMRAG of the zona glomerulosa of the adrenal cortex of a postnatal day 14 mouse, injected with  $^3\text{H}$ -thymidine, demonstrating DNA synthesis in the nucleus.  $\times 1,200$ . Bar=50 $\mu\text{m}$ . From Nagata (2001a), Permission from Academic Press.

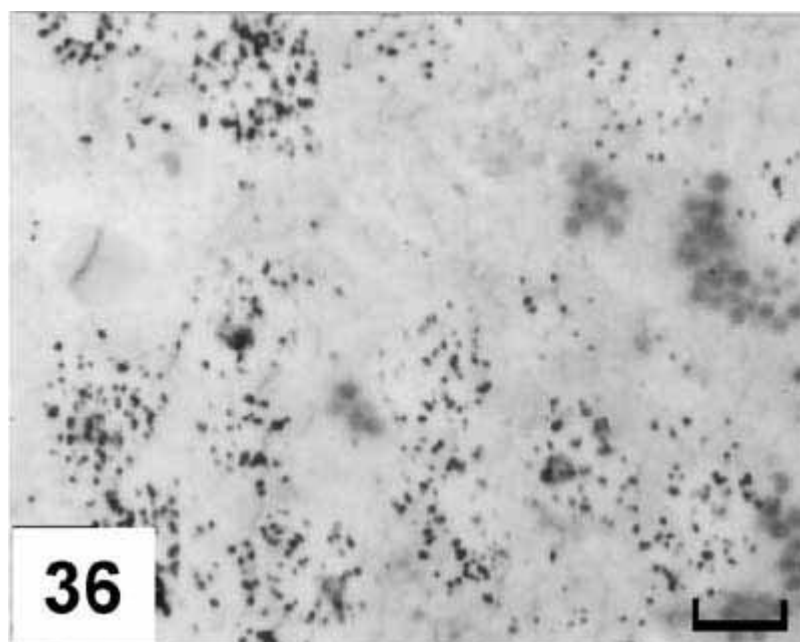


Figure 36. LMRAG of the zona glomerulosa of the adrenal cortex of a prenatal day 19 mouse, injected with  $^3\text{H}$ -uridine, demonstrating RNA synthesis in the nuclei, nucleoli and cytoplasm.  $\times 1,300$ . Bar= $50\mu\text{m}$ . From Nagata (2001a), Permission from Academic Press.

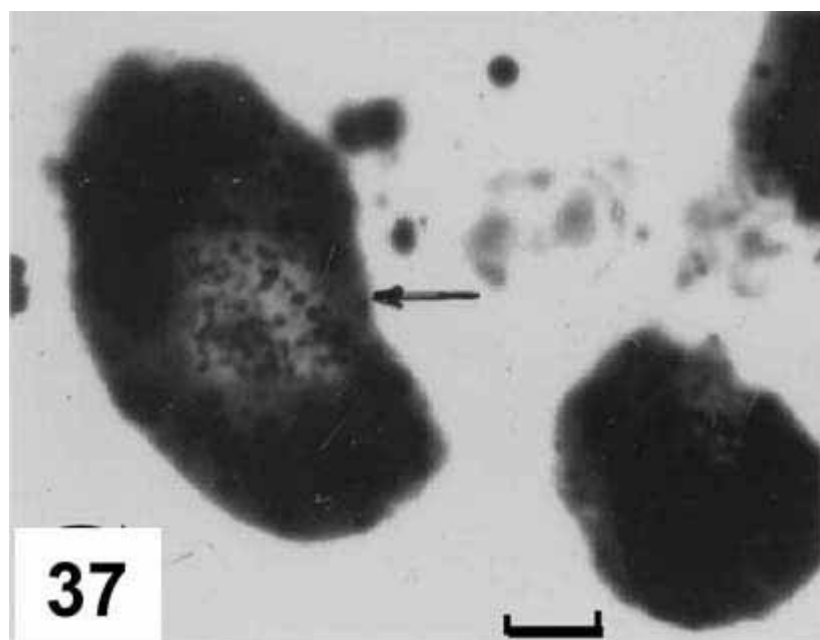


Figure 37. LMRAG of the interstitial tissue of the testis of a mouse at postnatal 12 months, labeled with  $^3\text{H}$ -thymidine *in vitro*, demonstrating DNA synthesis in the nucleus of a Leydig cell (arrow).  $\times 1,300$ . Bar= $50\mu\text{m}$ . From Nagata (2001a), Permission from Academic Press.



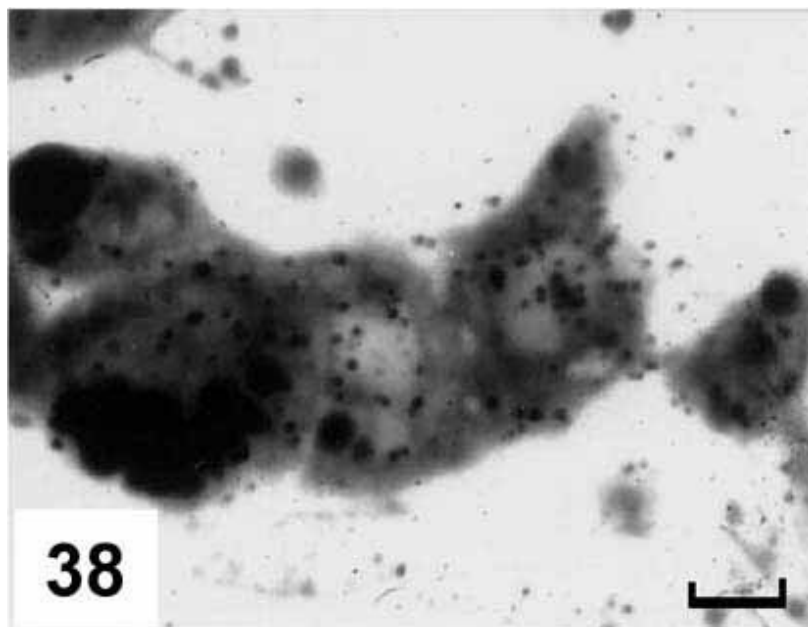


Figure 38. LMRAG of the interstitial tissue of the testis of a mouse at postnatal day 3, labeled with  $^3\text{H}$ -uridine *in vitro*, demonstrating RNA synthesis in several Leydig cells.  $\times 1,300$ . Bar= $50\mu\text{m}$ . From Nagata (2001a), Permission from Academic Press.

#### 4.9. The nervous system

The nervous system consists of the central (brain, spinal cord) and peripheral nervous system. We studied the DNA synthesis of the cerebella (Cui, 1995) and the localization of TGF- $\beta 1$  mRNA in the segments of the spinal cords (Nagata *et al.*, 1999b) of aging mice at various ages. The neuroblasts and glioblasts labeled with  $^3\text{H}$ -thymidine showing DNA synthesis were observed in the external granular layer of the cerebella of perinatal mice, from fetal day 19 (Fig. 39) to postnatal day 1, 3, 7 and 14 (Cui, 1995; Nagata *et al.*, 1999). The labeled cells disappeared from month 1 to year 1 (Fig. 41). The endothelial cells of the cerebellar vessels were progressively labeled from fetal to perinatal mice, reaching a peak at week 1, then decreased. The neuroblasts and glioblasts labeled with  $^3\text{H}$ -leucine showing protein synthesis were also observed in the external granular layer of the cerebella of perinatal mice, from fetal day 19 to postnatal day 1, 3, 7 and 14. Some Purkinje cells were recognized to be labeled on day 3. On the other hand, the localization of TGF- $\beta 1$  mRNA in the segments of the spinal cords of mice was observed by *in situ* hybridization technique using cryosections (Nagata *et al.*, 1999). The tissues of lower cervical segments of the spinal cords of BALB/C mice, from fetal day 12, 14, 16, 19 to postnatal day 1, 3, and week 1, 2, 3, 4, 6, 10, were studied (Fig. 40). The results demonstrated that TGF- $\beta 1$  mRNA was localized in the meninges surrounding the spinal cords but not in the spinal cord parenchyma.

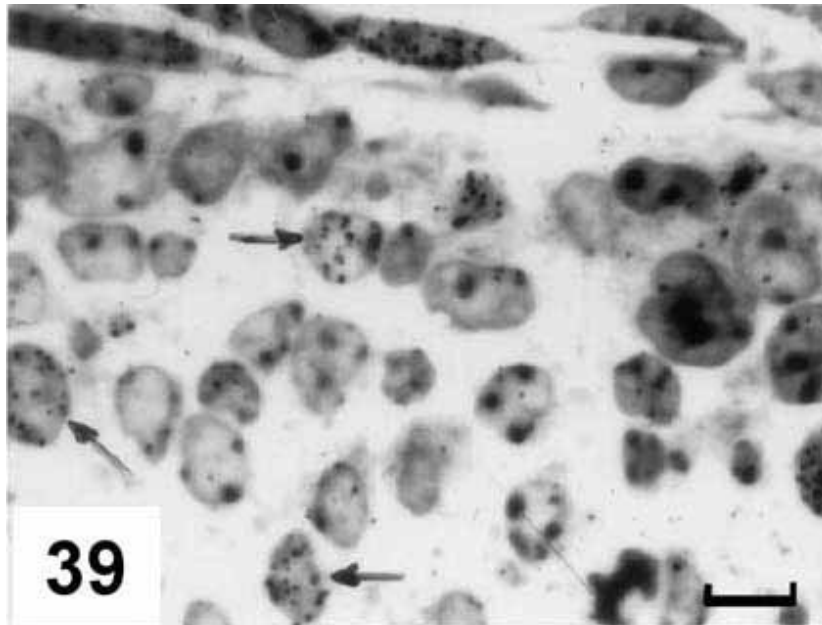


Figure 39. LMRAG of a fetal mouse cerebellum, labeled with  $^3\text{H}$ -thymidine, demonstrating DNA synthesis of a few neuroblasts (arrows).  $\times 1,200$ . Bar= $50\mu\text{m}$ . From Nagata (2001a), Permission from Academic Press.

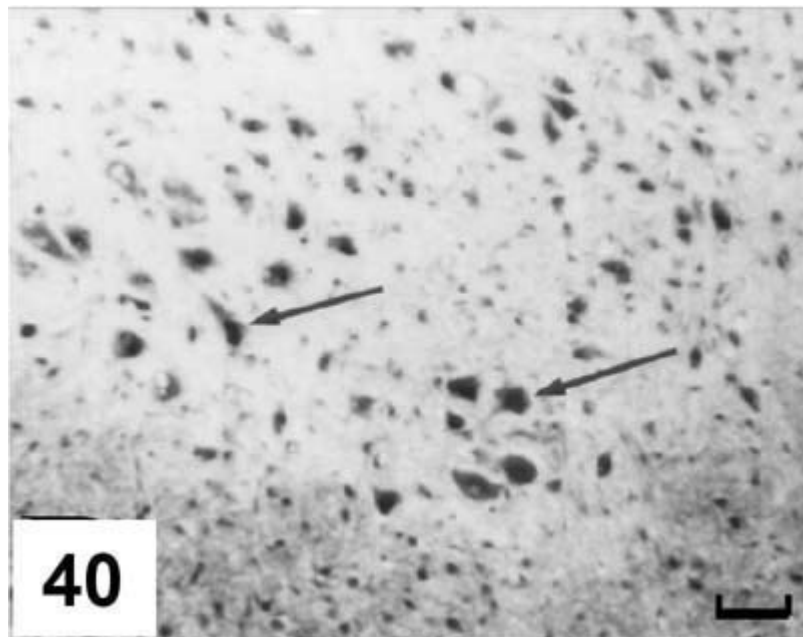


Figure 40. LM photograph of the spinal cord of a mouse at postnatal day 14 immunostained with rabbit anti-TGF- $\beta 1$  polyclonal IgG and biotinylated goat anti-rabbit IgG followed by ABC method. Note that the ventral horn motoneurons (arrows) are strongly positive, while the white matter (bottom) shows weak immunoreactivity.  $\times 100$ . Bar= $500\mu\text{m}$ . From Nagata (2001a), Permission from Academic Press.



Figure 41. Transitional curves of the labeling indices of neuroblasts and glioblasts in the extragranular layer of the cerebella of aging mice after injection with  $^3\text{H}$ -thymidine. Means + SD. A. Labeling indices of the neuroblasts. B. Labeling indices of the glioblasts. From Nagata (2002), Permission from Urban & Fischer Verlag.

#### 4.10. The sensory system

The sensory system consists of the visual (eye), stato-acoustic (ear), olfactory (nose), gustatory (tongue) organs and the skin. We studied the DNA, RNA and protein synthesis of the ocular tissues of chickens (Gunarso *et al.*, 1996, 1997) and the mice (Gao *et al.*, 1992a,b, 1993; Kong, 1993; Kong & Nagata, 1994; Kong *et al.*, 1992a,b; Cui *et al.*, 2000; Nagata, 2006a) and the skins of salamanders (Nagata, 1998c, 2007d) at various ages by LM and EM radioautography. The nucleic acid synthesis was first studied in the ocular tissues of chicken embryo from day 1 to day 14 incubation. It was shown that the labeled cells with  $^3\text{H}$ -thymidine were most frequently observed in the posterior region of the day 2 chick embryo optic vesicle and the labeled cells moved from the anterior to the posterior regions, decreasing from day 3 to 7 (Nagata, 1999c). On the other hand, numbers of silver grains incorporating  $^3\text{H}$ -uridine

increased from day 1 to day 7 and they were more in the anterior region than in the posterior region (Gunarso *et al.*, 1996). On the other hand, the nucleic acid synthesis in the ocular tissues of mice at various ages from embryo day 9, 12, 14, 16, 19 to postnatal day 1, 3, 7, 14, were also studied (Gao *et al.*, 1992a,b, 1993; Kong, 1993; Kong & Nagata, 1994; Kong *et al.*, 1992a,b; Cui *et al.*, 2000; Nagata 2006a). The labeling indices of the retina and the pigment epithelium with DNA synthesis were higher in early stages than later stages (Gao *et al.*, 1992a,b). Comparing the 3 regions of the retina in mice, the anterior, the equatorial and the posterior regions, the labeling indices of the anterior regions were higher than the other 2 regions. In the juvenile and adult stages, however, the labeled cells were localized at the middle of the bipolar-photoreceptor layer of the retina, which was supposed to be the undifferentiated zone (Kong, 1993; Kong & Nagata, 1994; Kong *et al.*, 1992a,b). In the cornea of aging mice, the labeled cells with DNA synthesis were localized in the epithelial cells from prenatal stage to postnatal day 1 to year 1. The labeling indices of the corneal epithelial cells increased from perinatal stage to postnatal month 1, reaching a peak, then decreased to year 1, while the indices of stromal and endothelial cells reached a peak at postnatal day 3 and disappeared from month 1 to year 1. In the ciliary bodies of aging mice, the labeled cells were localized in the ciliary, pigment epithelial, stromal and smooth muscle cells of mice from fetal day 19 to postnatal day 1 to week 1, but no labeled cells were found in any cell types from week 2 to year 1. The labeling indices of all the cell types were at maxima at fetal day 19 and decreased. The numbers of silver grains due to RNA synthesis, on the other hand, increased from fetal day 9 to postnatal day 1 in the retina, while they increased from fetal day 12 to postnatal day 7 in the pigment epithelial cells (Kong *et al.*, 1992b; Kong & Nagata, 1994). The distribution and localization of TGF- $\beta$ 1 and  $\beta$ FGF and their mRNAs in mice at various ages from fetal day 14, 16, 19 to postnatal day 1, 3, week 1, 2, 4, 6 and 10, were studied by *in situ* hybridization (Nagata & Kong, 1998).  $^{35}$ S-labeled oligonucleotide probes for TGF- $\beta$ 1 and  $\beta$ FGF were used to detect their mRNA demonstrating silver grains by radioautography. The silver grains were localized in the scleral layer as well as in the choroidal and pigment epithelial layer but not in the retina (Fig. 42). The distribution and localization of TGF- $\beta$ 1 and  $\beta$ FGF were also studied with the immunocytochemical method (Nagata & Kong, 1988). The posterior segments of mouse eyes, from embryonic days 14, 16 and 19 and postnatal days 1, 3, 5, 7, 17, 28, 42 and 70 were used. For immunostaining, cryo-sections were stained with rabbit anti-TGF- $\beta$ 1 and  $\beta$ FGF polyclonal antibodies followed by the ABC method. The results showed positive immunoreactivities localized in the ganglion cell layers and the vessels of the retina and choroid (Fig. 43). The protein and glycoprotein syntheses in the ocular tissues were studied in several groups of aging mice. In the retina of aging mice labeled with  $^3$ H-leucine incorporation showed silver grains in both the bipolar cells and photoreceptor cells at embryonic stage and early neonatal stage. The numbers of silver grains peaked at postnatal day 1 and decreased from day 14 to year 1 (Toriyama, 1995). The collagen synthesis in the ocular tissues was also demonstrated with  $^3$ H-proline which was incorporated into the endoplasmic reticulum and Golgi apparatus of stromal fibroblasts and intercellular matrices in the cornea and the trabecular meshworks in the iridocorneal angle in prenatal and neonatal mice. The numbers of silver grains increased from embryonic stage to neonatal stage, peaked at postnatal day 7 and decreased (Nagata, 1997c). The protein kinase C activity in rabbit ocular tissues were studied by immunocytochemistry which showed differential localization in the retinal neurons (Usuda *et al.*, 1991a).

The skins of juvenile salamanders at 4-8 weeks after hatching were labeled with  $^3$ H-thymidine which showed that some of the nuclei of the basal cells of the epidermis were labeled with silver grains at 4-6 weeks (Fig. 44), when the labeling indices were 20-25%, then the indices decreased from 8 to 9 weeks to around 5%, and finally to 3-5% at 10-12 weeks (Nagata, 1998c). In the senescent adults at 60 months (5 years), the labeling indices kept constant around 3% but never reached zero. The results showed that the epidermal cells belonged to the renewing cell population (Nagata, 2007d).



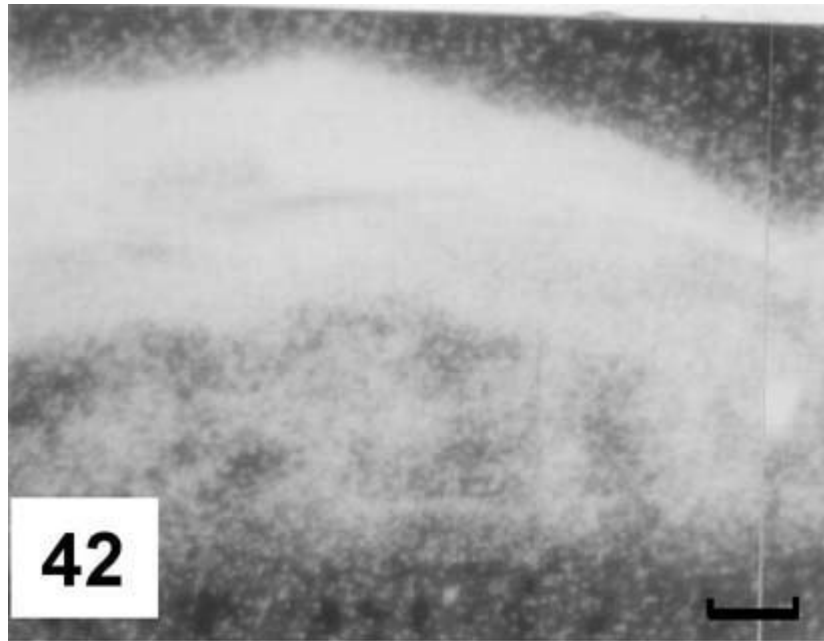


Figure 42. Dark-field photograph of the skleral layer (top), choroid layer (middle) and pigment epithelium (bottom) of an adult mouse, demonstrating intense silver grains (white dots) by *in situ* hybridization for TGF- $\beta$ 1 mRNA in the 3 layers. Compare this picture to the next picture. x600. Bar=100 $\mu$ m. From Nagata (2001a), Permission from Academic Press.

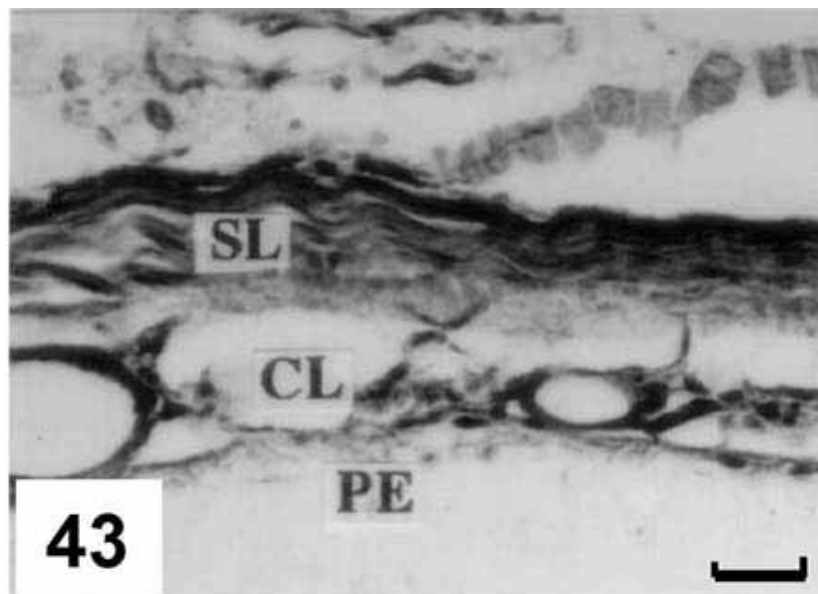


Figure 43. LM photograph of the skleral layer (SK), choroid layer (CL) and pigment epithelium (PE) of an adult mouse, demonstrating immunostaining for TGF- $\beta$ 1. The 3 layers show intense immunoreactivity. x600. Bar=100 $\mu$ m. From Nagata (2001a), Permission from Academic Press.

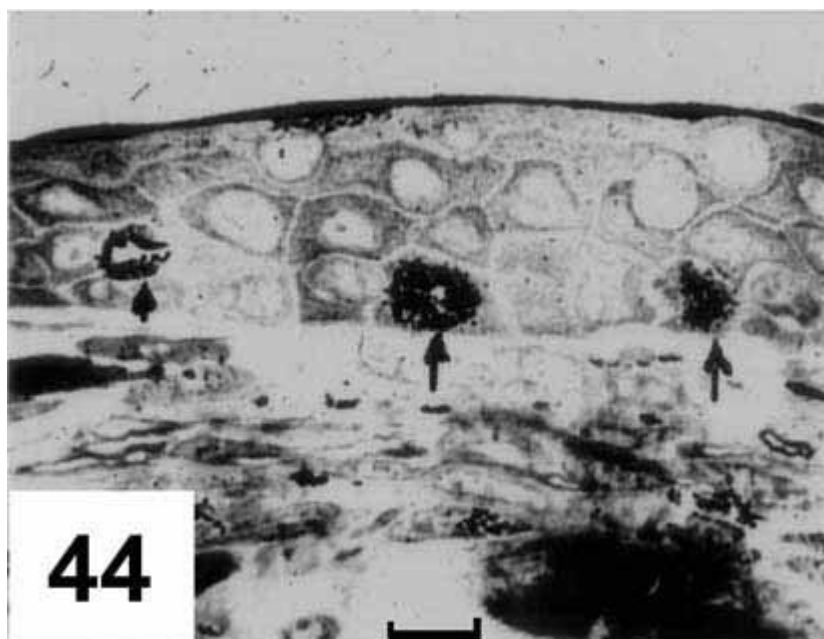


Figure 44. LM-RAG of the skin of a fore-limb of a salamander at 6 weeks after hatching, labeled with  $^3\text{H}$ -thymidine. Three nuclei (arrows) at the basal layer are labeled.  $\times 1,200$ . Bar= $50\mu\text{m}$ . From Nagata (2001a), Permission from Academic Press.

## 5. Concluding Remarks

The histochemical methods which were developed in our laboratory to demonstrate various chemical compounds in biological specimens at both light and electron microscopic levels were briefly described. The methods can be classified into 3 categories, chemical, physical and biological methods, which were first described in details, which should be designated as general histochemistry. On the other hand, the applications of these methods to all the organ systems of skeletal, muscular, circulatory, digestive, respiratory, urinary, reproductive, nervous and sensory organ systems of normal experimental animals, mainly mice, were described at the end, which should be designated as special histochemistry. We hope that these methods should be applied to various normal and pathological organs of various animals as well as to human materials in the future and this science, histochemistry general and special, would be further developed and established.

## 6. Acknowledgments

The author thanks Dr. Kiyokazu Kametani, Department of Instrumental Analysis, Research Center for Human and Environmental Sciences, Shinshu University, for his technical assistance during the course of this study. This study was supported in part by a grants-in-aid for scientific research, from the Ministry of Education, Science and Culture of Japan Government and a grant for promotion of characteristic research and education from the Japan Foundation for Promotion of Private Schools.

## 7. References

- Altmann R. Über die Fettumsetzungen im Organismus. Arch. Anat. Physiol. 1889; suppl.:86-104.
- Altmann R. Die Elementorganismen und ihre Beziehungen zu den Zellen. Leipzig: Veit und Comp, 1894.
- Bernhard W, Leduc EH. Ultrathin frozen sections. I. Methods and ultrastructural preservation. J Cell Biol 1967;34:757-71.
- Caspersson T. Über die chemischen Aufbau des Struktur des Zellkernes. Skandinav Arch Physiol 1936;73(8):1-151.

- Coons A H, Creech H J, Jones RN. Immunological properties of an antibody containing a fluorescent group. *Proc Exp Biol NY* 1941;47:200-2.
- Cui H. Light microscopic radioautographic study on DNA synthesis of nerve cells in the cerebella of aging mice. *Cell Mol Biol* 1995;41:1139-54.
- Cui H, Gao F, Nagata T. Light microscopic radioautographic study on protein synthesis in perinatal mice corneas. *Acta Histochem. Cytochem* 2000;33:31-7.
- Daddi L. Nouvelle methode pour colorer la graisse dans les tissue. *Arch Ital Biol* 1896;26:143-6.
- Danielli JE. Cytochemistry, a critical approach. New York, London: Wiley & Sons, Chapman and Hall, 1953
- Duan H, Nagata T. Glomerular extracellular matrices and anionic sites in aging ddY mice: a morphometric study. *Histochemistry* 1993;99: 81-91.
- Duan H, Gao F, Li S, Hayashi K, Nagata T. Aging changes and fine structure and DNA synthesis of esophageal epithelium in neonatal, adult and old mice. *J Clin Electron Microsc* 1992;25:452-3.
- Duan H, Gao F, Li S, Nagata T. Postnatal development of esophageal epithelium in mouse: a light and electron microscopic radioautographic study. *Cell Mol Biol* 1993;39:309-16.
- Eränkö O. Quantitative methods in histology and microscopic histochemistry. Rarger, Basel and New York, 1955.
- Enzyme Committee of the International Union of Biochemistry. Recommendation of the Nomenclature Committee of the International Union of Biochemistry on the Nomenclature and Classification of Enzymes. New York, San Francisco, London: Academic Press, 1979.
- Feulgen R, Rossenbeck H. Mikroskopisch-chemischetr Nachweiss einen Nukleinsäure von Typus der Thymonukleinsäure. *Z Physik Chem* 1924;135:203-48.
- Gao F. Study on the macromolecular synthesis in aging mouse seminiferous tubules by light and electron microscopic radioautography. *Cell Mol Biol* 1993;39:659-72.
- Gao F, Toriyama K, Nagata T. Light microscopic radioautographic study on the DNA synthesis of prenatal and postnatal aging mouse retina after labeled thymidine injection. *Cell Mol Biol* 1992a;38:661-8.
- Gao F, Li S, Duan H, Ma H, Nagata T. Electron microscopic radioautography on the DNA synthesis of prenatal and postnatal mice retina after labeled thymidine injection. *J Clin Electron Microsc* 1992b;25:721-2.
- Gao F, Toriyama K, Ma H, Nagata T. Light microscopic radioautographic study on DNA synthesis in aging mice corneas. *Cell Mol Biol* 1993;39:435-41.
- Gao F, Ma H, Sun L, Jin C, Nagata T. Electron microscopic radioautographic study on the nucleic acids and protein synthesis in the aging mouse testis. *Med Electron Microsc* 1994;27:360-2.
- Gersh I. The Altmann technique for fixation by drying while freezing. *Anat Rec* 1932;53:309-24.
- Gersh I. The preparation of frozen-dried tissues for electron microscopy. *J Biophys Biochem Cytol* 1956;2(suppl):37-43.
- Glick D. Technique of histo- and cytochemistry. New York: Interscience, 1949.
- Gomori G. Microtechnical demonstration of phosphatase in tissue sections. *Proc Soc Exp Biol Med* 1939;42:23-6.
- Gomori G. Microscopic Histochemistry. Chicago: Chicago University Press, 1952.
- Graumann W. (partly with Neuman K). *Handbuch der Histochemie (Handbook of Histochemistry)*. 27 volumes. Stuttgart: Gustav-Fischer Verlag, 1958-1998.
- Graumann W. *Progress in Histochemistry and Cytochemistry*. Jena: Urban & Fischer Verlag, vol 1, 1966, vol 38, 2003.
- Gunarso W, Gao F, Cui H, Ma H, Nagata T. A light and electron microscopic radioautographic study on RNA synthesis in the retina of chick embryo. *Acta Histochem* 1996;98:309-22.
- Gunarso W, Gao F, Nagata T. Development and DNA synthesis in the retina of chick embryo observed by light and electron microscopic radioautography. *Cell Mol Biol* 1997;43:189-201.
- Hanai T. Light microscopic radioautographic study of DNA synthesis in the kidneys of aging mice. *Cell Mol Biol* 1993;39:81-91.
- Hanai T, Nagata T. Study on the nucleic acid synthesis in the aging mouse kidney by light and electron

- microscopic radioautography. pp.209-214. In: Nagata T (editor). Radioautography in Medicine. Matsumoto: Shinshu University Press; 1994a.
- Hanai T, Nagata T. Electron microscopic study on nucleic acid synthesis in perinatal mouse kidney tissue. *Med Electron Microsc* 1994b;27:355-7.
- Hanai T, Usuda N, Morita T, Shimizu T, Nagata T. Proliferative activity in the kidneys of aging mice evaluated by PCNA/cyclin immunohistochemistry. *Cell Mol Biol* 1993;39:181-91.
- Hanai T, Usuda N, Morita T, Nagata T. Light microscopic lectin histochemistry in aging mouse kidney: study of compositional changes in glycoconjugates. *J Histochem Cytochem* 1994a;42:897-906.
- Hanai T, Usuda N, Morita T, Nagata T. Correspondence to changes in lectin binding pattern during fetal and postnatal development of renal corpuscles of rat kidney as revealed by light and electron microscopy. *Acta Histochem Cytochem* 1994b;27:185-188.
- Hayashi K, Gao F, Nagata T. Radioautographic study on <sup>3</sup>H-thymidine incorporation at different stages of muscle development in aging mice. *Cell Mol Biol* 1993;39:553-560.
- Ito M. The radioautographic studies on aging change of DNA synthesis and the ultrastructural development of mouse adrenal gland. *Cell Mol Biol* 1996;42:279-292.
- Ito M, Nagata T. Electron microscopic radioautographic studies on DNA synthesis and ultrastructure of aging mouse adrenal gland. *Med Electron Microsc* 1996;29:145-152.
- Jin C. Study on DNA synthesis of aging mouse colon by light and electron microscopic radioautography. *Cell Mol Biol* 1996;42:255-268.
- Jin C, Nagata T. Light microscopic radioautographic study on DNA synthesis in cecal epithelial cells of aging mice. *J Histochem Cytochem* 1995a;43:1223-1228.
- Jin C, Nagata T. Electron microscopic radioautographic study on DNA synthesis in cecal epithelial cells of aging mice. *Med Electron Microsc* 1995b;28:71-75.
- Joukura K, Nagata T. Aging changes of <sup>3</sup>H-glucosamine incorporation into mouse kidney observed by radioautography. *Acta Histochem Cytochem* 1995;28:494-494.
- Joukura K, Usuda N, Nagata T. Quantitative study on the aging change of glycoconjugates synthesis in aging mouse kidney. *Proc X<sup>th</sup> Int Cong Histochem Cytochem, Acta Histochem Cytochem* 1996;29(suppl):507-508.
- Kametani K. Detection of aluminum by energy dispersive X-ray microanalysis at high accelerating voltages with semi-thin sections of biological samples. *J Electron Microsc* 2002;51:265-274.
- Kametani K, Nagata T. Demonstration of aluminum in mouse tissues by X-ray microanalysis and energy spectroscopic imaging with electron energy loss spectrometry. *Ann Microsc* 2005;5:19-27.
- Kametani K, Nagata T. Quantitative elemental analysis on aluminum accumulation by HVTEM-EDX in liver tissues of mice orally administered with aluminum chloride. *Med Mol Morphol* 2006;39:97-105.
- Kametani K, Nagata T. Aluminum accumulation in several organs of mice orally administered with aluminum chloride as detected by EDX-HVTEM. *Ann Microsc* 2007;7:84-94.
- Kong Y. Electron microscopic radioautographic study on DNA synthesis in perinatal mouse retina. *Cell Mol Biol* 1993;39:55-64.
- Kong Y, Nagata T. Electron microscopic radioautographic study on nucleic acid synthesis of perinatal mouse retina. *Med Electron Microsc* 1994;27:366-368.
- Kong Y, Usuda N, Nagata T. Radioautographic study on DNA synthesis of the retina and retinal pigment epithelium of developing mouse embryo. *Cell Mol Biol* 1992a;38:263-372.
- Kong Y, Usuda N, Morita T, Hanai T, Nagata T. Study on RNA synthesis in the retina and retinal pigment epithelium of mice by light microscopic radioautography. *Cell Mol Biol* 1992b;38:669-678.
- Lehmann CG. *Lehrbuch der Physiologischen Chemie*. Leipzig: Vogel Verlag, 1842.
- Li S. Relationship between cellular DNA synthesis, PCNA expression and sex steroid hormone receptor status in the developing mouse ovary, uterus and oviduct. *Histochemistry* 1994;102:405-413.
- Li S, Nagata T. Nucleic acid synthesis in the developing mouse ovary, uterus and oviduct studied by light and electron microscopic radioautography. *Cell Mol Biol* 1995;41:185-195.
- Li S, Duan H, Nagata T. Age-related alterations of proteoglycan in mouse tracheal cartilage matrix: An



- electron histochemical analysis with the cationic dye of polyethylenimine. *Cell Mol Biol* 1994;40:129-135.
- Li S, Gao F, Duan H, Nagata T. Radioautographic study on the uptake of  $^{35}\text{SO}_4$  in mouse ovary during the estrus cycle. *J Clin Electron Microsc* 1992;25:709-710.
- Liang Y. Light microscopic radioautographic study on RNA synthesis in the adrenal glands of aging mice. *Acta Histochem. Cytochem* 1998;31:203-210.
- Liang Y, Ito M, Nagata T. Light and electron microscopic radioautographic studies on RNA synthesis in aging mouse adrenal gland. *Acta Anat Nippon* 1999;74:291-300.
- Lillie RD. Various oil soluble dyes as fat stains in supersaturated isopropanol technic. *Stain Technol* 1944;19:55-58.
- Lillie RD. *Histopathologic Technique and Practical Histochemistry*. New York: Blackstone, 1954.
- Lison L. *Histochimie et Cytochimie Animal, principes et methodes*. Paris: Gauthier-Villards, 1936.
- Lison L. *Histochimie et Cytochimie Animal, principes et methodes*. 3<sup>rd</sup> ed. Paris: Gauthier-Villards, 1960.
- Ma H. Light microscopic radioautographic study on DNA synthesis of the livers in aging mice. *Acta Anat Nippon* 1988;63:137-147.
- Ma H, Nagata T. Electron microscopic radioautographic study on DNA synthesis of the livers in aging mice. *J Clin Electron Microsc* 1988a;21:335-43.
- Ma H, Nagata T. Studies on DNA synthesis of aging mice by means of electron microscopic radioautography. *J Clin Electron Microsc* 1988b;21:715-716.
- Ma H, Nagata T. Electron microscopic radioautographic studies on DNA synthesis in the hepatocytes of aging mice as observed by image analysis. *Cell Mol Biol* 1990a;36:73-84.
- Ma H, Nagata T. Study on RNA synthesis in the livers of aging mice by means of electron microscopic radioautography. *Cell Mol Biol* 1990b;36:589-600.
- Ma H, Nagata T. Collagen and protein synthesis in the livers of aging mice as studied by electron microscopic radioautography. *Ann Microsc* 2000;1:13-22.
- Ma H, Gao F, Olea MT, Nagata T. Protein synthesis in the livers of aging mice studied by electron microscopic radioautography. *Cell Mol Biol* 1991;37:607-615.
- Miescher F. *Ein Beitrag zur Histochemie*. Leipzig: Vogel Verlag, 1874.
- Morita T. Radioautographic study on the aging change of  $^3\text{H}$ -glucosamine uptake in mouse ileum. *Cell Mol Biol* 1993;39:875-884.
- Morita T, Usuda N, Hanai T, Nagata T. Changes of colon epithelium proliferation due to individual aging with PCNA/cyclin immunostaining comparing with  $^3\text{H}$ -thymidine radioautography. *Histochemistry* 1994;101:13-20.
- Murata F, Nagata T. Fine structure and acid mucosubstance localization of the human basophilic leukocytes. *J Clin Electron Microsc* 1976;9:207-214.
- Murata F, Nagata T, Spicer SS. Fine structural localization of arylsulfatase B activity in the rabbit blood platelets. *Histochemistry* 1975;44:307-312.
- Murata F, Wholtman H, Spicer SS, Nagata T. Fine structural and ultracytochemical studies on the lymphocytes in three types of genetic mucopolysaccharidoses. *Virchows Arch. B Cell Pathol* 1977a;25:61-73.
- Murata F, Momose Y, Yoshida K, Ohno S, Nagata T. Nucleic acid and mucosubstance metabolism of the mastocytoma cells by means of electron microscopic radioautography. *Acta Pharmacol Toxicol* 1977c;41:58-59.
- Murata F, Momose Y, Nagata T. Demonstration of intracytoplasmic glycogen of megakaryocytes and blood platelets by means of the periodic acid-thiocarbohydrazide-silver proteinate method. *Histochemistry* 1977b;52:307-316.
- Murata F, Yoshida K, Ohno S, Nagata T. Ultrastructural localization of glycogen in the granulocytes of normal rabbit bone marrow. *Histochemistry* 1978a;58:103-111.
- Murata F, Yoshida K, Ohno S, Nagata T. Ultrastructural and electron microscopic radioautographic studies on the mastocytoma cells and mast cells. *J Clin Electron Microsc* 1978b;11:561-562.
- Murata F, Yoshida K, Ohno S, Nagata T. Mucosubstance of rabbit granulocytes studied by means of

- electron microscopic radioautography and X-ray microanalysis. *Proc. Ninth Internat. Cong. Electron Microsc.* 1978c; II: 64-65.
- Nagata T. On the relationship between cell division and cytochrome oxidase in the Yoshida sarcoma cells. *Shinshu Med J* 1956;5:383-386.
- Nagata T. Quantification of DNA contents in rat hepatocytes by means of microspectrophotometry, with special reference to binucleate cells. *Arch Histol Japon* 1961a;22:81-82.
- Nagata T. A new method for preparing specimens suitable to microspectrophotometry of binucleate cell nuclei stained with the Feulgen reaction. *Med J Shinshu Univ* 1961b;6:137-141.
- Nagata T. A quantitative study of the DNA contents in rat hepatic cell nuclei by means of microspectrophotometry, with special reference to binucleate cells. *Med J Shinshu Univ* 1961c;6:143-153.
- Nagata T. Theory and application of microspectrophotometry: Introduction to quantitative histochemistry. *Shinshu Med J* 1966;15:148-157.
- Nagata T. Application of microspectrophotometry to various substances. pp. 49-155. In: Isaka S, Nagata T, Inui N (editors). *Introduction to Microspectrophotometry*. Tokyo: Olympus Co.; 1972a.
- Nagata T. Electron microscopic dry-mounting autoradiography. *Proc 4<sup>th</sup> Internat Cong Histochem Cytochem*, Kyoto 1972b;43-44.
- Nagata T. Lipase. Vol. 2, pp. 132-148. In: Hayat MA (editor). *Electron Microscopy of Enzymes, Principles and Methods*. New York: Van Nostrand Reinhold Co.; 1974.
- Nagata T. Electron microscopic radioautography and analytical electron microscopy. *J Clin Electron Microsc* 1991;24:441-442.
- Nagata T. Radiolabeling of soluble and insoluble compounds as demonstrated by light and electron microscopy. pp. 9-21. In: Wegmann RJ, Wegmann MA (editors). *Recent Advances in Cellular and Molecular Biology, Molecular Biology of Pyridines, DNA, Peroxisomes, Organelles and Cell Movements*. Leuven: Peeters Press; 1992.
- Nagata T. Quantitative analysis of histochemical reactions: Image analysis of light and electron microscopic radioautograms. *Acta Histochem Cytochem* 1993;26:281-291.
- Nagata T. Introductory remarks to advances in cytochemistry with physical method. *Acta Histochem Cytochem* 1994a;27:465-9.
- Nagata T. Electron microscopic radioautography with cryo-fixation and dry-mounting procedure. *Acta Histochem Cytochem* 1994b;27:471-489.
- Nagata, T. Application of electron microscopic radioautography to clinical electron microscopy. *Med Electron Microsc* 1994c;27:191-212.
- Nagata T (editor). *Radioautography in Medicine*. Matsumoto: Shinshu Univ Press, 1994d.
- Nagata T. Light and electron microscopic radioautographic study on macromolecular synthesis in digestive organs of aging mice. *Cell Mol Biol* 1995a;41:21-38.
- Nagata T. Histochemistry of the organs: Application of histochemistry to anatomy. *Acta Anat Nippon* 1995b;70:448-471.
- Nagata T. Three-dimensional observation of whole mount cultured cells stained with histochemical reactions by ultrahigh voltage electron microscopy. *Cell Mol Biol* 1995c;41:783-792.
- Nagata T. Technique and application of electron microscopic radioautography. *J Electron Microsc* 1996a;45:258-274.
- Nagata T. Techniques of light and electron microscopic radioautography. In: *Histochemistry and Cytochemistry 1996*. *Proc X<sup>th</sup> Internat Congr Histochem Cytochem Acta Histochem Cytochem* 1996b;29 (suppl):343-344.
- Nagata T. Techniques and applications of microscopic radioautography. *Histol Histopathol* 1997a;12:1091-124.
- Nagata T. Three-dimensional observation on whole mount cultured cells and thick sections stained with histochemical reactions by high voltage electron microscopy. pp. 37-44. In: Motta P (editor). *Recent Advances in Microscopy of Cells, Tissues and Organs*. Roma: Antonio Delfino Editore; 1997b.
- Nagata T. Radioautographic study on collagen synthesis in the ocular tissues. *J Kaken Eye Res* 1997c;15:1-9.

- Nagata T. Biological microanalysis of radiolabeled and unlabeled compounds by radioautography and X-ray microanalysis. Proc. 30<sup>th</sup> International Scanning Microscopy Meeting, Chicago, May 10-15, 1997d, 1-2.
- Nagata T. Techniques of radioautography for medical and biological research. *Braz J Biol Med Res* 1998a;31:185-195.
- Nagata T. Radioautographology, the advocacy of a new concept. *Braz J Biol Med Res* 1998b;31:201-41.
- Nagata T. Radioautographic studies on DNA synthesis of the bone and skin of aging salamander. *Bull Nagano Women's Jr College* 1998c;6:1-14.
- Nagata T. 3D observation of cell organelles by high voltage electron microscopy. *Microscopy and Analysis, Asia Pacific Edition* 1999a;9:29-32.
- Nagata T. Application of histochemistry to anatomy: Histochemistry of the organs, a novel concept. Proc XV<sup>th</sup> Cong Internat Fed Assoc Anatom, Italy. *J Anat Embryol* 1999b;104(suppl): 486-487.
- Nagata T. Aging changes of macromolecular synthesis in various organ systems as observed by microscopic radioautography after incorporation of radiolabeled precursors. *Methods Find Exp Clin Pharmacol* 1999c;21:683-706.
- Nagata T. Three-dimensional observations on thick biological specimens by high voltage electron microscopy. *Image Analysis Stereolog* 2000a;19:51-56.
- Nagata T. Study of the effects of aging on macromolecular synthesis in mouse steroid secreting cells using microscopic radioautography. *Methods Find Exp Clin Pharmacol* 2000b;22:5-18.
- Nagata T. Three-dimensional high voltage electron microscopy of thick biological specimens. *Micron* 2000c;32:387-404.
- Nagata T. Electron microscopic radioautographic study on protein synthesis in pancreatic cells of perinatal and aging mice. *Bull Nagano Women's Jr College* 2000e;8:1-22.
- Nagata T. Light microscopic radioautographic study on radiosulfate incorporation into the tracheal cartilage in aging mice. *Acta Histochem Cytochem* 2000f;32:377-383.
- Nagata T. Special cytochemistry in cell biology. pp. 33-151. In: Jeon KW (editor). *International Review of Cytology, A Survey of Cell Biology*. New York: Academic Press; 2001a.
- Nagata T. Three-dimensional high voltage electron microscopy of thick biological specimens. *Micron* 2001b;32:387-404.
- Nagata T. Radioautographology, general and special. 37(2);59-226. In: Graumann W (editor). *Progress in Histochemistry and Cytochemistry*. Jena: Urban & Fischer Verlag; 2002.
- Nagata T. The utility value of high voltage electron microscopy for X-ray microanalysis. *Acta Histochem Cytochem* 2003;36:299-315.
- Nagata T. Recent advances in cytochemical methodology in medical and biological sciences. *SBPN Scientific J* 2004a;1(1-2): 5-56.
- Nagata T. X-ray microanalysis of biological specimens by high voltage electron microscopy. 39(4);185-320. In: Sasse D (editor). *Progress in Histochemistry and Cytochemistry*. Jena: Elsevier GmbH; 2004b.
- Nagata T. Sepecial histochemistry: Histochemistry of the organs-Application of histochemistry to special histology. Proc 16<sup>th</sup> Internat Cong IFAA, Kyoto 2004c;193-196.
- Nagata T. Aging changes of macromolecular synthesis in the uro-genital organs of rodents as revealed by radioautography and cytochemistry. *Annu Rev Biomed Sci* 2005;6:13-78.
- Nagata T. Aging changes of macromolecular synthesis in the avian and mammalian eyes as revealed by microscopic radioautography. *Annu Rev Biomed Sci* 2006a;8:33-67.
- Nagata T. Electron microscopic radioautographic study on protein synthesis in hepatocyte mitochondria of aging mice. *The Scientific World J* 2006b;6:1583-1598.
- Nagata T. Radioautographic study on DNA synthesis in the limb bones of aging salamanders. *Bull Shinshu Inst Alternat Med* 2006c;1:51-60.
- Nagata T. Macromolecular synthesis in hepatocyte mitochondria of aging mice as revealed by electron microscopic radioautography. I. Nucleic acid synthesis. 1;245-258. In: Vilas AM, Alvarez JD (editors). *Modern Research and Educational Topics in Microscopy*. Spain: Formatex, Badajoz; 2007a.

- Nagata T. Macromolecular synthesis in hepatocyte mitochondria of aging mice as revealed by electron microscopic radioautography. II. Protein synthesis. 1;259-271. In: Vilas AM, Alvarez JD (editors). Modern Research and Educational Topics in Microscopy. Spain: Formatex, Badajoz; 2007b.
- Nagata T. Electron microscopic radioautographic study on macromolecular synthesis in hepatocyte mitochondria of aging mice. J Cell Tiss Res 2007c;1303-1312.
- Nagata T. Radioautographic study on DNA synthesis in the skins of aging salamanders. Bull Shinshu Inst Alternat Med 2007d; 2: 43-53. .
- Nagata T. Electron microscopic radioautographic study on mitochondrial DNA synthesis in binucleate hepatocyte in aging mice. The Scientific World J 2007e;7:1008-1023.
- Nagata T. Electron microscopic radioautographic study on protein synthesis in adrenal cortical cells of developing mice. J Cell Tissue Res 2008;8:1303-1312.
- Nagata T, Iwadare N. Electron microscopic demonstration of phospholipase B activity in the liver and the kidney of the mouse. Histochemistry 1984;80:149-152.
- Nagata T, Kawahara I. Radioautographic study of the synthesis of sulfomucin in digestive organs of mice. J Trace Microprobe Analysis 1999;17:339-355.
- Nagata T, Kong Y. Distribution and localization of TGF $\beta$ 1 and  $\beta$ FGF, and their mRNAs in aging mice. Bull Nagano Women's Junior College 1998;6:87-105.
- Nagata T, Ma H. Electron microscopic radioautographic study on protein synthesis in amitotic hepatocytes of the aging mouse. Med Electron Microsc 2004;37:62-69.
- Nagata T, Ma H. Electron microscopic radioautographic study on mitochondrial DNA synthesis in hepatocytes of aging mouse. Ann Microsc 2005a;5:4-18.
- Nagata T, Ma H. Electron microscopic radioautographic study on RNA synthesis in hepatocyte mitochondria of aging mouse. Microsc. Res Tech 2005b;67:55-64.
- Nagata T, Matsumura K Radioautographic studies on DNA synthesis of the lungs of aging salamanders. Ann Microsc 2004;4:4-13.
- Nagata T, Murata F. Electron microscopic dry-mounting radioautography for diffusible compounds by means of ultracryotomy. Histochemistry 1977;54:75-82.
- Nagata T, Murata F. Esterase. pp 225-253. In: Takeuchi T, Ogawa, K (editors). Enzyme Histochemistry. Tokyo: Asakura Shoten, 1980.
- Nagata T, Fujiwara I, Shimamura K. On the argentaffine reaction of melanins and their precursors. Shinshu Med J 1957a;6:515-517.
- Nagata T, Fujiwara I, Shimamura K. On the distribution of calcium in the stratified squamous epithelia. Acta Anat Nippon 1957b;32:305-310.
- Nagata T, Nawa T. A radioautographic study on the nucleic acid synthesis of binucleate cells in cultivated fibroblasts of chick embryo. Med J Shinshu Univ 1966;11:1-5.
- Nagata T, Nawa T, Yokota S. A new technique for electron microscopic dry-mounting radioautography of soluble compounds. Histochemie 1969;18:241-249.
- Nagata T, Shimamura K. Radioautographic study on Ca absorption. I. Calcium absorption in the stomach of rat. Shinshu Med J 1958;3:83-90.
- Nagata T, Shimamura K. Radioautographic study on Ca absorption. II. Calcium absorption in the intestines of rat. Shinshu Med J 1959a;4:1-10.
- Nagata T, Shimamura K. Radioautographic study on Ca absorption. III. Distribution of radiocalcium in the liver and the kidney of rat after oral administration. Shinshu Med J 1959b;4:11-18.
- Nagata T, Sun L. Electron microscopic radioautographic study on DNA and RNA synthesis in pulmonary cells of aging mice. Ann Microsc 2007;7:36-59.
- Nagata T, Yoshida K, Murata F. Demonstration of hot and cold mercury in the human thyroid tissues by means of radioautography and chemography. Acta Pharmacol Toxicol 1977b;41:60-61.
- Nagata T, Cui H, Kong Y. The localization of TGF- $\beta$ 1 and its mRNA in the spinal cords of prenatal and postnatal aging mice demonstrated with immunohistochemical and *in situ* hybridization techniques. Bull Nagano Women's Jr College 1999;7:75-88.
- Nagata T, Ito M, Liang Y. Study of the effects of aging on macromolecular synthesis in mouse steroid secreting cells using microscopic radioautography. Methods Find Exp Clin Pharmacol 2000a;22:5-18.



- Nagata T, Ito M, Chen S. Aging changes of DNA synthesis in the submandibular glands of mice as observed by light and electron microscopic radioautography. *Ann Microsc* 2000b;1:4-12.
- Nawa T, Nagata T, Omochi S. An apparatus for freeze-drying of tissue. *Med J Shinshu Univ* 1965;10:1-11.
- Nawa T, Nagata T, Yokota S, Murata F, Omochi S. Two new models of freeze-drying apparatus for tissues. *Med J Shinshu Univ* 1969;14:1-15.
- Oguchi K, Nagata T. A radioautographic study of activated satellite cells in dystrophic chicken muscle. pp 16-17. In: *Current Research in Muscular Dystrophy in Japan*. Annu Rept Neurol Dis. Tokyo: Ministry of Welfare of Japan; 1980.
- Oguchi K, Nagata T. Electron microscopic radioautographic observation on activated satellite cells in dystrophy chickens. pp. 33-31. In: *Clinical Studies on the Etiology of Muscular Dystrophy*. Annu Rept Neurol Dis. Tokyo: Ministry of Welfare of Japan; 1981.
- Olea MT. An ultrastructural localization of lysosomal acid phosphatase activity in aging mouse spleen: a quantitative X-ray microanalytical study. *Acta Histochem Cytochem* 1991;24:201-208.
- Olea MT, Nagata T. X-ray microanalysis of cerium in mouse spleen cells demonstrating acid phosphatase activity using high voltage electron microscopy. *Cell Mol Biol* 1991;37:155-163.
- Olea MT, Nagata T. Simultaneous localization of  $^3\text{H}$ -thymidine incorporation and acid phosphatase activity in mouse spleen: EM radioautography and cytochemistry. *Cell Mol Biol* 1992a;38:115-122.
- Olea MT, Nagata T. A radioautographic study on RNA synthesis in aging mouse spleen after  $^3\text{H}$ -uridine labeling *in vitro*. *Cell Mol Biol* 1992b;38:399-405.
- Oliveira SF, Nagata T, Abrahamsohn .A, Zorn TMT. Electron microscopic radioautographic study on the incorporation of  $^3\text{H}$ -proline by mouse decidual cells. *Cell Mol Biol* 1991;37:315-323.
- Oliveira SF, Abrahamsohn PA, Nagata T, Zorn TMT. Incorporation of  $^3\text{H}$ -amino acids by endometrial stromal cells during decidualization in the mouse. A radioautographical study. *Cell Mol Biol* 1995;41:107-116.
- Ono S. Electron microscopy and electron probe X-ray microanalysis of human lumbar yellow ligaments by forzen-dried cryosections. *J Clin Electron Microsc* 1991;24:377-388.
- Ono S, Nagata T. X-ray microanalysis of Ca and S in human lumbar yellow ligaments. 1988;22:723-724.
- Ono S, Otsuka K, Terayama K, Nagata T. Quantitaive electron probe X-ray microanalysis of calsium and phosphorus in human lumbar yellow ligaments. 1994;27:323-325.
- Pearse AGE. *Histochemistry, Theoretical and Applied*. 1<sup>st</sup> ed . Boston: Little Brown Co., 1953.
- Pearse AGE. *Histochemistry, Theoretical and Applied*. 2<sup>nd</sup> ed. Boston: Little Brown Co., 1961.
- Pearse AGE. *Histochemistry, Theoretical and Applied*. 3<sup>rd</sup> ed. London: J & A Churchill Ltd., 1968.
- Pearse AGE. *Histochemistry, Theoretical and Applied*. 4<sup>th</sup> ed, vol 1. Edinburgh, London, New York: Churchill Livingstone, 1980.
- Pearse AGE. "Histochemistry, Theoretical and Applied." 4<sup>th</sup> ed, vol 2. Edinburgh, London, New York: Churchill Livingstone, 1985.
- Pearse AGE (edited by Stoward P). *Histochemistry, Theoretical and Applied*. 4<sup>th</sup> ed, vol 3. Edinburgh, London, New York: Churchill Livingstone, 1991.
- Raspail FV. Development de la fecale dans les organes de la fructification des cereales et analyse microscopique de la fecale, suivie d'experiences propres a expliquer la conversion en gommen. *Ann Sci Nat* 1825;6:224-39.
- Raspail FV. *Essai de Chimie Microscopique Appliquée à la Physilogie*. Paris, 1830.
- Roth J. The colloidal gold marker system for light and electron microscopic cytochemistry. vol. 2, pp 217-284. In: Bullock GR, Petrusz P (editors). *Techniques in Immunocytochemistry*. London, New York: Academic Press; 1983.
- Roth J, Binder M. Colloidal gold, ferritin and peroxidase for electron microscopic double labeling lectin technique. *J Histochem Cytochem* 1978;26:163-169.
- Roth J, Bendayan M, Orci L. Ultrastructural localization of intracellular antigens by the use of protein A-gold complex. *J Histochem Cytochem* 1978;26:1074-81.

- Sakai Y, Ikado S, Nagata T. Electron microscopic radioautography of satellite cells in regenerating muscles. *J Clin Electron Microsc* 1977;10:508-509.
- Sasse D. (editor), *Progress in Histochemistry and Cytochemistry*. Vol.39: No. 1, 2, 3, 4, Jena: Elsevier, 2004.
- Sasse D. (editor), *Progress in Histochemistry and Cytochemistry*. Vol.43: No. 1, 2, 3, 4, Jena: Elsevier, 2008.
- Sauren YMHF, Mierement RHP, Groot CG, Scherfft JP. Polyethyleneimine as a contrast agent for ultrastructural localization and characterization of proteoglycans in the matrix of cartilage and bone. *J Histochem Cytochem* 1991;39:331-340.
- Scott GH, Horning H. Microincineration of tissues. 2<sup>nd</sup> ed. In: Scott GH, Horning H (editors). *Cytology and Cell Physiology*. Oxford: Oxford Press, 1953.
- Shimizu T, Usuda N, Sugeno A, Masuda H, Hagiwara M, Hidaka H, Nagata T, Iida F. Immunohistochemical evidence for the over-expression of protein kinase C in proliferative diseases of human thyroid. *Cell Mol Biol* 1991;37:812-821.
- Singer SJ. Preparation of electron dense antibody conjugate. *Nature* 1959;183:1523-1524.
- Sternberger LA. The unlabeled antibody peroxidase-antiperoxidase (PAP) method. pp. 104-164. In: Sternberger LA (editor). *Immunohistochemistry*. New York: John Wiley & Sons, Inc.; 1979.
- Sun L. Age related changes of RNA synthesis in the lungs of aging mice by light and electron microscopic radioautography. *Cell Mol Biol* 1995;41:1061-1072.
- Sun L, Gao F, Duan H, Nagata T. Light microscopic radioautography of DNA synthesis in pulmonary cells in aging mice. pp 201-5. In: Nagata T (editor). *Radioautography in Medicine*. Matsumoto: Shinshu Univ Press; 1994.
- Sun L, Gao F, Nagata T. Study on the DNA synthesis of pulmonary cells in aging mice by light microscopic radioautography. *Cell Mol Biol* 1995a;41:851-859.
- Sun L, Gao F, Jin C, Duan H, Nagata T. An electron microscopic radioautographic study on the DNA synthesis of pulmonary tissue cells in aging mice. *Med Electron Microsc* 1995b;28:129-131.
- Sun L, Gao F, Jin C, Nagata T. DNA synthesis in the tracheae of aging mice by means of light and electron microscopic radioautography. *Acta Histochem Cytochem* 1997a;30:211-220.
- Sun L, Gao F, Nagata T. A light microscopic radioautographic study on protein synthesis in pulmonary cells of aging mice. *Acta Histochem Cytochem* 1997b;30:463-70.
- Suzuki K, Imada T, Gao F, Ma H, Nagata T. Radioautographic study of benidipine hydrochloride. - Localization in the mesenteric artery of spontaneous hypertensive rat. *Drug Res* 1994;44:129-133.
- Takamatsu H. Morphological study on alkaline phosphatase. *Manchurian Med J* 1938;29:1351-1351. [in Japanese].
- Takamatsu H. Morphological demonstration of alkaline phosphatase. *Trans Soc Pathol Jap* 1939;29:492-492. [in Japanese].
- Terauchi A, Mori T, Kanda H, Tsukada M, Nagata T. Radioautographic study of <sup>3</sup>H-taurine uptake in mouse skeletal muscle cells. *J Clin Electron Microsc* 1988;21:627-628.
- Terauchi A, Nagata T. Observation on incorporation of <sup>3</sup>H-taurine uptake in mouse skeletal muscle. pp 397-404. In: Nagata T (editor). *Radioautography in Medicine*. Matsumoto: Shinshu University Press; 1993.
- Thiéry JP. Mise en évidence des polysaccharides sur coupes fines en microscopie électronique. *J Microscopie* 1967;6:987-1018.
- Tokuyasu K. A technique for ultracryotomy of cell suspensions and tissues. *J Cell Biol* 1973;57:551-565.
- Toriyama K. Study on the aging changes of DNA and protein synthesis of bipolar and photoreceptor cells of mouse retina by light and electron microscopic radioautography. *Cell Mol Biol* 1995;41:593-601.
- Usuda N, Nagata T. Post-embedding immunoelectron microscopy of tissues processed by rapid freezing and freeze-substitution without chemical fixatives. Authors' response. *J Histochem Cytochem* 1991;39:546-547.
- Usuda N, Ma H, Hanai T, Yokota S, Hashimoto T, Nagata T. Immunoelectron microscopy of tissues processed by rapid freezing and freeze-substitution without chemical fixatives. Application to catalase in rat liver hepatocytes. *J Histochem Cytochem* 1990;38:617-623.

- Usuda N, Kong Y, Hagiwara M, Uchida C, Terasawa M, Nagata T, Hidaka H. Differential localization of protein kinase C in retinal neurons. *J Cell Biol* 1991a;112:1241-1247.
- Usuda N, Kuwabara T, Ichikawa R, Hashimoto T, Nagata T. Immunoelectron microscopic evidence for organ difference in the composition of peroxisome-specific membrane polypeptides among three rat organs: Liver, kidney and intestine. *J Histochem Cytochem* 1991b;39:1357-1366.
- Usuda N, Yokota S, Ichikawa R, Hashimoto T, Nagata T. Immunoelectron microscopic study of a new D-amino acid oxidase-immunoreactive subcompartment in rat liver peroxisomes. *J Histochem Cytochem* 1991c;39:95-102.
- Usuda N, Hayashi S, Fujiwara S, Noguchi T, Nagata T, Rao MS, Alvares K, Reddy JK, Yeldandi AB. Uric acid degrading enzymes, urate oxidase and allantoinase, are associated with different subcellular organelles in frog liver and kidney. *J Cell Sci* 1994;107:1073-1091.
- Usuda N, Hanai T, Nagata T. Immunogold studies on peroxisomes: review of the localization of specific proteins in vertebrate peroxisomes. *Microsc Res Tech* 1995;31:79-92.
- Usuda N, Nakazawa A, Terasawa M, Reddy JK, Nagata T. Immunocytochemical study of the ultrastructure of peroxisomes and the effects of peroxisome proliferators. 804;297-309. In Reddy JK, Suga T, Mannaerts GP, Lazarow PB, Subramani S (editors). *Peroxisomes, Biology and Role in Toxicology and Disease*. New York: Ann New York Acad Sci; 1996.
- Watanabe I, Nagata T. Changes of glucide synthesis in the submandibular glands of aging mice as observed by light and electron microscopic radioautography. *Ann Microsc* 2002;2:4-14.
- Widström G. Über die Verwendbarkeit der Schiffschen Fuchsin-schwefeligsäure-Reaktion zur quantitativen Bestimmung von Thymonukleinsäure. *Biochem Z* 1928;199:298-308.
- Xiao-Lin P, Koide N, Kobayashi S, Kobayashi M, Sugeno A, Iida F, Katsuyama T, Usuda N, Nagata T. Assessment of proliferative activity of glandular cells in hyperfunctioning parathyroid gland using flow cytometric and immunohistochemical methods. *World J Surg* 1996;20:361-367.
- Yamada AT. Timely and topologically defined protein synthesis in the periimplanting mouse endometrium revealed by light and electron microscopic radioautography. *Cell Mol Biol* 1993;39:1-12.
- Yamada AT, Nagata T. Ribonucleic acid and protein synthesis in the uterus of pregnant mouse during activation of implantation window. *Med Electron Microsc* 1992a;27:363-365.
- Yamada AT, Nagata T. Light and electron microscopic radioautography of DNA synthesis in the endometria of pregnant-ovariectomized mice during activation of implantation window. *Cell Mol Biol* 1992b;38:763-774.
- Yamada AT, Nagata T. Light and electron microscopic radioautography of RNA synthesis of peri-implanting pregnant mouse during activation of receptivity for blastocyst implantation. *Cell Mol Biol* 1993;38:211-33.
- Yanagiya N. Ultrastructural and histochemical changes of mitochondria in global ischemic cardiac muscle of rat. *Cell Mol Biol* 1994;40:1151-1164.
- Yanagiya N, Usuda N, Hayashi K, Nagata T. Ultrastructural changes in myocardial and endothelial cells in the microvasculature of the rat heart after global ischemia. *Med Electron Microsc* 1994;27:73-79.
- Yokota S, Nagata T. Study on mouse liver urate oxidase. III. Fine localization of urate oxidase in liver cells revealed by means of ultracryotomy-immunoferritin method. *Histochemistry* 1973;39:243-250.
- Yokota S, Nagata T. Ultrastructural localization of catalase on ultracryotomic sections of mouse liver by ferritin-conjugated antibody technique. *Histochemistry* 1974;40:165-74.
- Yokota S, Nagata T. Urate oxidase. 5;72-97. In: Hayat MA (editor). *Electron Microscopy of Enzymes, Principles and Methods*. New York: Van Nostrand Reinhold Co.; 1977.
- Watanabe I, Nagata T. Aging changes of glucide synthesis in the submandibular glands of aging mice as observed by light and electron microscopic radioautography. *Ann Microsc* 2002;2:4-15.